Cognition and maps : reading and scene comprehension extensively overlap topological viusal, auditory and somatomotor maps in the human cortex

Cognition and Maps:

Reading and scene comprehension extensively overlap topological visual, auditory and somatomotor maps in the human cortex

Mariam Reeny Sood

Submitted for PhD in Psychology

June 2016

Birkbeck, University of London

Supervisor: Prof. Martin I. Sereno

Declaration:

I, Mariam Reeny Sood, confirm that the work presented in this thesis is my own. Where information has been derived from other sources, I confirm that this has been indicated in the thesis.

Signed: Mariam Sood

Date: 09-06-2016

Abstract

Cortical mapping techniques using fMRI have been instrumental in identifying the boundaries of topological maps in early sensory areas. The presence of topological maps beyond early sensory areas raises the possibility that they might play a significant role in other cognitive systems, and that topological mapping might help to delineate areas involved in higher cognitive processes. This thesis investigates the three way interplay between the full extent of topologically mapped sensory-motor regions (detected using retinotopic, tonotopic and somatomotor mapping) and activation observed during two high level comprehension specific tasks in the same set of subjects across the whole cortex.

In the first set of studies, I combined surface based visual, auditory, and somatomotor mapping methods with a naturalistic reading comprehension task to provide a qualitative and quantitative assessment of the cortical overlap between sensory-motor maps in all major modalities, and reading processing regions. The results suggest that cortical activation during naturalistic reading comprehension overlaps more extensively with topological sensory-motor maps than has been heretofore appreciated. To further differentiate the activations observed during the reading study, a separate fMRI study involving a purely picture-based narrative scene comprehension task was carried out on the same set of subjects. The results from the cumulative dataset suggest that the reading and scene activations are centred around the same regions in the occipito-parietal, temporal and frontal cortex. The shared activations between reading and scene also largely overlap with topological cortical maps. Additionally, there are regions overlapping with maps in occipito-parietal, temporal and frontal cortex that are distinct to either reading or scene processing.

Finally, the mapping studies also identified several previously unreported maps in the cortex including a visual and a tonotopic map in the cingulate cortex, and several tonotopic maps in the frontal cortex.

Acknowledgements

First and foremost I want to thank my principal supervisor Prof. Martin (Marty) Sereno, for his excellent mentoring and invaluable support through out my PhD. I greatly appreciate Marty's intellectual generosity, the time he has invested in me, the consideration and patience he has shown me through out, and the independence he gave me to pursue my research interests. I am truly grateful for all the knowledge, inspiration, and skills I gained from Marty.

My sincere thanks also go to: Dr. Frederic Dick, my second supervisor for his guidance and for introducing me to key neuroimaging software at the start of my PhD; Staff at BUCNI, especially Trevor Brooks and Preetha Shaji for help with the scanner; to the participants for their participation in all five experiments described in this thesis, and to my colleagues for their help and company. I also want to express my sincere gratitude to ESRC for the postgraduate studentship without which I would not have been able to do this PhD, and to Marty for funding my scanning costs.

On my personal front, I want to thank my parents for instilling in me reverence for knowledge and my past teachers for their intellectual encouragement and support. I would also like to thank my friends whose encouragement was a source of comfort while making the decision to switch to neuroscience research. Most importantly, I would like to thank my husband Anuj for believing in me and for helping me execute my crazy plans. I am grateful to both Anuj and our son Siddhant for their unconditional love and support which was instrumental for my physical and mental happiness.

Contents

List of Figures

List of Tables

Chapter 1

General Introduction

Topological (neighbor-preserving) remapping is a key principle of organization of sensory and motor areas within the mammalian brain. In primary sensory and motor cortices, these representations initially reflect the spatial layout of the receptors; for instance retinotopic maps in visual cortex topologically encode retinal locations, tonotopic maps in auditory cortex represent positions along the cochlear hair cell line, which correspond to sound frequency, and somatotopic maps in the somatosensory cortex represent locations on the body surface. Disrupting these maps has been shown to affect subsequent sensory processing and behaviour (Sperry, 1944; Kaas, 1997). Traditionally it has been assumed that topological mapping was limited to lower level cortex (e.g., Hebb, 1949). But the entire cortex is characterized by the overwhelming predominance of local connections (Lund et al., 1993; Schmahmann and Pandya, 2009; Markov et al., 2011; Ercsey-Ravasz et al., 2013), suggesting that maps of some form may extend to the highest levels. The last few decades of electrophysiological investigations in monkeys and neuroimaging research on humans has shown that topological organization extends well into higher-level cortical areas (Felleman and Van Essen, 1991; Sereno and Allman, 1991; Wandell et al., 2007; Huang and Sereno, 2013). In contrast to lower-level maps, however, localized activity in higher-level maps is affected as much by spatial attention as by the spatial characteristics of the stimuli (Saygin and Sereno, 2008). In frontal cortex, there is evidence that topological maps may serve as a convenient method of allocating working memory, or maintaining pointers to specific content (Hagler and Sereno, 2006), even for tasks not overtly referencing position; for example, the exact areas that showed more robust activity during an identity two-back task (in which location was ignored), than during a location two-back task (in which identity was ignored) turned out to contain retinotopic maps. A significant role for topological maps in other complex mental operations has been suggested before (e.g., Simmons and Barsalou, 2003; Thivierge and Marcus, 2007), but direct neuroimaging evidence supporting this idea has been scant.

The primary aim of this thesis is to advance the conceptual understanding of the level of interplay between topological visual, auditory and somatomotor cortical maps and higher level cognitive processes. To this end, I undertook five main scanning experiments. The first major body of work investigated the extent of overlap between cortical reading comprehension regions and brain areas that possess a topological visual, auditory or

somatomotor map based on an fMRI study comprising nearly 80 separate sessions. Following on from the first project, I did another fMRI study on the same subset of subjects using a purely picture-based comprehension task. The data from this study titled 'Narrative scene comprehension' was combined with the four sets of cortical mapping and reading comprehension data I had already collected, providing a unique data set that combined narrative reading and scene comprehension with visual, auditory and somatomotor mapping in the same set of subjects. The data set from these five studies brings much improved accuracy and clarity to several important debates in the field including the degree to which sensory-motor regions are involved in reading/pictorial comprehension, the significance of maps in higher-level cortical areas, the significance of comprehension-specific activity in lower-level visual/auditory/somatomotor areas, and the degree to which serial assembly processes in linguistic and non-linguistic comprehension utilise the same set of uni- and multi-modal areas. Finally, siting reading and scene processing regions with respect to topological cortical maps provide a more precise way to compare activations across individuals and groups as well as studies. This is particularly important for refining functional localisations in less well-understood regions such as frontal cortex.

On the methodological front, there were two different types of analysis utilized in this thesis. The mapping experiments were analysed using a linear Fourier based phase-encoded analysis technique while the high-level cognitive experiments (reading and scene) utilized a closely related GLM (general linear model) based mass univariate analysis (see Rio et al., 2013 for more details). In all studies, I employed a fully surface-based group analysis stream as opposed to volume-based group analysis commonly used in high-level cognitive experiments (merely displaying a 3-D averaged result on an average surface gains none of the benefits of surface-based averaging). The cerebral cortex has the topology of a 2-D sheet. Many relevant dimensions (e.g., retinotopy, somatotopy, tonotopy) vary much more rapidly tangential to the cortical surface than they do perpendicular to the cortical surface, through the several millimetres of cortical thickness. Distances measured in 3-D space between two points — but also used in standard pre-fitting 3-D smoothing — can substantially underestimate the true distance along the cortical sheet due to its folded nature (Fischl et al., 1999a,b). This artifactual within-subject blurring is then made worse by 3-D averaging of between-subject variability in the idiosyncratic secondary crinkling of major sulcal cortical

folding patterns. Surface based techniques make it possible to restrict smoothing to directions parallel to the cortical sheet, and to employ inter-subject 2-D alignment based on the patterns of sulci and gyri after secondary crinkles have been removed, which reduces both kinds of artifactual blurring and improves cross subject averaging (Fischl et al., 1999b); this also provides a less biased estimate of overlap.

The five core experiments that form the cornerstone of this thesis are described in three chapters (chapters 2-4). All experiments in this thesis were conducted on the same set of subjects. Each chapter is designed to be self contained with a separate introduction, methods, results and discussion. The scanner set-up, imaging parameters and data analysis methods are discussed in each individual chapters. A reference chapter, chapter 6 provides an overview of the basic concepts of MRI/fMRI and the relevant pulse sequences used.

In chapter 2, I detail the retinotopic, tonotopic and somatomotor mapping experiments undertaken. The mapping datasets presented here provides a comprehensive picture of cortical maps of three major modalities- visual, auditory and somatomotor across the whole cortex in the same set of subjects. The new large data sets benefitted from the latest multi-band pulse sequences, and the most up-to-date sensory mapping stimuli. The mapping experiments also uncovered several new, previously unreported topological sensory maps. Specifically, several new tonotopic maps were found in the frontal cortex, two of which partially overlap with retinotopy in the region. Then, in the cingulate cortex, two additional new maps were found— a visual map and a tonotopic map. The cingulate visual map may constitute the “supplementary eye fields”; the data presented here may provide the first observation of topological organization within the human equivalent of the non-human primate dorsomedial frontal eye fields. Additionally the map datasets presented here illustrates where topological sensory-motor maps of different modalities intersect. Chapter 3 details the naturalistic reading comprehension experiment and provides a qualitative and quantitative assessment of the level of overlap between activations observed during naturalistic, narrative reading comprehension and topological sensory-motor maps, which are driven by relatively low-level sensory-motor stimuli. The results suggest that cortical activation during naturalistic reading comprehension overlaps more extensively with topological sensory-motor maps than has been heretofore appreciated. In chapter 4, a similar overlap analysis is carried out using a narrative scene comprehension experiment, and the

assessment from the combined data set from the previous chapters is presented. This combined data set provides a unique view of where reading and scene comprehension regions are localized relative to both low-level and high-level topological maps and how they compare and contrast. Finally, in chapter 5, I provide a general discussion combining all the findings in this thesis.

A slightly revised version of the results presented in chapters 2 and 3 are reported in the peer reviewed publication: “Areas activated during naturalistic reading comprehension overlap topological visual, auditory, and somatomotor maps”. Sood, MR and Sereno MI (in press, Human Brain Mapping)

~~~
~~~

Chapter 2

Cortical Visual, Auditory and Somatomotor maps

*This chapter is derived in part from: “Areas activated during naturalistic reading comprehension overlap topological visual, auditory, and somatomotor maps”. Sood, MR and Sereno MI (in press, Human Brain Mapping).

Precis

This chapter details the cortical mapping experiments which form an integral part of this thesis. The mapping study presented here provides a comprehensive picture of cortical maps of three major modalities- visual, auditory and somatomotor across the whole cortex in the same set of subjects, also revealing the 'multisensory' regions where maps of different modalities overlap. The findings described here report several new, previously unreported retinotopic and tonotopic maps in the frontal/cingulate cortex. The dataset benefitted from the latest multi-band pulse sequences that allowed mapping the whole brain without losing temporal SNR, as well as from optimised sensory mapping stimuli which together may account for why it was possible to visualise more of these maps. The stimulus programs for retinotopic mapping and somatomotor mapping were provided by Martin Sereno. The stimulus program for tonotopic mapping was taken unchanged from previous study by Dick et al. (2012). Custom software for cortical surface based phase encoded analysis were provided by Martin Sereno and extended for the current study.

2.1 Introduction

Topological maps refer to a collection of axonal projections from one neural region to another such that the spatial representations and neighbour relations on the sending surface is preserved on the target surface. Much of the neocortex of each hemisphere in a primate brain consists of a mosaic of topological maps relating to visual, auditory, somatosensory, motor and limbic areas. This thesis focuses on visual, auditory and somatomotor maps on the cerebral cortex and the discussion in this chapter is restricted to these categories of maps.

Visual retinotopic maps are the paradigm case for topological neural maps. The spatial arrangement of the visual field is reflected in the retinal activation pattern which in turn is maintained in its projections to primary visual cortex (V1, in Brodmann area 17, see figure 2.1) via dorsal lateral geniculate nucleus (dLGN) and to the midbrain (tectum or superior colliculus). In both cases, the axonal mapping preserves both left-right and top-bottom ordering. This orderly arrangement (congruent with the retinal locations) of visual activation on the cortical surface, especially in the posterior occipital cortex is commonly termed as retinotopic maps.

Retinotopy was originally discovered more than a century ago when Inouye (1909) an ophthalmologist and then Holmes (1916, 1918), a neurologist observed strong correlations between visual field deficits and the location of battlefield lesions within V1. Their analysis of these observations defined the retinotopic maps in V1 and established several important characteristics of the V1 map. They noted that, V1 in each hemisphere encodes the opposite hemifield (one half of visual space) and that a larger fraction of the cortical surface is devoted to the central fovea (varying cortical magnification factor). Subsequent electrophysiological measurements in animals led to the discovery of multiple maps adjacent to V1, such as V2 and V3 (Thompson et al., 1950; Clare and Bishop, 1954; Cowey, 1964; Hubel and Wiesel, 1965; Tusa et al., 1978). The organization and perceptual significance of the human V1 map were confirmed by experiments showing that local electrical stimulation in the V1 map gives rise to a sensation of light (phosphene) at the corresponding visual field location. In early 1990's, with the introduction of fMRI (Ogawa and Lee, 1990; Ogawa et al., 1990) and novel data-analysis methods (Engel et al., 1994), it became possible to non-invasively investigate retinotopic maps in intact human visual cortex. The ensuing discoveries made it clear that visual topology is not restricted to posterior occipital cortex as envisaged traditionally, but that visual maps extend into parietal, lateral and ventral posterior cortex, as well as frontal and temporal cortex (for a review see Wandell et al., 2007). Unlike the maps in many earlier visual areas (posterior occipital cortex), however, the maps in parietal and frontal cortex only became evident when the subject was required to engage spatial attention (Saygin and Sereno, 2008).

The mapping of motor and somatosensory cortex also has a long illustrious history. It has been known for well more than a century, that motor cortex is organised in a gross topographical manner when Ferrier (1874) published the first report from the monkey brain establishing a systematic map of the body along the precentral gyrus with the legs at the top of the brain and the mouth near the bottom. Leyton and Sherrington (1917) provided the first detailed 'motor map' of the primate motor cortex and established precisely the true extent of the motor area. A similar topographic organisation of motor cortex was later found in human subjects by Penfield and colleagues (Penfield and Boldrey, 1937; Penfield and Rasmussen, 1950) who stimulated pre- and post- central sites during surgery for removal of tumours or

epileptic foci. They found that the majority of effective sites for motor activation were in the precentral gyrus and movements of the hand were most commonly elicited.

There is no clear consensus on exactly how many cortical motor areas exist (for reviews, see Rizzolatti et al., 1998; Graziano, 2006). The original cytoarchitectonic maps of the human cortex differentiated between precentral and intermediate precentral cortex (Brodmann's areas 4 and 6 respectively). The location of the primary motor cortex (area 4) is most obvious on histological examination due to the presence of the distinctive Betz (giant pyramidal) cells, especially in the representation of the lower limbs. Though the Betz cells do not compose the entire motor output of the cortex, they nonetheless provide a clear marker for the primary motor cortex. The primary motor cortex in humans (as well as in monkeys) is located on the anterior wall of the central sulcus. It extends anteriorly out of the sulcus partly onto the precentral gyrus and dorsally to the top of the hemisphere and partially onto the medial wall of the hemisphere. Anteriorly, the primary motor cortex is bordered by a set of areas that lie on the precentral gyrus and that are generally considered to compose the lateral premotor cortex (area 6). The functional distinction between "primary" motor cortex (area 4) and "premotor" cortex (lateral area 6) was proposed originally by Fulton (1935) based on lesion studies on monkeys. Although the exact boundaries between 'primary motor cortex' and 'premotor cortex' is contentious, it is now known that this region can be further fractionated and that the topological motor maps found here are distinct from those in primary motor cortex (Rizzolati et al., 1998). There is a further smaller, distinct set of maps found on the medial wall of area 6, known since mid 20th century as 'supplementary motor area' (Penfield and Welch, 1951, Woolsey et al. 1952). Although the majority of key insights in motor mapping have come from electrophysiological recordings on human and non-human primates, these findings have been largely replicated in functional neuroimaging studies in humans (Grafton et al., 1991; Chainay et al., 2004; Meier et al., 2008; Zeharia et al., 2012).

The research on motor cortex historically was done largely in parallel with that of somatosensory system and this resulted in the discovery of primary somatosensory cortex, located adjacent to primary motor cortex in the posterior bank of central sulcus and extending onto the postcentral gyrus, in the parietal lobe. The primary somatosensory cortex, or SI was originally defined by electrophysiological mapping procedures as a single somatotopic representation of the body surface (Penfield and Rasmussen, 1950; Woolsey, 1964). From the

initial mapping studies, Marshall and colleagues (Marshall et al., 1937) recognised that SI of monkeys included the four strip-like architectonic fields of Brodmann- areas 3a, 3b, 1 and 2, although significance of these architectonic fields were not known. Later a number of studies combining micro electrode mapping with the study of cortical histology demonstrated that each of the four architectonic fields of SI of monkeys contains a separate body representation (Merzenich and Kaas, 1980; Kaas, 1983) organised somatotopically with a ventral-dorsal face-foot mapping. Each of the SI subregions is functionally specialized in the processing of somatosensory information. Areas 3a and 2 receive proprioceptive information from receptors in the muscles and joints, whereas areas 3b and 1 are the major arrival points for information from touch receptors on the skin.

On the lateral side of the face representation in SI, there is a secondary somatosensory cortex SII. This set of maps was originally discovered in cats by Adrian (1940), later confirmed to be present in monkeys (Woolsey, 1943, 1944; Woolsey and Wang, 1945; Woolsey and Fairman, 1946) and in humans (Penfield and Rasmussen, 1950; Penfield and Jasper, 1954). Non-invasive neuroimaging studies further supported the existence of human SII and its location within the upper bank of the lateral sulcus (Hari et al., 1984; Seitz and Roland, 1992; Burton et al., 1993; Lin et al., 1996; Hodge et al., 1998; Maldjian et al., 1999; Polonara et al., 1999; Francis et al., 2000, Disbrow et al., 2000, Venkatesan et al., 2014). As with SI, SII was eventually divided into multiple, separate body representations.

Apart from the primary and secondary somatosensory cortices, the ventral intraparietal (VIP) cortex is a site of multi sensory maps (Sereno and Huang, 2014). VIP was originally defined in macaque monkeys as a visual area containing neurons with large receptive fields that also had aligned somatosensory receptive fields on the face and shoulders (Colby et al., 1993). A human homologue region was discovered in parietal cortex using functional magnetic resonance imaging (fMRI) that responds to somatosensory, visual and auditory stimuli (Bremmer et al., 2001). Further more, it was established using fMRI that this site contains a multi sensory topographic map in which visual space is superimposed and aligned with a somatosensory map (Sereno and Huang, 2006).

In the auditory system, the nerve fibres in the cochlear ganglion receive synapses from cochlear hair cells in the inner ear which are laid out along the length of the basilar membrane. Because the mechanical and electrical properties of the basilar membrane

gradually change along its length, hair cells are tuned to progressively higher frequencies when traversing the cochlea from its apex to its base. Thus, the inner ear acts as a sound frequency analyser, and the input to the auditory cortex is topologically ordered according to sound frequency. Currently, frequency is the only acoustic parameter that is unequivocally held to be topologically mapped, although other parameters like sound intensity (Bilecen et al., 2002; Pantev et al., 1989), tuning band-width (Moerel et al., 2012; Seifritz et al., 2006), and modulation rate (Langner et al., 1997; Barton et al., 2012; Herdener et al., 2013) have been suggested to form complementary maps. So far, the research in this field has been

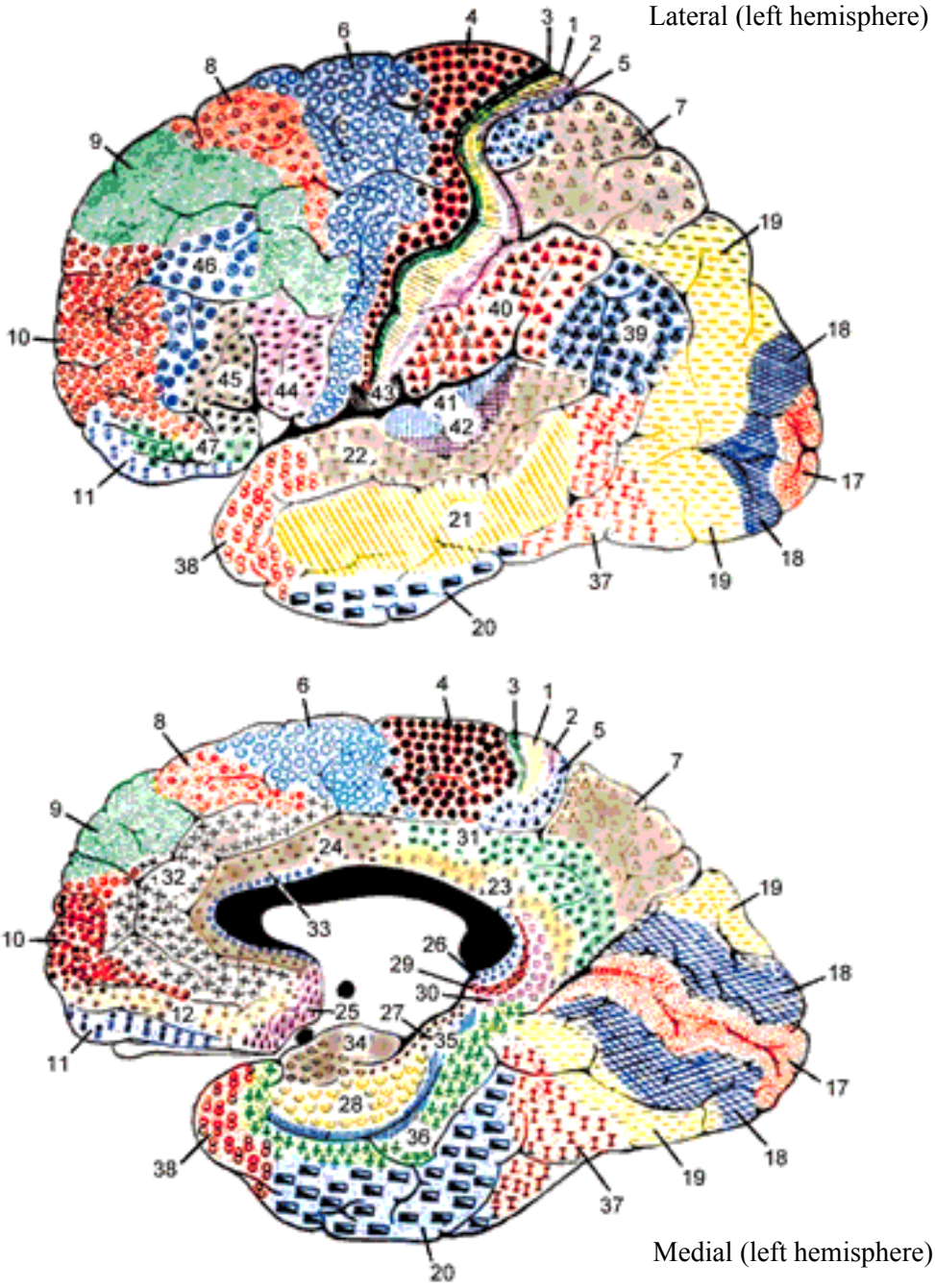

Figure 2.1: Brodmann (1909) areas (adapted from Internet)

mainly focussed on characterising the organisation of auditory cortex (Brodmann areas 41, 42) in the temporal lobe and the literature on tonotopy mainly focusses on tonotopy in auditory cortex. Based on a combined knowledge of electrophysiology, cortical architecture and connectivity, the auditory cortical organisation emerging in non-human primates consists of an elongated core comprised of up to three elongated, roughly collinear tonotopic fields (primary auditory field A1, followed by a rostral field R and an even more rostral temporal field RT) surrounded by several belt fields, which in turn are further surrounded by higher-order parabelt regions (Kaas and Hacket, 2000). Although there is far less consensus on human auditory cortex organisation, most studies agree on an elongated core region along the crest of HG that appears similar in shape to the elongated posterior-to-anterior auditory core in the monkey (Hackett et al., 2001; Talavage et al., 2004; Dick et al., 2012; Da Costa et al., 2013). The gradient of tonotopy is neither parallel nor perpendicular to the axis of Heschl's gyrus.

Retinotopic, tonotopic and somatomotor mapping was carried out on the same set of human subjects using fMRI phase-encoded cortical mapping techniques. The following sections of this chapter detail the methodology and results of the mapping study. These results are combined with the results in the experiments described in chapters 3 and 4 to provide a comprehensive assessment of where and by how much activation due to higher level cognition overlap with cortical sensory-motor maps.

2.2 Materials and Methods

2.2.1 Subjects

20 right-handed native English speakers (9 women) participated in these experiments. The mean age was 28 (ranging from 19 to 58). All participants were neurologically healthy with normal or corrected to normal vision and normal hearing capacity. The experimental protocols were approved by local ethics committees and participants gave their informed written consent prior to the scanning session. All 20 participants took part in the Retinotopic mapping experiment. 18 of the same participants took part in the Auditory mapping experiment and 17 of the same participants took part in Somatomotor mapping experiment.

2.2.2 Experimental Stimuli and Design

The mapping experiments differ from reading and scene experiments (typical high-level cognitive experiments) described in chapters 3 and 4 both in stimulus design and data analysis methods. Mapping experiments are based on the assumption that when a stimulus changes periodically along a particular dimension, the signal of neuronal populations selective for this stimulus dimension will also be periodically modulated. The stimulus design hence utilises a periodically varying dimension and the data analysis utilises a Fourier based phase-encoded analysis which can detect the different frequencies and phases present in the signal. For example in retinotopic mapping, a thin rotating wedge will traverse two different locations in the visual field at two different times, but at the same frequency; therefore there is a delay (phase difference) between the times when two different neurons that respond to two different locations in the visual field are stimulated. Applying a fast Fourier transform to the time series output of the MRI signal at each voxel will detect the different frequencies and phases in the signal, allowing us to differentiate the neurons that has responded to stimulation at different visual field locations (for a review, see Engel, 2012).

The concept of stimulus design and analysis is same for all three mapping experiments. However the the stimulus content and the dimension that is varied differs. So for tonotopic mapping, participants heard different frequency sounds, where the frequency is periodically modulated. In somatomotor mapping, participants were asked to move different body parts in a periodic manner.

Retinotopic Mapping: In the retinotopic mapping experiment, the polar angle of the visual field was mapped using a phase-encoded stimulus very similar to that used in previous recent work by Sereno et al. (2013). The stimulus (figure 2.2) consisted of a continuously rotating thin wedge (18 deg wide) populated with a random-coloured checkerboard with 35% luminance contrast (not gamma-corrected). The checkerboard was overlaid with white dot fields moving in 500 msec periods of coherent motion that extended slightly beyond the checkerboard wedge to 21.6 deg wide (each new flow period had randomly chosen contraction/dilation and clockwise/anti-clockwise components, dots had 50% average luminance contrast), as well as two simultaneous asynchronous streams of random objects (tiffs with a transparent background, 0.5 sec duration, 0.1 sec gap) and random black letters (0.4 sec duration, 0.1 sec gap); both were scaled with eccentricity to fit within the confines of

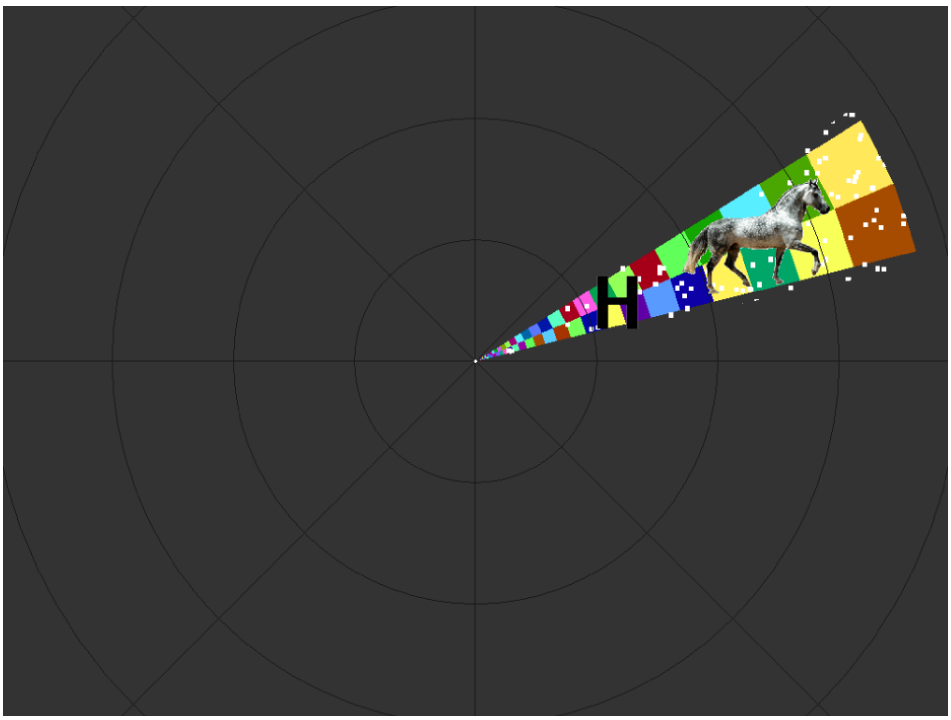

Figure 2.2: Retinotopic Mapping Stimulus

the 21.6 deg wide wedge, and were rotated together with the wedge. The objects had an additional random radial (inward or outward, rescaled) motion. This stimulus was designed to evoke activation in the maximum number of lower-level and higher-level visual areas. The participant was presented with the periodic stimulus (64 sec per full rotation cycle, 8 cycles/ run). 512 second runs (4 in total) alternated between clockwise and anti-clockwise rotation of wedges. Participants were required to fixate on the centre dot at all times. Additionally they were instructed to monitor for occasional numbers (among the letters) and occasional upside down objects (among the right-side-up objects) to maintain a high and continuous level of peripheral attention to the entire wedge during central fixation.

Auditory Mapping: In the auditory mapping experiment, the tonotopically organized cortical areas were mapped using a frequency-modulated stimulus taken unchanged from the previous study by Dick et al. (2012). The stimulus consisted of bandpass-filtered nonlinguistic vocalizations adapted from the Montreal Affective Voices (Belin et al., 2008), a series of recordings by actors (only male voices were utilized in the stimulus) producing sounds associated with a set of eight emotions. Each run consisted of eight 64 sec band-pass-filtered cycles, where the centre filter frequency repeatedly logarithmically ascended from 150 to 9600 Hz, or repeatedly descended from 9600 to 150 Hz (no gap at the wrap-around point). The session consisted of 4 runs alternating between ascending and descending

frequency sweeps. During scanning, subjects were asked to monitor the stimuli and press a button whenever they heard laughter (laughter targets were distributed non-periodically through the stimulus train). The band pass filter made this task challenging.

Somatomotor Mapping: In order to reveal sensory and motor maps in primary and secondary somatosensory and motor cortical areas, participants were asked to move different body parts in response to periodic auditory cues (spoken name of the body part to be moved, rendered using Mac OS X text-to-speech with "Alex" voice). Each run consisted of 8 cycles of 64 sec, and in each cycle participants successively moved 11 different body parts progressing from tongue to toe. Runs (4 in total) alternated between movement cycles in each direction (from tongue to toe and toe to tongue). The stimuli were presented by an in-house C/OpenGL program and the conceptual design is similar to that described in Zeharia et al. (2012). The participants were allowed to familiarise themselves with the auditory cues and practice the controlled movements prior to the scan.

Auditory instructions:

say tchuh-tchuh; say pup-pup; crinkle eyebrows; touch thumb index; wave wrist; contract biceps; pull in stomach; squeeze buttocks; contract quads; wave ankle; rub big toe

2.2.3 Experimental Set-Up

For retinotopic mapping experiment, the stimuli were projected into the bore using an Eiki LC-XG300 XGA video projector onto a translucent direct-view screen at the participant's upper chest level. All polar angles of the visual field were stimulated out to an eccentricity of at least 54 degrees of visual angle (much larger than the usual 8-12 degrees of all-polar-angles eccentricity achieved when a standard screen is viewed via a mirror). This avoids artifactual periodic modulation of voxels representing visual field locations beyond the outer edge of the stimulus due to surround inhibition. A black matte shroud situated just outside the bore blocked the beam from making low-angle reflections off the top of the bore. The rear of the head coil was elevated with a wooden wedge and thinner bed cushions were used to help naturally tilt the head forward. For auditory and somatomotor mapping, the stimuli were delivered binaurally using in-house safety-enhanced Sensimetrics (Malden) S14 earbuds and cushions. During all scanning sessions, memory foam cushions (NoMoCo Inc.) were placed around the head to provide additional passive scanner acoustical noise attenuation and to

stabilise head position. Responses were made via an optical-to-USB response box (LUMItouch, Photon Control, Burnaby, Canada) situated under their right hand.

2.2.4 Imaging Parameters

Functional images were acquired on a 1.5 T whole-body TIM Avanto System (Siemens Healthcare), at the Birkbeck /University College London Centre for NeuroImaging (BUCNI), with RF body transmit and a 32-channel receive head coil. For the first 3 subjects, images were acquired using the standard product EPI pulse sequence (24 slices, 3.2x3.2x3.8mm, 64x64, flip=90°, TE=39ms, TR=2sec) (Mansfield, 1977), while the remaining sessions used multiband EPI (40 slices, 3.2x3.2x3.2mm, flip=75°, TE=54.8ms, TR=1sec, accel=4) (Moeller et al., 2011). Individual scans had 260 volumes for standard EPI and 520 volumes for multiband EPI. To allow longitudinal relaxation to reach equilibrium, 4/8 initial volumes were discarded from each run for standard/multiband EPI. For each imaging session, a short (3 min) T1-weighted 3D MPRAGE (88 partitions, voxel resolution 1x1x2mm, flip angle=7°, TE=4ms, TI=1000ms, TR=1370ms, mSENSE acceleration=2x, slab-selective excitation) was acquired with the same orientation and slice block center as the functional data ('alignment scan'), for initial alignment with the high-resolution scans used to reconstruct the subject's cortical surface. Two high resolution T1-weighted MPRAGE (176 partitions, 1x1x1mm, flip angle=7^{o}, TI=1000ms, TE=3.57ms, TR=8.4ms) were acquired along with the fMRI sessions for cortical surface reconstruction (using FreeSurfer 5).

2.3 Data Analysis

2.3.1 Anatomical image processing

For each subject, the cortical surface was reconstructed with FreeSurfer (version 5; Dale et al., 1999) from the aligned average of the two high-resolution T1-weighted MPRAGE scans. Both mapping experiments and the high-level cognitive experiments (chapters 3, 4) employ a cross-subject surface-based analysis stream that begins by sampling responses and statistics to individual reconstructed cortices (cross-subject 3D averaging was not used at any point in the cortical pipeline).

2.3.2 Analysis of phase-encoded mapping data

The first level single subject data from each run was motion corrected and registered to the last functional scan (across all runs) using AFNI's 3dvolreg (Cox, 2012) function (using heptic interpolation). The functional images were registered with the cortical surface using a multi-stage registration pipeline. This involved first registering the 'alignment' scan to the high resolution MPRAGE, and then transferring that registration to the functional EPI images. These steps were done using FSL's FLIRT tool (version 5; Jenkinson and Smith, 2001; Jenkinson et al., 2002) and were then fine tuned using FreeSurfer's bbregister (Greve and Fischl, 2010). The final combined and fine-tuned 4x4 registration matrix aligns functional EPI to high-resolution MPRAGE (the matrix actually transforms 3D surface coordinates to 3D EPI block coordinates). The final registrations (EPI -> hi-res MPRAGE) were manually checked to ensure accuracy. The time courses from all the runs were averaged (after time-reversing the runs in the clockwise rotation for retinotopy, the upward frequency sweep for auditory, and the toe-to-tongue movement direction for the somatomotor map). The time reversed scans were time-shifted to compensate for hemodynamic delay before averaging. The averaged time courses were analyzed using Fourier methods (Bandettini et al., 1993; Engel et al., 1994, 1997; Sereno et al., 1995). Voxels preferentially responding to a particular point in the stimulus cycle will show higher amplitude at the stimulus frequency than at any other 'noise' frequency, after excluding (i.e., equivalent to linearly regressing out) the 3 lowest temporal frequencies as motion artifact. For retinotopic data, the phase of this vector at the stimulus frequency indicates the polar angle of the stimulus location. For auditory data, the phase indicates a particular point on the stimulus frequency ramp. For somatomotor data, this corresponds to the location of the moving body part. The individual and group analysis methods utilized a cortical surface based stream that were previously described (Sereno et al., 1995; Hagler et al., 2007; Huang et al., 2012) and briefly summarized below.

The single subject analysis utilized the procedure described in Huang et al. (2012) where a fast Fourier transform was performed on the average time courses of each voxel. An F-statistic value was obtained for each voxel by comparing the power at the stimulus frequency (eight cycles per scan) to the average power at the remaining frequencies. For individual subject's activation illustrated below, the F-statistic was thresholded at

$p<0.001$(corresponding to $F(2,232)=7.12$ for subject 1 who was scanned on standard EPI with 256 time points and $F(2,488)=7$ for subject 2 and subject 3 who were scanned on multiband EPI with 512 time points). Surface-based cluster size exclusion (Hagler et al., 2007) was used to correct for multiple comparisons with cortex surface clusters smaller than 30 mm^2 excluded, achieving a corrected p-value of 0.01 (csurf programs: randsurfclust, for estimating required minimum cluster size, and surfclust, for cluster exclusion).

Group analysis of phase-encoded mapping data was performed using the methodology developed by Hagler et al. (2006) in which the real and imaginary components of the signal at the stimulus frequency were averaged across the subjects, preserving any phase information consistent across subjects. This was performed by projecting each participant's phase-encoded map to the FreeSurfer spherical atlas (FreeSurfer mri_surf2surf), performing ten steps of complex-valued surface-based smoothing (~3mm FWHM in 2D) and averaging across subjects at each vertex in the common surface coordinate system. Second-level surface-based cluster size exclusion was used to correct for multiple comparisons, with vertex level F-statistics thresholded at $p<0.01$/$p<0.05$ and cortical surface clusters smaller than 40 mm^2/92mm^2 excluded, achieving a corrected p-value of 0.05 and then sampling back onto the average subject (fsaverage) surface for viewing. The fsaverage "inflated_avg" surface (made by averaging inflated surfaces) was used instead of the fsaverage "inflated" surface (made by averaging folded surfaces and then inflating the average) because it represents original average surface area better. This is because folding variations (sulcal crinkles) are removed before surface-averaging, making inflated_avg, more appropriate for displaying surface-averaged data (mesh defects in the north and south icosahedral poles of FreeSurfer5's inflated_avg were corrected before using it for display. Corrected and flattened inflated_avg surfaces are available here: http://www.cogsci.ucsd.edu/~sereno/.tmp/dist/csurf/fsaverage-adds.tgz).

2.4 Results

The figures 2.3-2.10 illustrates the cross-subject average results. The sensory-motor maps are illustrated for two separate vertex thresholds; $p<0.05$ (lower threshold) and $p<0.01$ (higher threshold), corrected for multiple comparisons using cluster thresholding at $p<0.05$.

Among the 17 subjects who took part in somatomotor experiment, data from 2 subjects were excluded owing to high stimulus correlated head motion during the task. No exclusions were made for retinotopic and tonotopic experiments.

2.4.1 Retinotopic maps

The retinotopic maps (amplitude in Fig 2.9A, phase in Fig. 2.3 and Fig 2.4) branch out anteriorly from the occipital pole into several 'streams' (numbered 1-5 in black in Fig. 2.3). In all phase maps, lower visual field is green, horizontal meridian is blue, and upper visual field is red (all contralateral). One stream extends through area MT into the superior temporal sulcus and reaches the posterior lateral sulcus (leaving a few disconnected regions in between, which join up as threshold is slightly lowered). A second stream stretches along the intraparietal sulcus and arrives at the superior part of the postcentral sulcus. A third stream spreads across the parieto-occipital sulcus (POS) into the medial posterior parietal cortex and precuneus, ending at the cingulate sulcus visual area (Huang and Sereno, 2013). A fourth stream runs across the POS into retrosplenial cortex at the isthmus of the cingulate gyrus (iCG) and continues to the edge of cortex just under the splenium of the corpus callosum. Finally, a fifth stream follows the collateral sulcus and fusiform gyrus into the ventral occipitotemporal lobe. A further disconnected set of retinotopic maps, including the frontal eye fields (FEF), frontal poly-sensory zone (Huang et al., 2012), and dorsolateral prefrontal cortex (DLPFC) are found in the frontal cortex. These maps are similar to those reported previously in Huang and Sereno (2013) using the same stimulus. The cingulate visual map found adjacent to SMA (Cv, in figure 2.3) probably corresponds to human dorsomedial frontal eye-fields.

The mapped regions in both lower and higher level visual areas unanimously preferred contralateral visual stimulation. The retinotopic activation pattern in individual subjects closely follows the average pattern. It should be noted that the apparent lack of retinotopy in the result figures around the fovea is an artifact expected with central fixation (no periodic signal change since the subject is fixating at all times); these regions are also known to be retinotopic (e.g., Schira et al., 2009).

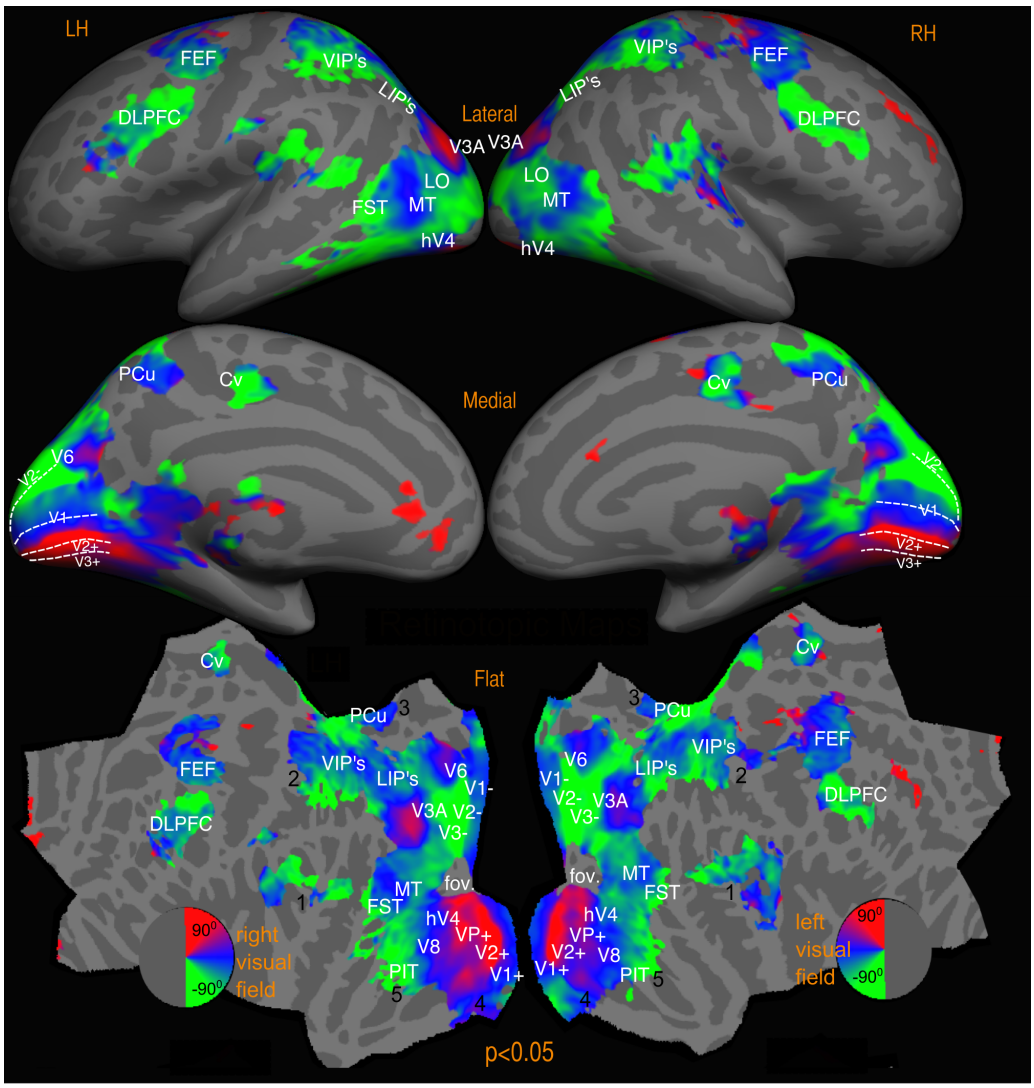

Figure 2.3: Group retinotopy (lower threshold).

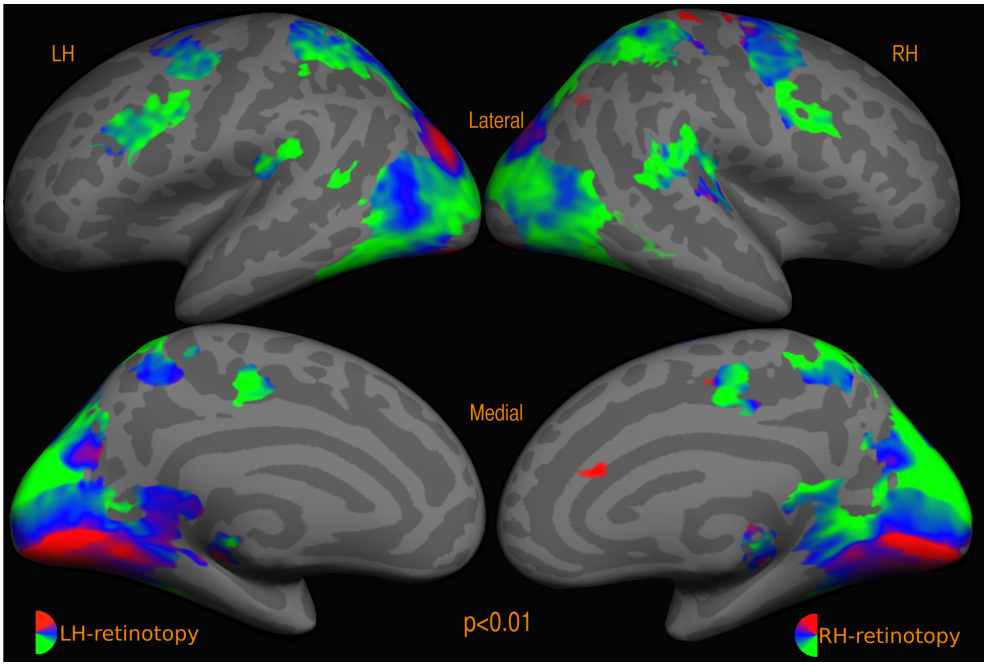

Figure 2.4: Group retinotopy (higher threshold)

2.4.2 Tonotopic maps

Tonotopy is observed in several regions on the cortex (amplitude in Fig 2.9B, phase in Fig. 2.5 and Fig 2.6). In all phase maps, lower frequencies are green, middle frequencies blue, and high frequencies red. The tonotopic maps in and around primary auditory cortex in the lateral fissure are well known and followed characteristic features previously reported in the literature (e.g., Talavage et al., 2000; 2004; Formisano et al., 2003). In both the group maps and the individual subject maps, there is a high-to-low-to-high frequency progression across Heschl's gyrus (HG), moving diagonally (medially and anteriorly) across the temporal plane. This region is flanked by higher frequency representation anteromedially towards the planum polare (PP) and posteromedially towards the planum temporale (PT). Posterior to HG on the lateral PT on the superior temporal gyrus, an additional low frequency focus, and two small high frequency foci are also observed. A few subjects also exhibited tonotopic responses extending inferiorly beyond the fundus of the superior temporal gyrus onto the middle temporal gyrus.

Tonotopic maps were also found in several frontal regions. In the cross subject average those regions are most significant in inferior frontal cortex, occupying a region on the precentral gyrus that extends posteriorly into the central sulcus and anteriorly into the precentral sulcus, reaching the inferior/anterior end of the precentral sulcus. While tonotopy in human frontal lobe has received scant attention so far, our results suggest that consistent frontal tonotopy is observed with only a moderate degree of variation across subjects.

Finally, a distinct tonotopic region was found in both hemispheres in the anterior cingulate region (ACa in Fig. 2.5). The anterior cingulate tonotopic region is immediately anterior to the cingulate visual map (Cv) described above, and does not overlap it.

2.4.3 Somatomotor maps

Figures 2.7 and 2.8 illustrate the group level somatomotor maps on the inflated surface (also see amplitude, Fig. 2.9C). The somatomotor mapping revealed a highly significant ventral-to-dorsal face-to-leg somatotopic representation in M-I proper and premotor cortex, as well as in a number of post-central areas including primary somatosensory cortex (including areas 3a, 3b, 1, and 2), parts of area 5, two small maps in the upper bank of the lateral sulcus (S-II and related areas), and most of VIP+, where a characteristically medially

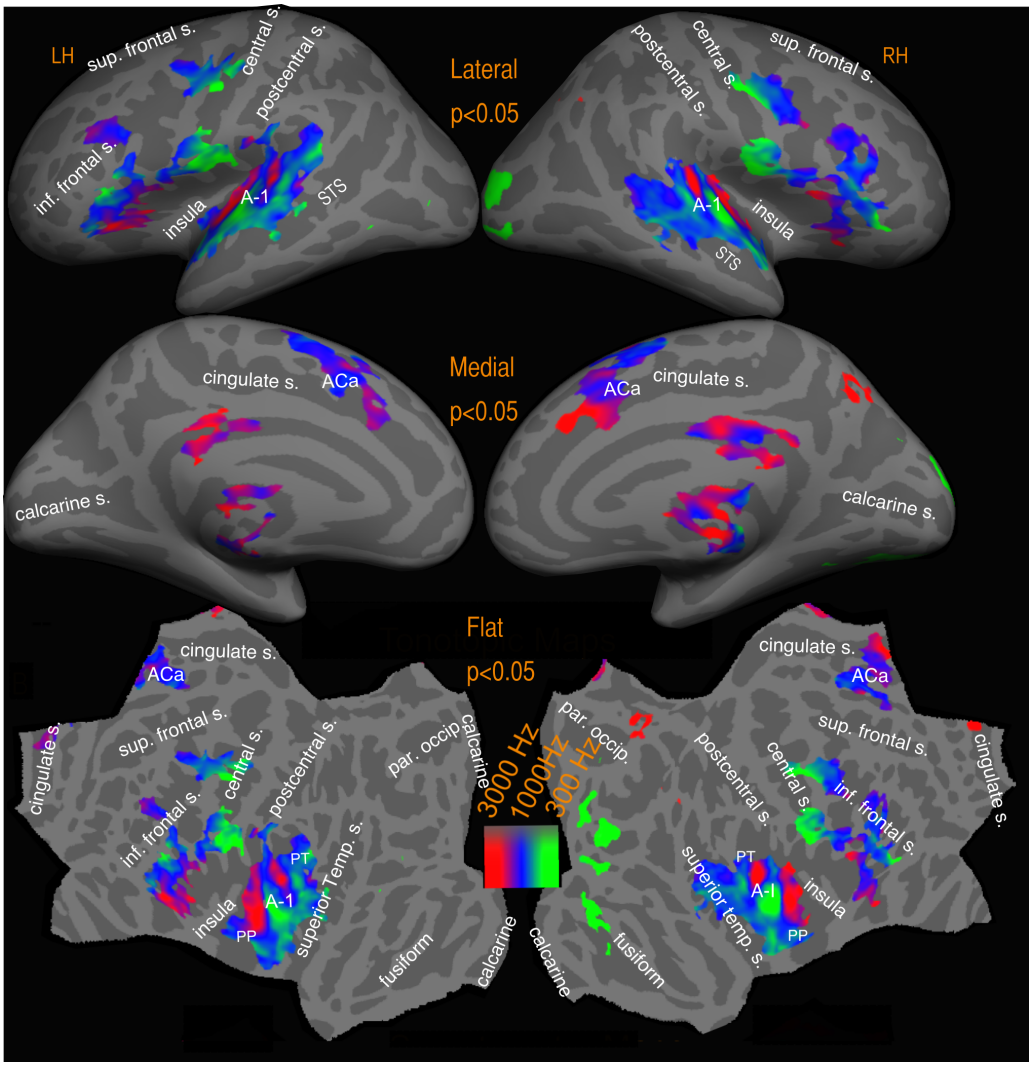

Figure 2.5: Group tonotopy (lower threshold)

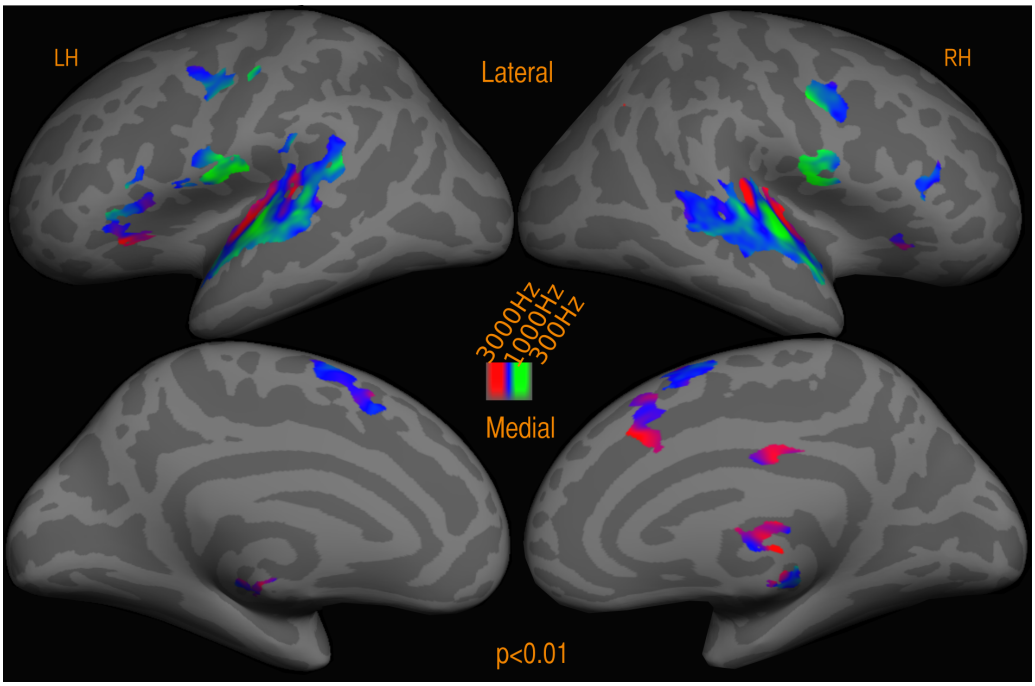

Figure 2.6: Group tonotopy (higher threshold)

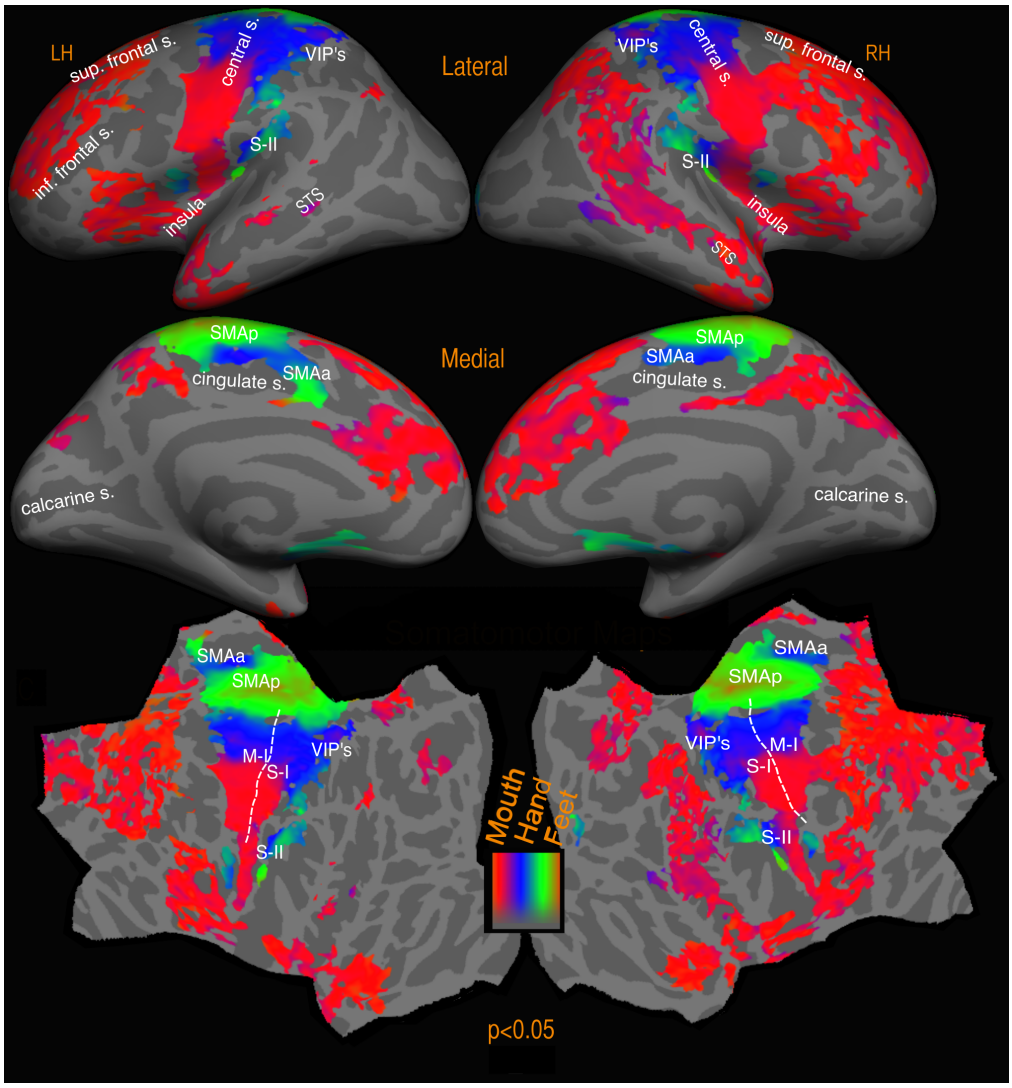

Figure 2.7: Group somatomotor (lower threshold)

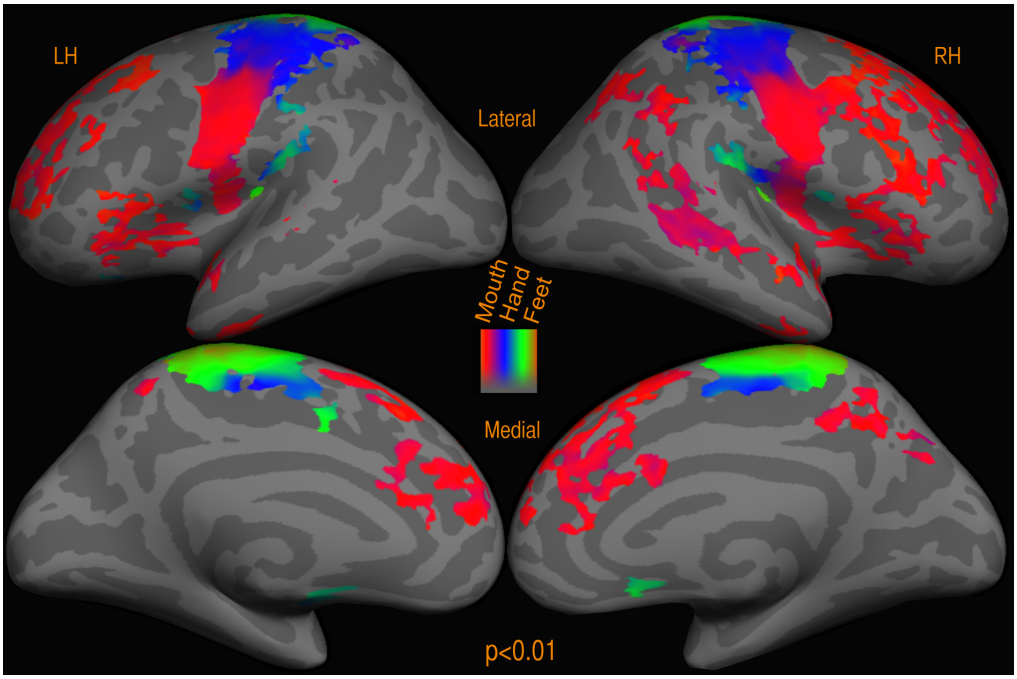

Figure 2.8: Group somatomotor (higher threshold)

displaced face representation is identified in the postcentral sulcus (red), as well as a more medial lower-visual-field-overlapping lower body representation areas recently revealed in Huang et al.'s (2012) mapping study that used an air puff body suit. Finally, the somatomotor activation involved two additional smaller body representations (leg-to-face and face-to-leg) on the medial surface moving posterior to anterior in supplementary motor area (SMA) at both group and individual level. Though neither of these appears to reach all the way to the face (red) in the average, the reason for this is that inter-subject variation in the exact location of these small maps resulted in flattening the phase range in the average; a full face representation was visible in a number of other individual subjects (data not shown). During mapping of the face, participants softly mouthed syllables, which they were nevertheless able to hear, and which are similar to speech sounds, which possibly explains some face-correlated activation observed in temporal auditory areas. In order to assess the possible

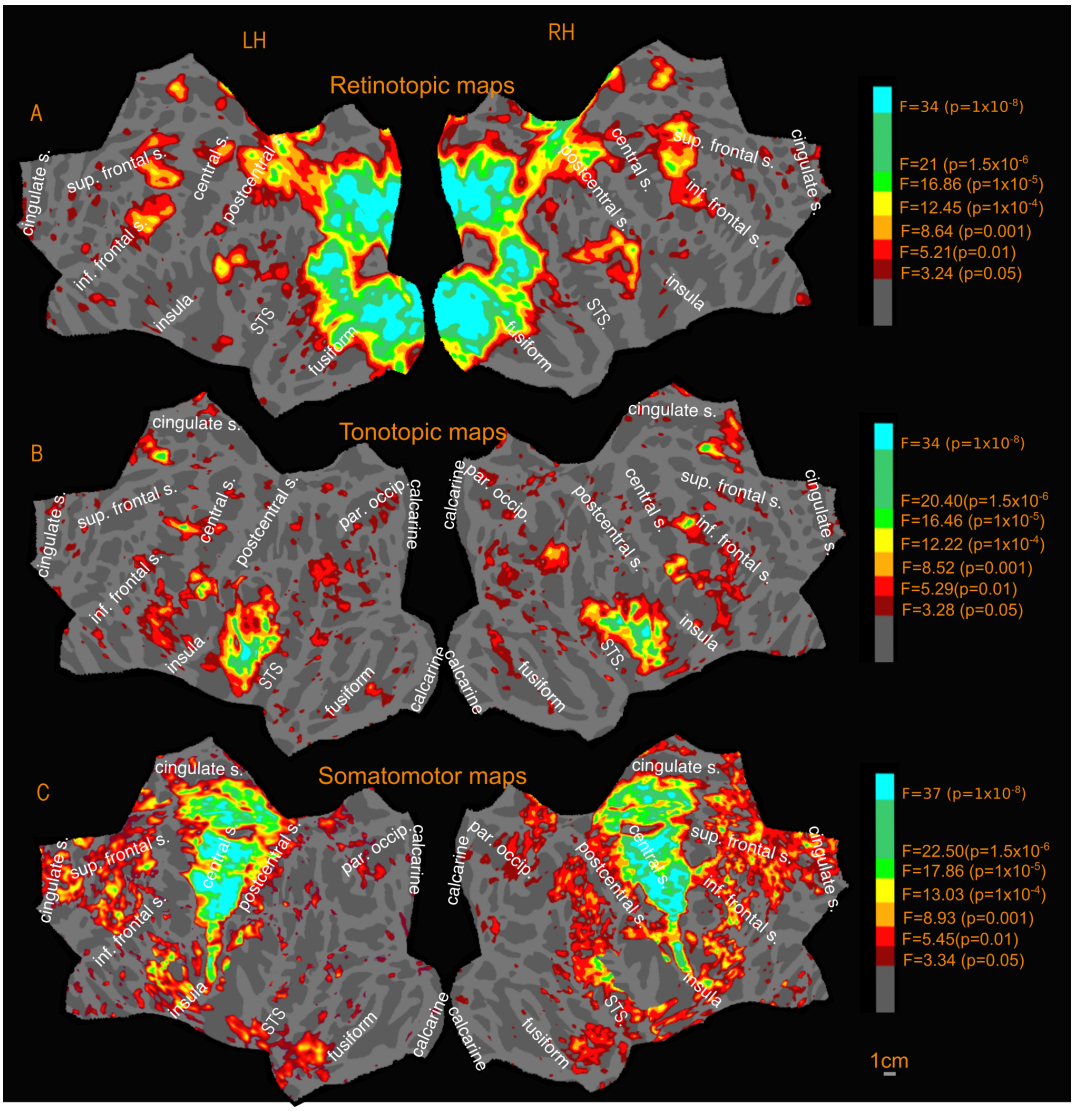

Figure 2.9: Activation amplitude profile (uncorrected) of Sensory-motor maps

auditory contribution, I analyzed the activation due to the auditory cue itself, (by doing a Fourier analysis at the higher frequency at which auditory cue occurred, 88 cycles/scan and thresholded at $p<0.05$), and masked out the activated regions. These masked regions mainly involved the auditory cortex and small regions in the insula, frontal cortex and medial anterior cingulate.

There was also a moderate apparently face-correlated activation in anterior frontal areas and the anterior temporal lobe. This was likely caused by B0 deformations due to changing the distribution of air in the oral cavity during active mouth movements (these brain regions are closest to the oral cavity). There was no map-like structure (phase spread or reversals) in the apparent activity in these regions, nor any overlap with reading activation. By contrast, the region on the anterior bank of the central sulcus near the border between the face and hand representations of M-I -- which is substantially further away from the oral cavity -- was a topologically organised poly-sensory zone activated also by passive visual and auditory stimulation, as can be seen in Fig. 2.10.

2.4.4 Overlap between retinotopic, tonotopic and somatomotor maps

There were multi sensory maps in several locations including lateral prefrontal and in the extreme superior, posterior part of the lateral sulcus near the supra marginal gyrus as well as in VIP. Note that the term 'multisensory' is defined in the restricted sense of voxels that contain topological maps in more than one modality (not voxels that merely respond to more than one modality). In the posterior, superior lateral sulcus zone, the visual maps overlap separately with the tonotopic maps and the SII maps. The ventral intraparietal region is a multisensory region, where visual and somatosensory maps overlap, in agreement with recent findings of superimposed visual and somatosensory maps in the region (Huang et al., 2012). In the frontal cortex, there are several overlapping zones. Near to the inferior frontal gyrus, retinotopic and tonotopic maps overlap, with retinotopic maps lying dorsal to the tonotopic maps in the region. There is a region on the anterior bank of the central sulcus near the border between the face and hand representations of M-I where all three maps overlap. This region had been identified by Huang et al. (2012) to be the human homolog of the 'polysensory zone', PZ, in monkeys (Graziano and Cooke, 2006) that responds to both air puffs on the face and to looming visual stimuli. The results presented here suggest that in addition to

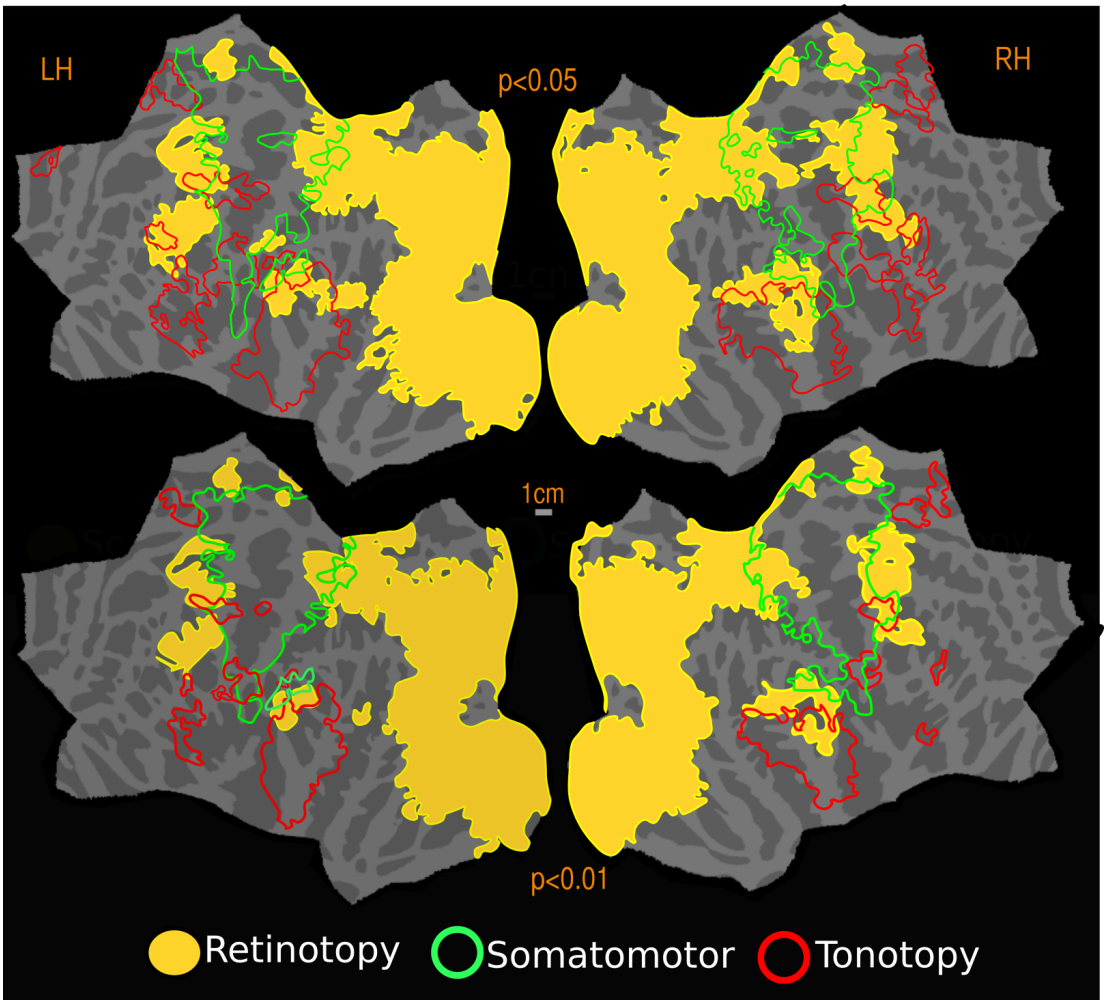

Figure 2.10: Group All maps. Reported p values are vertex thresholds used before cluster thresholding. All activations are cluster thresholded to p<0.05.

retinotopic and somatomotor maps, there are also overlapping tonotopic maps in the region. In fact, this is the only region in the cortex where all three modality maps overlap.

2.5 Discussion

The results presented here provide a comprehensive view of the topological sensory-motor maps in three major modalities- visual, auditory and somatomotor across the whole brain in the same set of subjects.

The data confirms the previous findings of retinotopic maps in posterior occipital, frontal, parietal and temporal cortex, the tonotopic maps in lateral sulcus/superior temporal cortex and the somatomotor maps in the somatomotor cortex. Additionally, the mapping experiments uncovered several sensory maps previously unreported in the literature.

In non-human primates, it has long been known that the anterior cingulate supplementary motor areas are directly adjoined by the dorsomedial frontal eye fields in primates (Schiller and Chou, 1998; Purcell et al., 2012). So far, there have not been any reports on topological maps in a similar region in humans. This data may provide the first observation of the topological organization of the human equivalent of the dorsomedial frontal eye fields (Cv in Figure 2.3), which posses a retinotopic map of the contralateral visual field. Their location is more inferior than in non-human primates, in line with similar superior-toward-medial-wall movements of parietal retinotopic areas in humans that are comparable to LIP. While retinotopy in this region is reported here for the first time, there have been a number of previous reports of activation in this region associated with visuo-spatial attention and eye movements (Mesulam et al., 2001; Pierrot-Deseilligny et al., 2004; McDowell et al., 2008; Jamadar et al., 2013; O'Reilly et al., 2013). The results presented in chapters 3 and 4 also suggest that the activation seen here during high level cognitive tasks is more relevant for eye movements or/and spatial attention.

Adjacent to the dorsomedial retinotopic map, a tonotopic map, previously unreported in the literature and hereafter referred to as the dorsomedial frontal 'ear' fields (ACa in Figure 2.5) is found. The anterior cingulate retinotopic map and the tonotopic map are separated by SMA map and do not overlap each other or SMA. The data presented in Chapter 3, shows that there is strong reading activation aligned with the tonotopic map in this region and unlike the reading activation in the anterior cingulate retinotopic region, this activation is stronger when subjects are engaged in comprehending the reading passages, and is only present in the left hemisphere.

Several previously unreported tonotopic maps were found in the frontal cortex. All frontal tonotopic maps partially overlap with retinotopic maps in this region as well. In the polysensory zone, it was found that there is an overlapping tonotopic map in addition to previously reported visual and motor maps. In the superior posterior lateral sulcus region, there is significant presence of all three maps, and visual maps overlap separately with somatomotor maps and tonotopic maps. The data also confirms the previous findings that the region surrounding VIP is both visual and somatosensory.

~~~
~~~

Chapter 3

Cortical reading comprehension regions and topological sensory-motor maps

*This chapter is derived in part from: “Areas activated during naturalistic reading comprehension overlap topological visual, auditory, and somatomotor maps”. Sood, MR and Sereno MI (in press, Human Brain Mapping).

Precis

This chapter builds on the results from the previous chapter. The same set of subjects participated in a naturalistic reading comprehension task, and the data was combined with those from the topological mapping experiments to provide a qualitative and quantitative assessment of the cortical overlap between topological sensory-motor maps in all major modalities and regions involved in reading comprehension. The results suggest that cortical activation during naturalistic reading comprehension overlaps more extensively with topological sensory-motor maps than has been heretofore appreciated. Reading activation in regions adjacent to the occipital lobe and inferior parietal lobes completely overlaps visual maps, whereas most of frontal activation for reading in dorsolateral and ventral prefrontal cortex overlaps both visual and auditory maps. Even classical language regions in superior temporal cortex are partially overlapped by topological visual and auditory maps. By contrast, the main overlap with somatomotor maps is restricted to dorsolateral frontal cortex. The data analysis uses a general linear model (GLM) based mass univariate analysis, with group analysis carried out on the average cortical surface. The overlap analysis described in this chapter and next, was done using custom code added to MGH freesurfer.

3.1 Introduction

The investigations on the neural basis of language processing started in earnest more than a century back with the seminal work of Broca and Wernicke on aphasic patients suffering from neurological disorders affecting language. The aphasias were the first demonstrations that selective damage to the brain could affect one class of learned behaviour while sparing other classes, and thus gave origin to the modern field of study of brain-behaviour relationships. Because language is a uniquely human faculty, aphasia research was central to our understanding of language and the brain until the advent of neuroimaging in 1990's. Insights from neuroimaging research has given rise to a set of alternate proposals on how language processing takes place in the brain. In this section, I will briefly summarise the history of language research in relation to the brain and the current state of the field.

Some cases of aphasia had been described before the mid-1800's, but it was Paul Broca who in 1861 initiated the modern study of the relationships of language functions to the brain. Based on his observations on two aphasic patients with similar linguistic disabilities, Broca characterised a type of aphasia now called Broca's aphasia, where the patient's comprehension abilities were relatively spared while the patient had severe trouble in articulating speech as well as in writing. On superficial examination of his patient's brains on autopsy, Broca defined the posterior third of the inferior frontal gyrus as the site of critical lesion (Broca, 1861; Broca 1865; Berker et al., 1986).

Following on from Broca's work, Carl Wernicke (Wernicke, 1874) established that there was characteristic differences between the aphasias produced by the damage in the left temporal lobe, in what is now called Wernicke's area, and those produced by lesions in the frontal lobe in Broca's area. In Wernicke's aphasia the speech output can be rapid and effortless but it is remarkably empty and conveys little or no information. The Wernicke's aphasic may, in writing, produce well-formed letters, but the output exhibits the same linguistic defects which are observed in the patient's speech. Wernicke went on to propose a comprehensive model of language processing within the brain. Wernicke postulated that language processing is carried out by two connected centres in the brain- an area lying near the auditory cortex, now called Wernicke's area, responsible for storing the auditory representations of words and Broca's area in frontal cortex, responsible for motor representations necessary to produce speech sounds. In addition, Wernicke predicted a third type of aphasia, resulting from the disruption of the flow of information between the two language centres, where the patient would have speech output similar to that in Wernicke's aphasia, but have normal comprehension of auditory input. These predictions were later supported and that type of aphasia was called 'conduction aphasia'.

A decade after Wernicke's publication, Lichtheim (1885) reported two patients- one who could not comprehend and the other who was non-fluent, both with preserved repetition. Because Wernicke's language processing model could not account for these, Lichtheim introduced to Wernicke's model an additional module that stores the concepts or meaning of words, later called the 'semantic field'. This functional module, connected to both Broca's and Wernicke's areas was postulated to be anatomically distributed in the brain. Based on his model, Lichtheim argued that in his patients, either the connection between Wernicke's area

and the semantic field was disrupted leading to normal repetition but lack of comprehension or the connection between semantic field and Broca's area was disrupted leading to normal repetition, but non-fluent speech. However Lichtheim's model could not adequately account for certain other findings in aphasia- for example, the abnormal speech output seen in Wernicke's aphasia (Nadeau et al., 2000).

Although Broca's and Wernicke's concept of localised language processing centres dominated the late 19th and early 20th century, not all contemporaries agreed with this model. Notable among them was John Hughlings Jackson, a contemporary of Broca, who rejected the view that specific brain centres are specialised for certain behaviours, and argued that language and other behaviours are organised hierarchically and in a more distributed way in the brain (Head, 1915). Jackson observed that his aphasic patients who have lost the ability to say certain words, could still say these same words under different circumstances, such as in an emotional situation. Based on his observations, Jackson argued that there may be various centres for different modes of behaviour. Jackson influenced views of many leading neurologists in mid 20th century and the prominent view was that language processing is far more distributed than originally envisaged. In 1960's however, Geshwind revived the 19th century models of Wernicke and extended them to explain in a more differentiated way why particular aspects of language function may break down while others are preserved (Geshwind, 1970).

With the advent of neuroimaging in 1990's, it became possible to examine the neural basis of language processing in normal healthy volunteers. Although lesion-deficit aphasia research provided us with many insights, it must be noted that the human brain's vascular anatomy causes a selection bias in the types of patients seen after a stroke. Lesions to Broca's and Wernicke's area are overrepresented, as left middle cerebral artery which serves the classical language regions is the one most often occluded in a survivable stroke. More recent research suggests that "Broca's" and "Wernicke's" areas are far more spread out than was originally envisaged. In fact, a surgical lesion confined to the originally defined Broca's area in an awake patient doesn't result in Broca's aphasia! (Mohr, 1976). Lesions in surrounding frontal cortex, underlying white matter, basal ganglia, insula, and parts of anterior superior temporal gyrus are all reported to result in Broca's aphasia (Mohr et al., 1978; Basso et al., 1985; Alexander et al., 1990). When the preserved brains of Broca's patients were examined

using high-resolution MRI, they turned out to have lesions far beyond the surface lesions observed by Broca (Dronkers et al., 2007). Similarly, there is no universal agreement on the cortical areas that constitute Wernicke's region. Lesions in superior temporal cortex, supramarginal gyrus, angular gyrus and insula have all been implicated with Wernicke's aphasia (Bogen & Bogen, 1976). Among other kinds of aphasia, a particularly interesting one is transcortical sensory aphasia ('across from the language cortex' aphasia), where the patient exhibits poor Wernicke-like comprehension, yet is still able to repeat words. The brain lesion in these cases is most often in inferior temporal cortex or parietal cortex or both, and commonly involves visual areas in the lateral aspect of the adjoining occipital lobe and in the white matter underneath (Mayeux, & Kandel, 1991; Rubens and Kertesz, 1983).

The last two decades of neuroimaging research has confirmed the significance of fronto-temporal regions for language, but has also provided ample evidence for the distributed nature of language processing, with activated regions extending well beyond the classical language regions in the left hemisphere. A line of enquiry that has gained considerable experimental support in recent times is that sensory-motor regions play a more significant role in language processing than was originally appreciated. This is a contentious area, and different researchers have staked out a spectrum of positions. Do sensorimotor areas have a mere concomitant role (Mahon, & Caramazza, 2008) or is comprehension actually rooted in sensory-motor networks (Pulvermüller, & Fadiga, 2010; Gallese, & Lakoff, 2005), or do they work in tandem with amodal regions (Binder, & Desai, 2011)? Among those supporting a prominent role for sensory-motor networks, opinion is divided on which modality (if any) plays the most important major role. Arguments have focused on 'action' (Pulvermüller, & Fadiga, 2010) as well as 'vision' (Sereno, 2014).

In the study presented here, I used fMRI to directly assess the extent of overlap between cortical regions involved in naturalistic reading comprehension and those that have a topological sensory or motor map. It has generally been assumed that the activation observed in temporal and frontal areas during reading falls beyond the bounds of sensory-motor maps, but this assumption has not been explicitly tested across all modalities in the same group of subjects. Recent advances in cortical surface-based mapping techniques have had less exposure in the language literature; for example, 'sensorimotor' regions are often defined only by anatomical features, or by basic, non-attention demanding tasks. In this study, I look

at the full extent of topologically mapped sensory-motor regions that can be reliably detected using retinotopic, tonotopic and somatomotor mapping and assess where and by how much they intersect with brain regions involved in reading comprehension in the same subjects. To this end, each subject in the study participated in a separate fMRI session consisting of naturalistic reading comprehension task in addition to the mapping experiments - retinotopic mapping, tonotopic mapping, and somatomotor mapping described in previous chapter. On the methodological front, a fully surface-based group analysis is employed as opposed to volume-based group analyses commonly used in language studies (merely displaying a 3-D averaged result on an average surface gains none of the benefits of surface-based averaging). The cerebral cortex has the topology of a 2-D sheet. Many relevant dimensions (e.g., retinotopy, somatotopy, tonotopy) vary much more rapidly tangential to the cortical surface than they do perpendicular to the cortical surface, through the several millimeters of cortical thickness. Distances measured in 3-D space between two points -- but also used in standard pre-fitting 3-D smoothing -- can substantially underestimate the true distance along the cortical sheet due to its folded nature (Fischl et al., 1999a,b). This artifactual within-subject blurring is then made worse by 3-D averaging of between-subject variability in the secondary crinkling of cortical folding patterns. Surface-based techniques make it possible to restrict smoothing to directions parallel to the cortical sheet, and to employ inter-subject 2-D alignment based on the patterns of sulci and gyri after secondary crinkles have been removed, which reduces both kinds of artifactual blurring and improves cross subject averaging (Fischl et al., 1999b); this also provides a less biased estimate of overlap. Finally, siting language regions with respect to topological cortical maps provides a more precise way to compare activations across individuals and groups as well as studies. Topological mapping is a time-tested method for accurately defining the boundaries of cortical areas. This is particularly important for refining functional localization in less well-understood regions such as frontal cortex.

3.2 Materials and Methods

3.2.1 Subjects

The same set of subjects who took part in the mapping experiments took part in the naturalistic reading comprehension experiment described in this chapter. All 20 subjects participated.

3.2.2 Experimental Stimuli and Design

Reading Experiment: The reading experiment consisted of a naturalistic reading task with precisely controlled saccade patterns where comprehension blocks contained a short narrative passage in English. The experiment was a random-order block design with 3 conditions and a central fixation screen. Each condition block was 16 sec long. During the experimental condition, a passage in English was presented one word at a time for 16 sec (64 words in total, average rate 4 words/sec). Each word was briefly presented on the screen at its natural reading position within the text. All other words appeared as grayed rectangles. The space between successive words/rectangles was set to 35% of the average word length. The exact display time of a particular word was made a piecewise linear function of the rendered word length. Vera.ttf, a san-serif typeface was parsed by FreeType 2.4.11 and rendered and measured in OpenGL using FTGL 2.1.3. The minimum display duration of a word was clamped to 175 msec, which was 70% of the average word duration of 250 msec. Words with widths more than 70% of the average word width were then given linearly increasing display durations with a slope chosen so the total paragraph duration equaled the desired block length (16 sec). This resulted in virtually identical duration/word-length slopes across different 64-word paragraphs. The guided reading experience felt much more subjectively natural when duration was controlled by word length than when a fixed word duration was used. In order to control for low level visual processing, there were two other conditions.

The condition 2 consisted of the 'Hindi' version of the English passage (simple substitution of characters from the font, lekhani_dynamic.ttf, not a translation, so rendered word lengths remained identical) using presentation mode and fixation durations identical to the English condition. In the third condition, Dot, a 0.5 deg visual angle dot instead of a word briefly replaced each of the grayed rectangles, again with the same varying fixation durations and

rectangle lengths. The baseline condition (condition 0) presented a single central fixation dot. The experiment consisted of 4 runs, where each run was comprised of 32 blocks presented in a random order. Participants, who had no familiarity with ‘Hindi’ were instructed to do their best to comprehend the English passages in all 4 runs and to follow the Hindi script 'words', or dot in the other two conditions. The passages were self-contained and unrelated to each other. The level of comprehension achieved for the English passages was measured with a questionnaire afterward. Participants were informed of this quality control process before the scan. The stimulus presentation technique used here, where each English word, Hindi word or dot was briefly presented in its natural reading position with all other words grayed out served several purposes. In the spirit of the classic attention study by Posner (1980), the

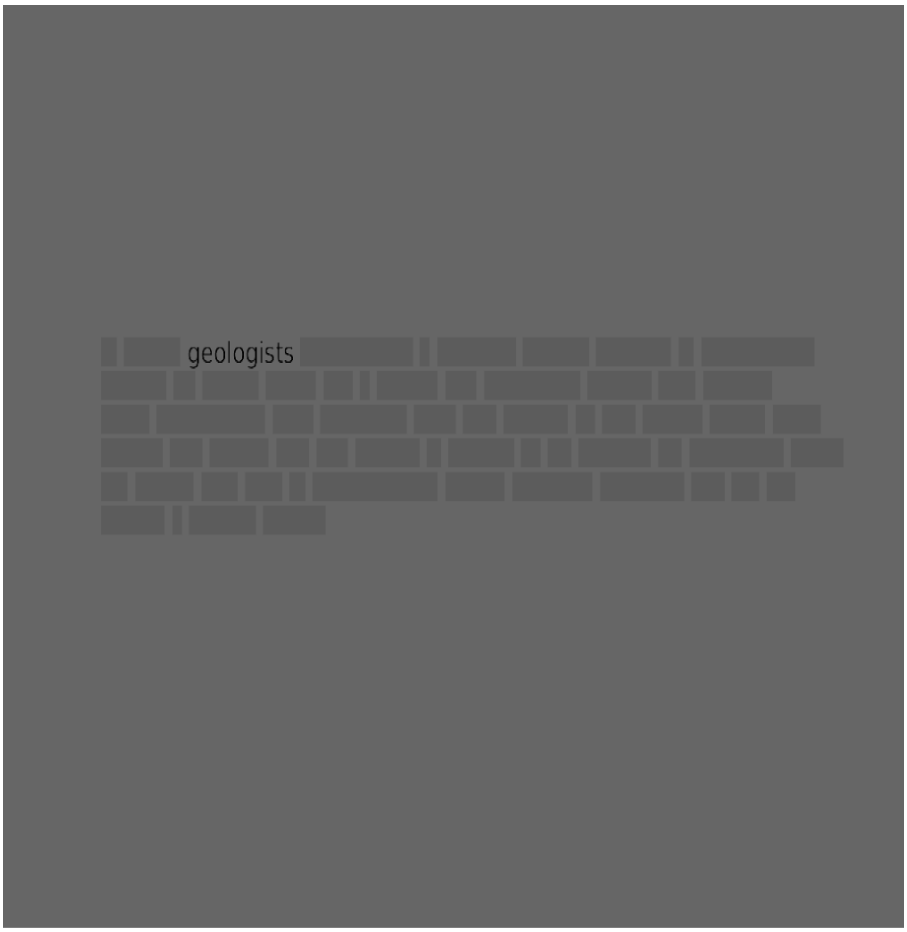

Sample Text

'In 1911, geologists discovered a strange glacial feature in Antartica, known as Blood Falls. It's a bright red waterfall, nearly five stories high. Geologists first believed that the colour of the water came from algae, but today the red colour is known to be caused by microbes living off sulphur and iron in oxygen-free water trapped beneath the ice for nearly 2 million years.'

Figure 3.1 Naturalistic reading comprehension: English screen

subject's exogenous attention is automatically drawn towards each newly highlighted position, where the word or dot appears, in a manner very similar to natural reading. The subjects moved their eyes along with the highlighted word and reported a naturalistic reading experience, which was aided by a naturalistic (word-length dependent) fixation duration. Additionally this presentation mode also ensured that participants made controlled eye saccades (and extremely similar eye movements across conditions) as opposed to uncontrolled eye movements if the passages were presented in its entirety. In order to further ensure that participants stayed attentive and made similar eye-movements for all conditions, they were instructed to press a button when the color of an English word, a Hindi pseudo word, a dot, or the central fixation dot occasionally changed from black to off-white (for an average of 0.25 seconds). The responses to button press events were logged and analyzed to assess the quality of task execution. Button press events were modeled as an extra regressor and used as an additional quality control check during data analysis. The English screen of the experiment and a sample English passage are shown in Figure 1. The stimulus was programmed in C/OpenGL/X11 (stimulus program available on request). An optimized random order of the conditions within each run was generated using AFNI's (Cox, 2012) RSFgen program.

3.2.3 Experimental Set-Up

The experimental set-up used was exactly same as that used for retinotopic mapping discussed in chapter 2. The stimuli were projected into the bore using an Eiki LC-XG300 XGA video projector onto a translucent direct-view screen at the participant's upper chest level. A black matte shroud situated just outside the bore blocked the beam from making low-angle reflections off the top of the bore. The rear of the head coil was elevated with a wooden wedge and thinner bed cushions were used to help naturally tilt the head forward. During all scanning sessions, memory foam cushions (NoMoCo Inc.) were packed around the head to provide additional passive scanner acoustical noise attenuation and to stabilize head position. Responses were made via an optical-to-USB response box (LUMItouch, Photon Control, Burnaby, Canada) situated under their right hand.

3.2.4 Imaging Parameters

Functional images were acquired on a 1.5 T whole-body TIM Avanto System (Siemens Healthcare), at the Birkbeck /University College London Centre for NeuroImaging (BUCNI), with RF body transmit and a 32-channel receive head coil. For the first ~3 subjects, images were acquired using the standard product EPI pulse sequence (24 slices, 3.2x3.2x3.8mm, 64x64, flip=90°, TE=39ms, TR=2sec), while the remaining (~17) sessions used multiband EPI (40 slices, 3.2x3.2x3.2mm, flip=75°, TE=54.8ms, TR=1sec, accel=4) (Moeller et al., 2011). Individual scans had 260 volumes for standard EPI and 520 volumes for multiband EPI. To allow longitudinal relaxation to reach equilibrium, 4/8 initial volumes were discarded from each run for standard/multiband EPI. For each imaging session, a short (3 min) T1-weighted 3D MPRAGE (88 partitions, voxel resolution 1x1x2mm, flip angle=7^{o}, TE=4ms, TI=1000ms, TR=1370ms, mSENSE acceleration=2x, slab-selective excitation) was acquired with the same orientation and slice block center as the functional data ('alignment scan'), for initial alignment with the high-resolution scans used to reconstruct the subject's cortical surface. Two high resolution T1-weighted MPRAGE (176 partitions, 1x1x1mm, flip angle=7^{o}, TI=1000ms, TE=3.57ms, TR=8.4ms) were acquired along with the fMRI sessions for cortical surface reconstruction (using FreeSurfer 5).

3.3 Data Analysis: Reading comprehension data

The data analysis methods employed here utilises GLM based mass univariate analysis (for an overview, see Monti, 2011), and the main parameter of interest is response amplitude. The single subject analysis was done in FSL (Smith et al., 2004) and across-subject group analysis was carried out on the cortical surface using FreeSurfer tools (for general guidance on the methods see- http://surfer.nmr.mgh.harvard.edu/fswiki/FsTutorial/FslFeatFreeSurfer).

For the reading experiment, single subject fMRI data was motion corrected and skull stripped using FSL tools (MCFLIRT and BET). First level fMRI analysis was carried out by applying the General Linear Model (GLM) within FEAT using FILM prewhitening (FSL, version 5) with motion outliers (detected by fsl_motion_outliers) being added as confound regressors if there was more than 1 mm motion (as identified by MCFLIRT). A small number of scans with excessive motion above the threshold of 1 mm were excluded from analysis.

High-pass temporal filtering of the data and the model was set to 100 seconds based on the power spectra of the design matrices (estimated by cutoffcalc; part of FSL). Three main explanatory variables were modelled and controlled: Reading English text, viewing Hindi text and viewing dot 'text'. Button press responses to target color change were modelled as the fourth regressor. In order to capture slight deviations from the model, temporal derivatives of all explanatory variables convolved with FEAT's double gamma haemodynamic response function (HRF) were included. The registration from functional to anatomical (6 DOF) and standard space (12 DOF) was first done using FSL's FLIRT and further optimized using boundary based registration (bbregister; FreeSurfer) similar to the procedure for the phase-encoded mapping data. A fixed effects analysis was performed across runs from an individual subject (usually 4 runs unless a run was excluded due to excessive motion/ lack of attention as evidenced by poor performance on qualitative assessment/ lack of response to the targets) to get group FEAT (GFEAT) results of first-level contrast of parameter estimates (COPEs) and their variance estimates (VARCOPEs) in the standard space. Across-subject group analysis was then carried out on the cortical surface using FreeSurfer tools. The GFEAT results of each subject were first sampled to individual cortical surfaces and then resampled to the spherical common average reconstructed surface (fsaverage inflated_avg surface is used as described in previous chapter). Surface based spatial smoothing of 3 mm FWHM was applied on the icosahedral sphere. A mixed effects GLM group analysis was performed on the average surface using the mri_glmfit program from FreeSurfer. Significance maps ($p<0.01$) were then corrected for multiple comparisons with cluster-based Monte-Carlo simulations with 10,000 permutations of white Gaussian noise using the FreeSurfer program mri_glmfit-sim. Finally corrected significance values ($p<0.05$) of reading activation were displayed on the average surface.

The single subject raw data was not spatially smoothed (both for phase-encoded analysis and reading analysis). As with the phase-encoded data, a 10 step (~3mm FWHM) surface level smoothing was applied for final illustration of the results. Hence, 3D Gaussian random field based cluster correction provided by FSL was not appropriate for multiple comparison correction of the reading data. I have instead used the surface based cluster correction similar to that employed for phase-encoded data analysis. The GFEAT results were sampled to their respective anatomical surface, thresholded at $p<0.001$ ($Z=3.09$) and corrected for multiple

comparisons with cortex surface clusters smaller than 30 mm^2 excluded, achieving a corrected p-value of 0.01.

The target (font color change) presentation timings and the button press events were logged during the experiment and analyzed to assess the performance of the task. A target was considered as detected if there was a response (a key press event) within 1 second after the colour change event had ended. For each participant, the number of targets detected and the mean response time in each condition were calculated. The cross-subject mean response time and target detection rates were assessed for significant differences across conditions.

Overlap analysis: All overlaps were calculated using "original vertex-wise area" in FreeSurfer. Original vertex-wise area in FreeSurfer is defined as the sum of 1/3 the area of each adjacent triangular face on the FreeSurfer "white" surface (refined gray/white matter boundary estimate). That single-vertex sum is not exactly constant across vertices because of slight non-uniformities in the final relaxed state of the surface tessellation. However, the sum of vertex-wise areas over a connected region of vertices exactly represents the summed original area of the enclosed triangles (plus the 1/3 fraction of triangles associated with the boundary vertices; along a straight edge of vertices, this last contribution corresponds to half of the area of the triangles just beyond the edge). The minimum areal increment that can be measured is roughly the average original vertex-wise area, which is ~0.6 sq mm.

3.4 Results

I first discuss the results obtained for reading experiment, followed by the overlap analysis results of reading activation with topological visual, auditory and somatomotor maps. For the result figures corresponding to reading experiment results, the amplitude of the vertex wise response for all relevant contrasts for a stairstep of t-values is illustrated. The overlap figures use transparent overlays to indicate reading activations over single modality phase hue maps, finally leading up to a summary outline figure containing all four kinds of data. The reading contrast used for overlap analysis is English vs. Hindi. Brain activation observed for English vs. Hindi contrast partially overlapped with retinotopic, tonotopic and somatomotor maps. For clarity, in overlap figures, only positive activation after thresholding and cluster correction is shown. The overlap results for different modalities are illustrated for several

individual subjects and then for the group as a whole. For the cross-subject average, the sensory-motor maps are illustrated for two separate vertex thresholds; $p<0.05$ (lower threshold) and $p<0.01$ (higher threshold), corrected for multiple comparisons using cluster thresholding at $p<0.05$. Because the phase-encoded analysis effectively spreads the same amount of imaging data over a larger number of different effective conditions (e.g., different polar angles, sound frequencies, body parts) than the Reading experiment does, the regression analysis carried out on reading data will have more power. Hence the Reading data illustrated here uses a vertex threshold of $p<0.01$ in all cross-average images. For the individual subjects, results are illustrated at a higher vertex threshold of $p<0.001$, corrected to $p<0.01$ for both reading and mapping data due to the higher amount of noise present in single subject data.

The individual subject data are illustrated here to show that in general the pattern of activity was similar to cross-subject average. The majority of subjects showed reading activation patterns similar to subject-1 and subject-2, while subject-3 had more restrained reading activation. All three of the individual subjects illustrated here had superlative comprehension task performance (vivid post-scan explanations correctly citing most of the text concepts presented to them during the task); all were in their early 20's.

Among the 20 subjects who took part in reading experiment, data from 3 subjects were excluded from the analysis owing to unsatisfactory performance in the target detection task and/or assessment of poor comprehension following the session and/or excessive movement (>1 mm). The activation for the target detection regressor (button press regressor) was used as an extra quality check to decide whether the subject performed the task as per the instructions during each run.

3.4.1 Target detection response

Figures 3.2 shows the target detection response results based on the performance of the included subjects. The average response time for the group when the target occurred in English, Hindi, Dot and Fixation conditions are depicted in Figure 3.2A. On average, participants took 0.47 seconds ± 0.01 (SEM) to respond to the target when it occurred in English/Hindi conditions and 0.42 seconds ± 0.01 (SEM) and 0.44 seconds ± 0.02 (SEM) when they occurred in Dot/Off conditions. A Wilcoxon matched-pairs signed-ranks test

indicated no significant differences between 'English' (median= 0.45 seconds) and 'Hindi' (median=0.46 seconds) (Z=-1.681, p=0.098). The differences between 'English' and 'Dot' (median=0.42 seconds) and 'English' and 'Off' (median = 0.40 seconds) conditions were found to be significant (Z=-2.96, p=0.002 for English-Dot and Z=-2.02, p=0.043 for English-Off).

Figure 3.2B depicts the average target detection success rate across all participants for different conditions. Across all runs, there were 20 targets for the English condition, 18 for the Hindi condition, 23 for the Dot and 7 for Off condition. All participants except one (see below) had comparable detection performance irrespective of the condition in which the target occurred. One participant did not respond to all 7 targets that fell on the fixation, though she consistently performed in all other conditions. All other quality measures were satisfactory for this subject and her data suggested that she did fixate during Off condition (the fovea had no activation in English vs. Fixation). I have therefore conservatively considered her data as valid. On average, the mean success rate for detecting targets when they occurred in English, Hindi, Dot and Off were 91.6%, 89.1%, 87.5% and 86.6% respectively. The average for Off condition is less mainly because of one outlier, the above mentioned subject. Excluding her data, the average success rate for Off condition was 92%. A Wilcoxon matched-pairs signed-ranks test was carried out to assess statistical significance of the average success rate. The median success rate for English, Hindi, Dot and Off were 90%, 89%, 87% and 100% respectively. There were no significant differences between English and any of the other conditions (English-Hindi: Z=-1.733, p=0.087; English-Dot: Z=-1.949, p=0.051; English-Off: Z=-0.94, p=0.94).

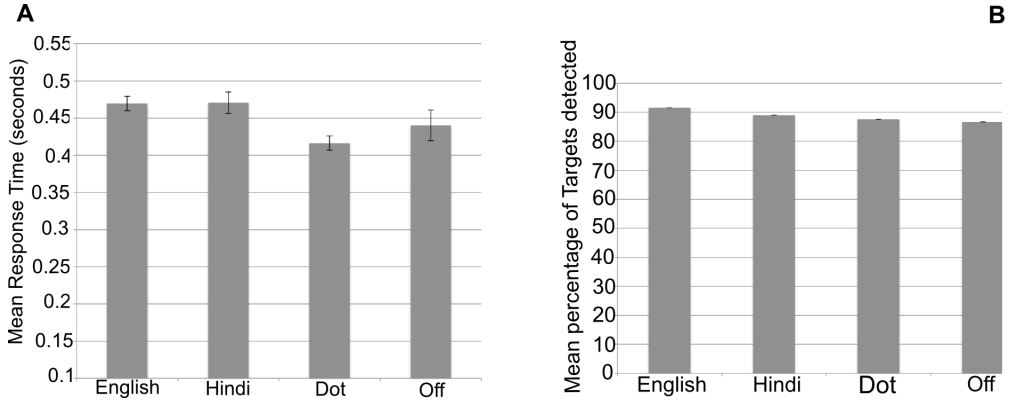

Figure 3.2: Target detection Performance results (Reading Experiment). Error bars represent one standard error from the mean.

3.4.2 Reading Activation

Figure 3.3 and Figure 3.4 illustrate the average cross-subject activation for a stairstep of t-values (all beyond a minimum threshold of $p<0.05$, uncorrected) for each condition (English, Hindi and Dot) relative to fixation (Fig. 3.3), and those for two main contrasts, Hindi vs. Dot) and English vs. Hindi (Fig. 3.4). The main contrast used to assess reading comprehension is English vs. Hindi. In the later figures depicting overlap with sensory-motor maps, bright yellow regions outlined in black depict the regions that showed significantly higher activation when reading English compared to Hindi. In all subjects, activation for English > Hindi was more widespread and pronounced in left hemisphere than in right hemisphere, as expected. The right hemisphere regions activated were very nearly a mirror image subset of the left hemisphere counterparts.

The cross-subject reading activation for English vs. Hindi (Figure 3.4A) was spread around 3 main connected regions in the left hemisphere. The first region was anterior to the occipital pole, extending laterally into the occipital cortex with two 'offshoots'. The first offshoot stretched across the intraparietal sulcus, covering regions in the inferior and superior parietal lobules. The second offshoot stretched nearly half the length of the inferior temporal gyrus and extended ventrally onto the fusiform gyrus joining the medial activation that extended from calcarine fissure to the fusiform gyrus. Less extensive but prominent activation was observed in medial regions in the cuneus, precuneus and at the isthmus of the cingulate gyrus. For English, Hindi, and Dot (versus Fixation), roughly the same regions in the occipital and parieral lobe were activated. However, the activation differences were most significant in those regions for English vs. Hindi.

The second main region (English vs. Hindi) is the superior temporal cortex, covering regions along the superior temporal gyrus and sulcus extending well into the middle temporal gyrus and supramarginal gyrus. Except for a small region in posterior STS, the Hindi and Dot conditions do not have any significant temporal lobe activation. Although cross-subject reading activation did not have significant activation in more anterior temporal cortex, the EPI pulse sequence used for 3 subjects (of the 17 included subjects) didn't include this region within its scanning block, which might partially explain why no activation is observed in anterior most regions of temporal cortex in cross-subject average. Among the subjects

illustrated here, subject 1 was scanned using EPI, while subjects 2 and 3 were scanned using multi band sequence which ensured full brain coverage.

The third region included two distinct frontal regions -- one near the precentral sulcus and another near the inferior frontal sulcus in the pars opercularis region. The right hemisphere activation profile was similar but covering a smaller total extent of cortical area. The activation near the precentral sulcus was present for Hindi and Dot conditions as well, with no significant differences in the Hindi vs. Dot contrast (Fig. 4D). The activation observed for English in inferior frontal region near pars opercularis was absent in both Hindi and Dot conditions.

The reading activations of subject-1 and subject-2 were strikingly similar to the cross-subject profile, with activated regions corresponding to the three main regions just described in the left hemisphere. Individual subject-3 (see below) showed the greatest variation from

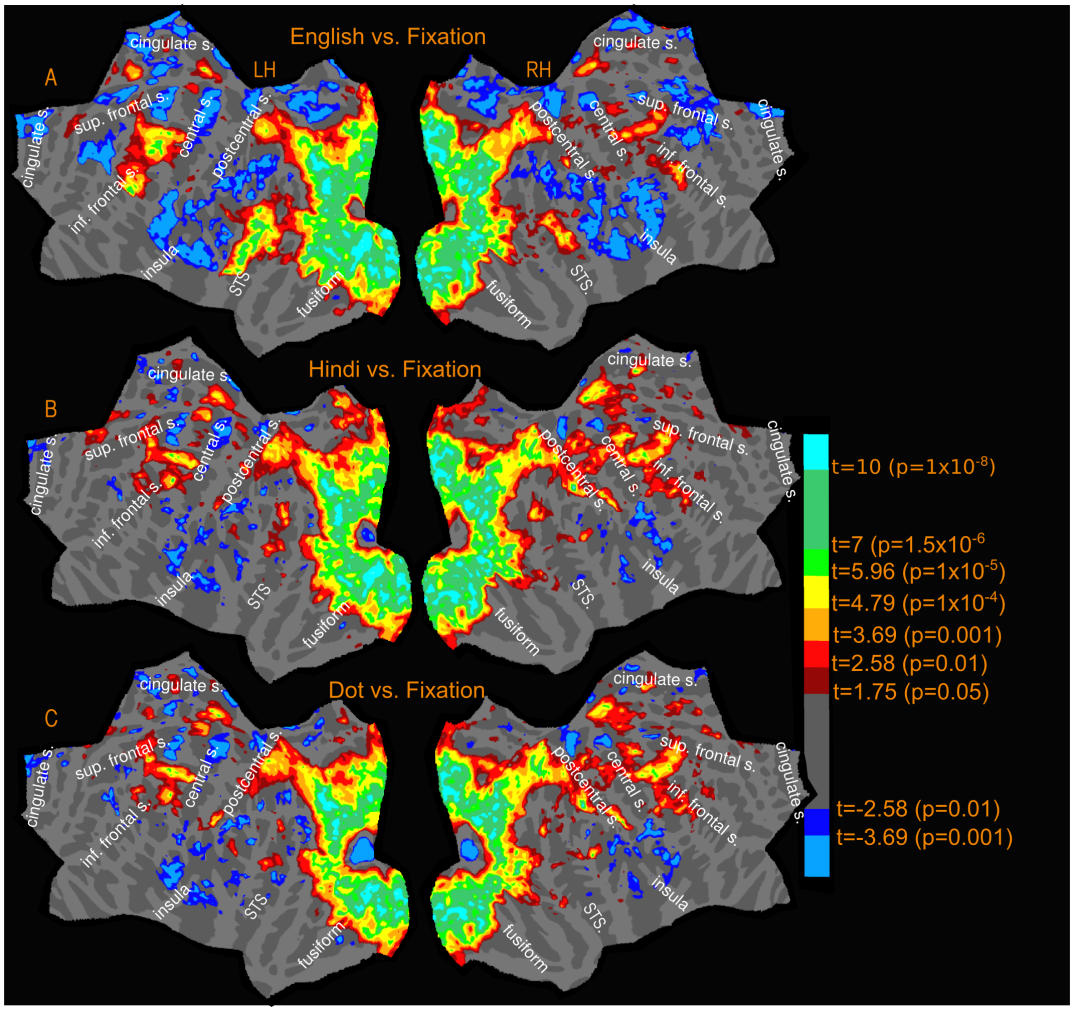

Figure 3. 3: Reading Experiment- Activation amplitude profile (uncorrected)

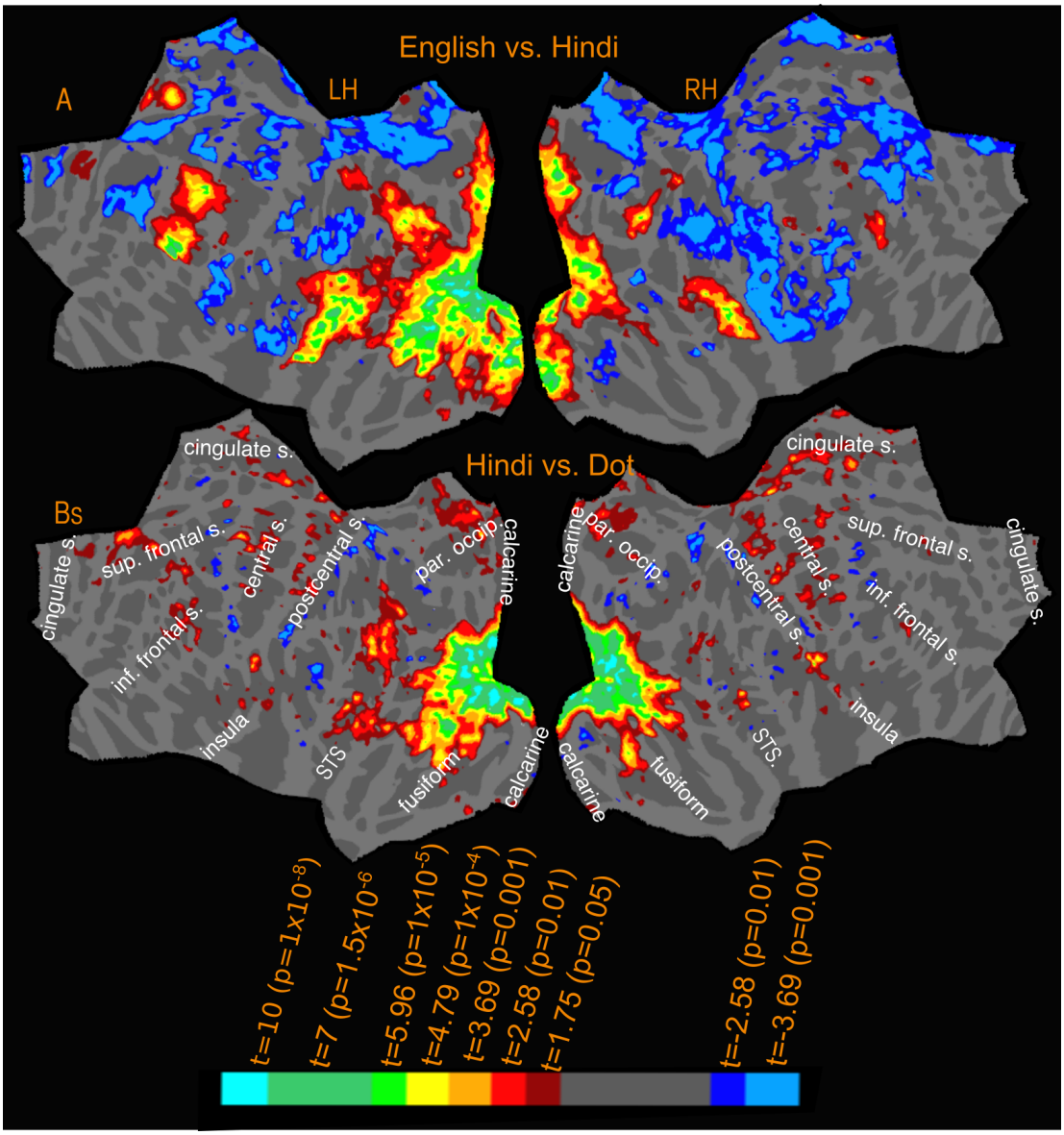

Figure 3.4: Reading Experiment- Activation amplitude profile (uncorrected)- continued

the average, with more extensive activation observed in superior temporal sulcus and middle temporal gyrus, but then less extensive activation elsewhere in the cortex.

3.4.3 Overlap of reading (English vs. Hindi) activation with visual, auditory, and somatomotor maps

Figures 3.5-3.11 show the overlap of reading (English vs. Hindi) activation with topological visual, auditory and somatomotor maps. For the cross-subject activations, the visual, auditory, and somatomotor activations are assessed for two different hard vertexwise thresholds before cluster exclusion correction: $p<0.01$ (higher threshold) and $p<0.05$ (lower threshold). Reading activation uses a single higher hard vertex threshold of $p<0.01$. For single subject activations, reading, retinotopic, and tonontopic maps are hard thresholded at

$p<0.001$, corrected to $p<0.01$. The overlap estimates below, are expressed as the percentage of reading activation intersecting with sensory-motor maps. The quantitative results include an overall estimate, where the percentage of total reading activation overlapping with retinotopic, tonotopic and somatomotor maps are reported for each hemisphere. Additionally, each region (frontal, temporal and occipito-parietal) for reading activation is considered separately, and corresponding overlap is expressed as a percentage of the regional reading activation. The quantitative estimates are summarized in Table 3.1.

Reading overlap with retinotopic maps: The retinotopy/reading overlap for the cross-subject surface average is shown in Figure 3.5. The reading activation in the whole of occipital and parietal cortex in both hemispheres fall within retinotopically mapped regions. In the left hemisphere, the overlapping regions include early visual areas such as V1, V2, ventral V3, extending to posterior inferior temporal cortex all the way to the lateral surface reaching MT and immediately surrounding areas, after which the lateral activation is attenuated. There is a more discontinuous overlap on the superior bank of the calcarine sulcus, with V1 and V2 activated, but little activation in dorsal V3. There is a strong activation again in the vicinity of V3A and immediately anterior areas. The retinotopic branch extending across MT overlaps with the reading activation in the posterior STS. The rest of the reading activation in the STS is outside the bounds of any retinotopy. In the frontal cortex, there is substantial overlap with both maps in the FEF region as well as more laterally located dorsolateral prefrontal cortex. In the right hemisphere, reading activation in occipital cortex is largely limited to early visual areas V1 and V2. On the lateral occipital side, significant activation is observed immediately anterior to V3A. The STS activation overlaps partially with retinotopic maps in the posterior STS regions, and the right frontal activation overlaps partially with retinotopy in the frontal cortex. The reading activation around the fovea region is considered as overlapping with retinotopy, as the lack of retinotopy in this region is an artifact expected with central fixation (no periodic signal change will be present since the subject is fixating at all times); however, these regions are known to be retinotopic (e.g., Schira et al., 2009) and are considered so for overlap analysis.

With regards to quantitative overlap estimate, over the entire cortex, at the higher threshold, more than 70% of the cross-subject reading activation in both hemispheres falls within retinotopic areas (LH: 75%, RH: 73%); the overlap is more than 80% at the lower

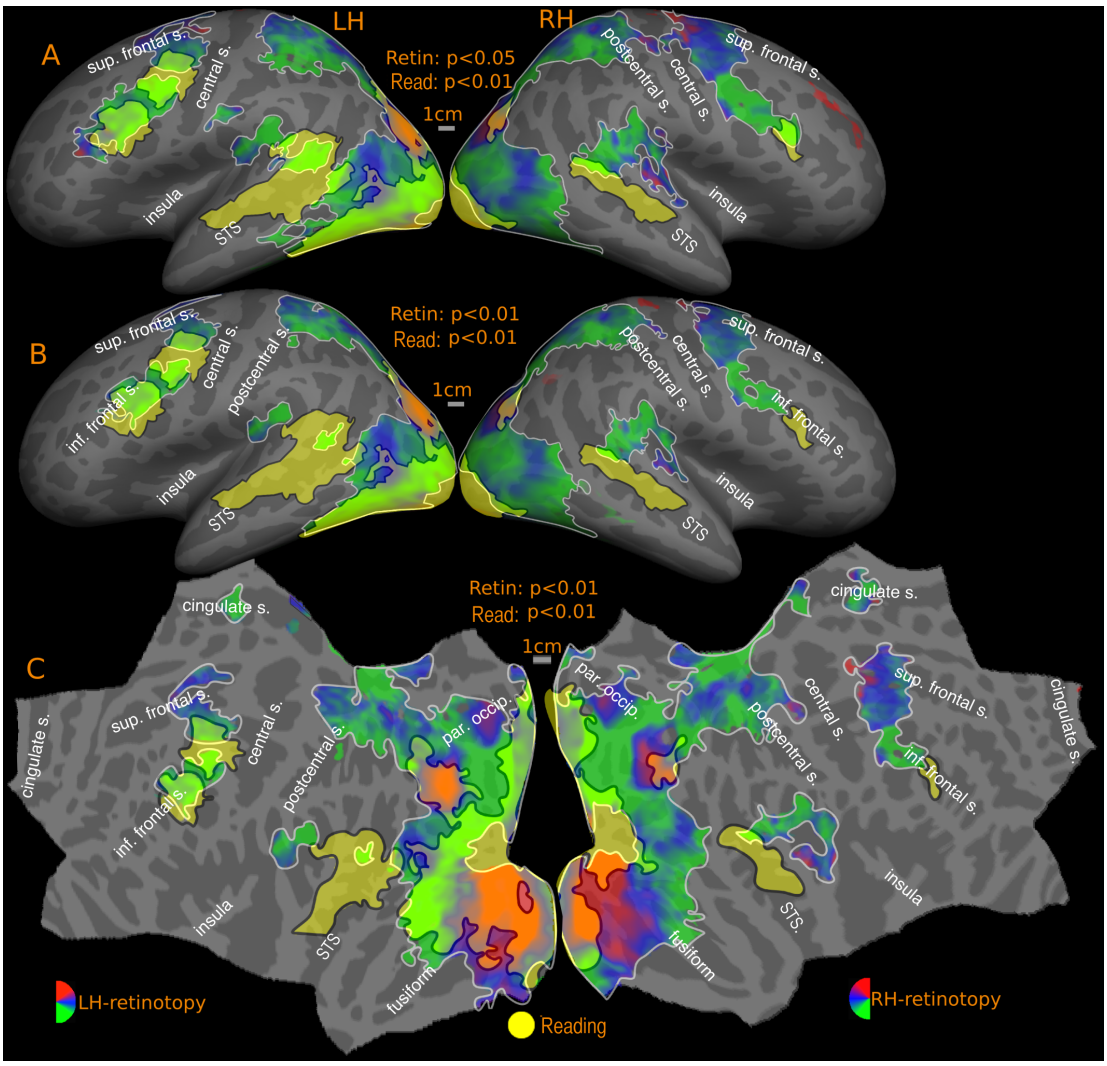

Figure 3.5: Overlap of READING (English vs. Hindi) with RETINOTOPIC maps- GROUP
Reported p values are vertex thresholds used before cluster thresholding. All activations are cluster thresholded to p<0.05. Reading activation is illustrated at p<0.01 (vertex threshold) in A and B. Retinotopic activation is illustrated at two different vertex thresholds- p<0.05 (A) and p<0.01 (B). C represents the flattened version of B.

threshold (LH: 81%, RH: 81%) (see Fig 9). I previously described three main regions of reading activation -- occipito-parietal, superior temporal and frontal. The reading activation in region-1, which includes the occipital lobe, inferior temporal lobe, and superior parietal lobe falls completely within retinotopic regions in both hemispheres (100% overlap). In reading region-2, the superior temporal cortex, in the left hemisphere, the overlaps were 7% (higher threshold) and 26% (lower threshold). In the right hemisphere, the overlaps were 8% (higher threshold) and 15% (lower threshold). For reading region-3, frontal cortex, which includes precentral and inferior frontal cortex, there is a 55% overlap with retinotopy at the higher threshold in the left hemisphere, which rises to 70% at the lower retinotopy threshold. In the right hemisphere, the frontal retinotopic maps lie just outside the borders of right

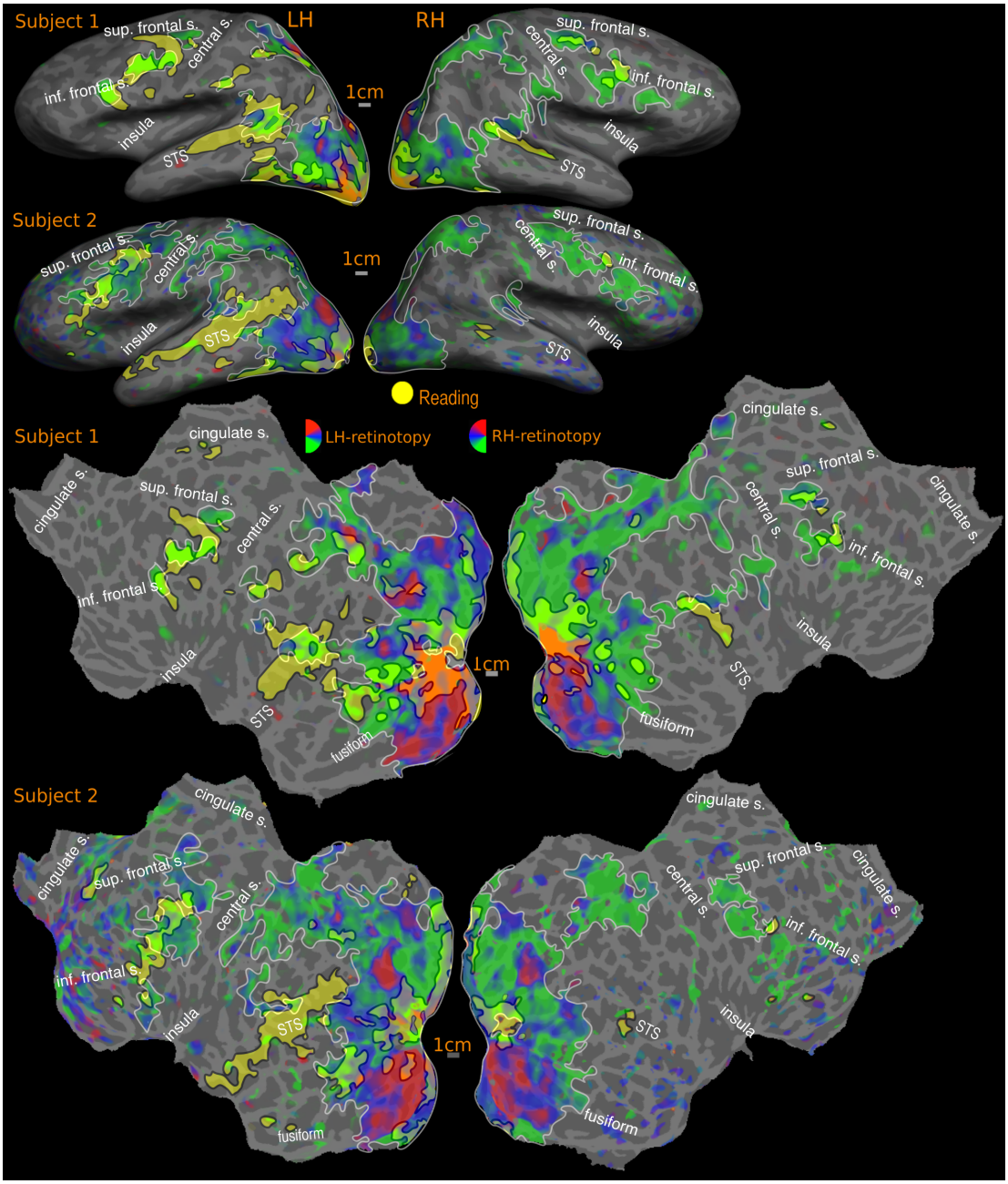

Figure 3.6: Overlap of READING (English vs. Hindi) with RETINOTOPIC maps- individual subjects-1 and 2.

Activations are illustrated at $p<0.001$, corrected to $p<0.01$. Only colors used in the figure are red, blue, green (to represent sensory-motor maps) and yellow (to represent language). Any other colors perceived are the result of overlap of colors (e.g. orange where red and yellow overlaps)

hemisphere reading activation in frontal cortex at the higher threshold; at the lower retinotopy threshold, they extend to cover almost 62% of the right hemisphere frontal reading activation.

For two individual subjects subject-1 and subject-2 (Fig. 3.6), the overall left hemisphere retinotopy/reading overlap is 53% (subject-1: 58% and subject-2: 48%), while the right hemisphere overlap is above 80% (subject-1: 83% and subject-2: 81%). Zooming in to

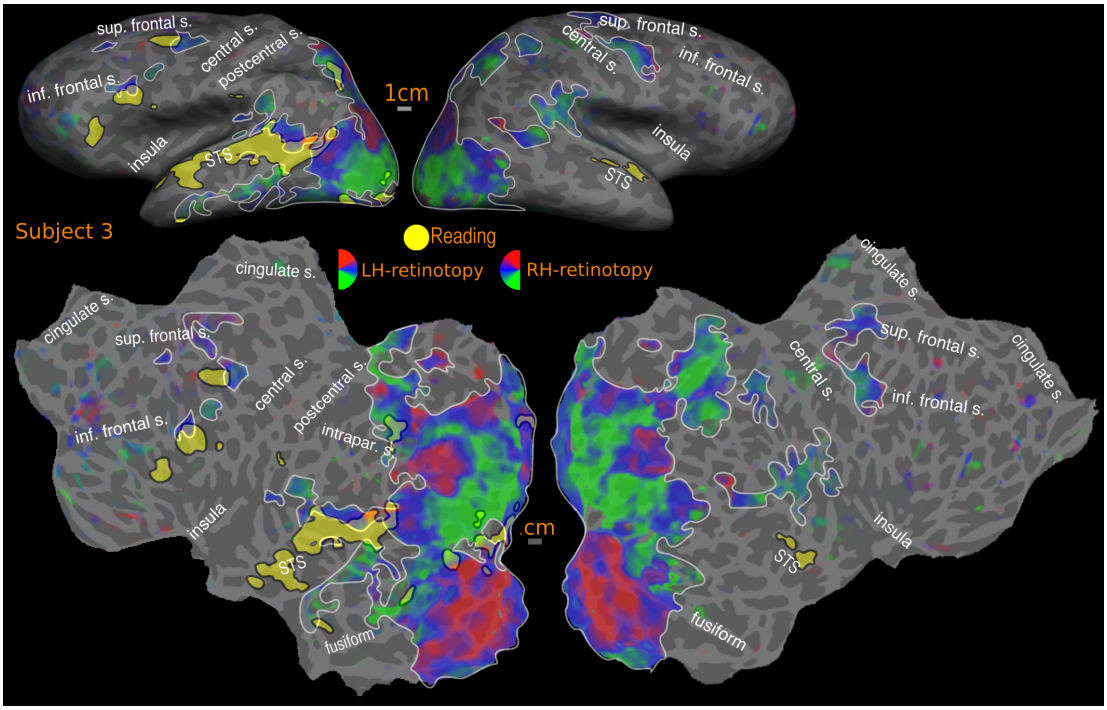

Figure 3.7: Overlap of READING (English vs. Hindi) with RETINOTOPIC maps- individual subject-3.

Activations are illustrated at p<0.001, corrected to p<0.01.

individual regions, as with the cross-subject average, there is almost 100% overlap between reading and retinotopy in occipito-parietal cortex in both hemispheres. In the left hemisphere frontal and temporal reading areas, overlap with retinotopy is 34% and 17% in subject-1 and 40% and 5% in subject-2. The corresponding overlaps for the right hemisphere of these subjects are 69% (frontal) and 18% (temporal) for subject-1, and 38% (frontal) and 0% (temporal) for subject-2.

In subject-3 (Fig. 3.7), the frontal and temporal reading profile varies considerably and has a lower overlap (LH: 28%, RH: Nil) with retinotopic maps than it does with tonotopic maps (see below). The individual left hemisphere overlap figures in frontal and temporal cortex are 11% and 13%. There is no overlap in the right hemisphere.

The retinotopic map underlays illustrated in Figures 3.5-3.7 use the same colour scale as the average (lower contralateral field green, horizontal meridian blue, upper field red). In the group results, in both hemispheres, the occipital reading activation overlaps roughly equally with lower, middle, and upper visual fields. In higher-level retinotopic areas, there was a slight predominance of horizontal meridian and lower visual fields. There are two reasons for this. First, because retinotopic maps in higher-level visual areas are smaller, slight inter-subject displacements in the location of these maps has a tendency to reduce the range of

polar angles in the average map. This 'regression toward the horizontal meridian' results in an overrepresentation of the horizontal meridian in the average. Another possible source of a horizontal meridian and particularly lower field emphasis is that subjects in the direct-view experiments had to lower their gaze somewhat to fixate the center of the close-up screen. Given that there is evidence for head-centered remapping of receptive fields in some higher visual areas (e.g., see Sereno and Huang, 2006), the lowered gaze may have remapped the entire visual field slightly toward the lower field in these higher level areas, resulting in an overemphasis of the lower field in both individual subjects as well as the average.

Reading overlap with tonotopic maps: The most obvious overlap is in temporal cortex, where the reading task consistently activates an anterior-posteriorly elongated region in superior temporal cortex. In the left hemisphere average, the center of the superior temporal reading activation is slightly inferior to the center of the tonotopic activation (Fig. 3.8, and compare Fig. 3.4A and 2.9B) with overlap on the superior temporal gyrus and part of the upper bank of the STS. The inferior edge of the reading activation in turn overlaps the superior edge of middle temporal visual areas. Most subjects (and the average) showed more reading overlap with retinotopic maps than tonotopic maps. However, this was reversed in some subjects (e.g. subject-3). In the right hemisphere average, the smaller superior temporal reading activation almost completely overlaps tonotopy.

The frontal lobe reading activation also overlaps partially with frontal tonotopic maps. These are also potential sites of multi-sensory integration since these region contain both retinotopic and tonotopic maps. These findings are consistent in the cross-subject average as well as in individuals. Though the cluster correction filter removed it as being too small to be valid (and hence it is not formally included in overlap analysis), there is a small but strong reading activation ($t>4.7$, $p<10^{-4}$) in anterior cingulate, which overlaps almost completely with the tonotopic map in the region. This region is only activated while reading English.

The overall tonotopy/reading overlap (Fig. 3.8) estimate is 6% (LH) and 13% (RH) for the higher threshold, and 10% (LH) and 20% (RH) for the lower threshold in the cross-subject average. In left temporal cortex, the level of overlap is 20% at the higher threshold and 26% at the lower threshold. In the right hemisphere, more of the temporal reading activation falls within tonotopy (74% at higher threshold, 85% at lower threshold). The tonotopic maps also

overlap with frontal reading activation in both hemispheres: 10% (high threshold) and 22% (low threshold) in left hemisphere and 6% (high threshold) and 84% (low threshold) in the right hemisphere.

The typical individual subjects (Fig. 3.9) exhibit a similar profile (overall overlap: subject-1: LH: 6%, RH: 10%; subject-2: LH: 14%, RH: 7%). In subject-1, 8% of frontal and 17% of temporal lobe activation in left hemisphere overlaps with tonotopy. The corresponding figures for right hemisphere are 8% frontal and 71% temporal. For subject-2, the left hemisphere overlap is 51% frontal and 23% temporal and for the right hemisphere, 33% frontal and 29% temporal. Subject-3 has especially extensive tonotopic maps and shows a higher degree of overall overlap with tonotopy than with retinotopic areas (overall: 32% in left hemisphere and 54% in right hemisphere). Around 44% of frontal and 39% of temporal lobe left hemisphere activation falls within tonotopically defined regions. In the right hemisphere, nearly 61% of temporal reading activation overlaps with tonotopy. No significant frontal reading activation is observed for subject-3 in the right hemisphere; and there are tonotopic maps in this region.

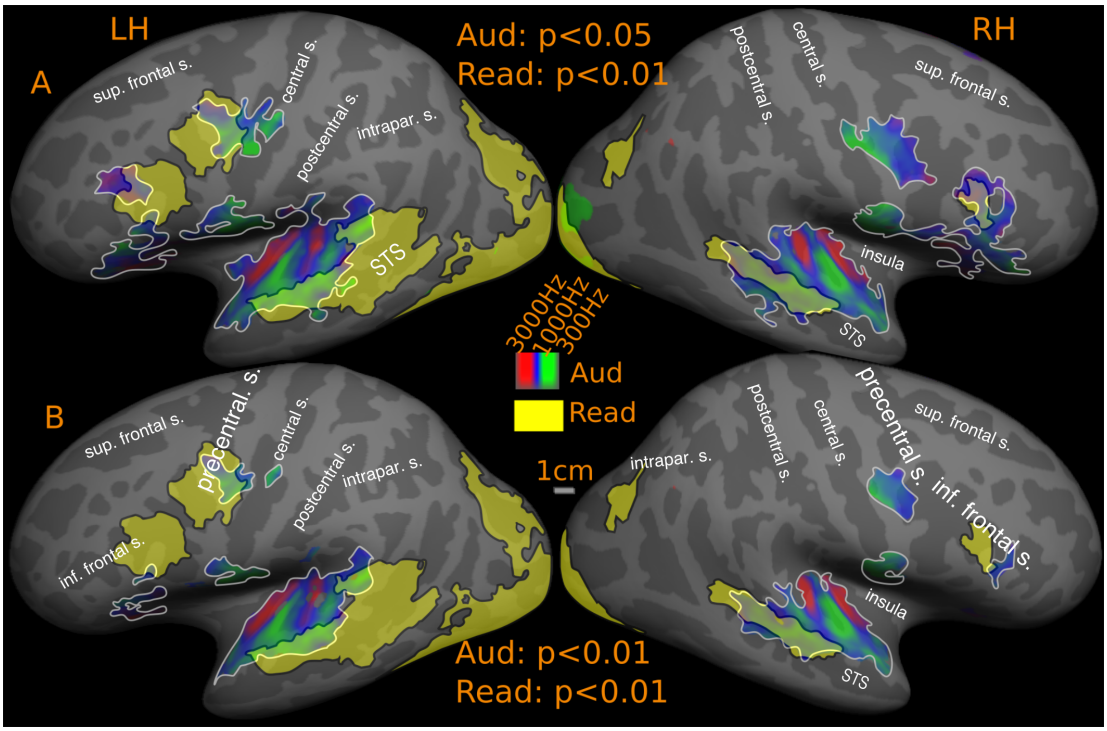

Figure 3.8: Overlap of READING (English vs. Hindi) with TONOTOPIC maps- GROUP
Reported p values are vertex thresholds used before cluster thresholding. All activations are cluster thresholded to p<0.05. Reading activation is illustrated at p<0.01 (vertex threshold) in A and B. Tonotopic activation is illustrated at two different vertex thresholds- p<0.05 (A) and p<0.01 (B).

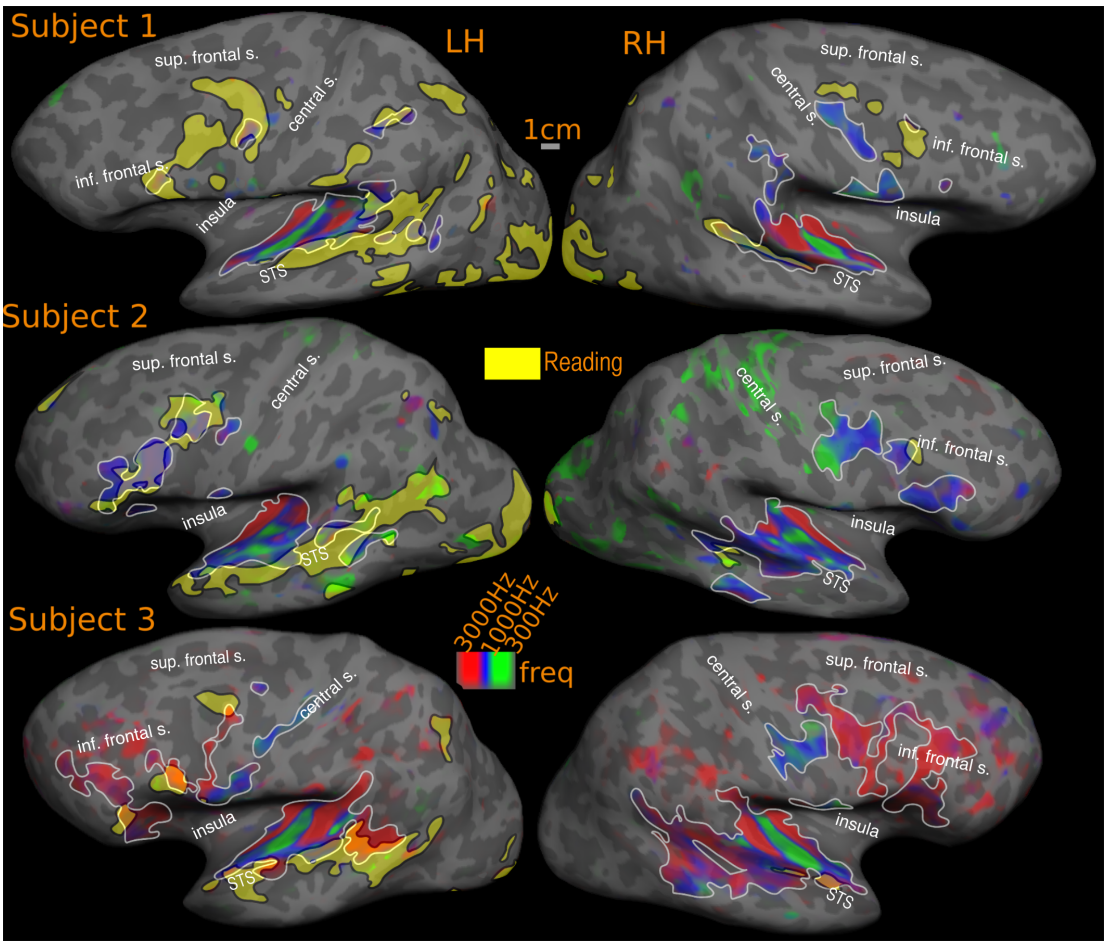

Figure 3.9: Overlap of READING (English vs. Hindi) with TONOTOPIC maps- individual SUBJECTS

Activations are illustrated at $p<0.001$, corrected to $p<0.01$.

In the group results, the majority of the overlap between reading and tonotopy in the temporal lobe falls within the low to middle frequency range. For example, in the left STG, only 0.7% of temporal reading activation overlaps high frequencies. In the right temporal cortex, reading/tonotopy overlaps occur within the mid-low frequency range avoiding high frequency regions in the lateral sulcus. The situation in frontal cortex is more mixed. In the left frontal cortex, the overlapping region lying between precentral and central sulcus is dominated by mid-low frequencies closer to central sulcus and by high-mid frequencies closer to the precentral sulcus. In the pars opercularis region, there are two separate overlaps, the more dorsal overlap region is predominantly high-mid range frequencies while the more ventral region is predominantly mid range frequencies. In the right hemisphere, the overlap is only with the pars opercularis activation, where the tonotopic maps overlapping with reading has a high-mid frequency distribution.

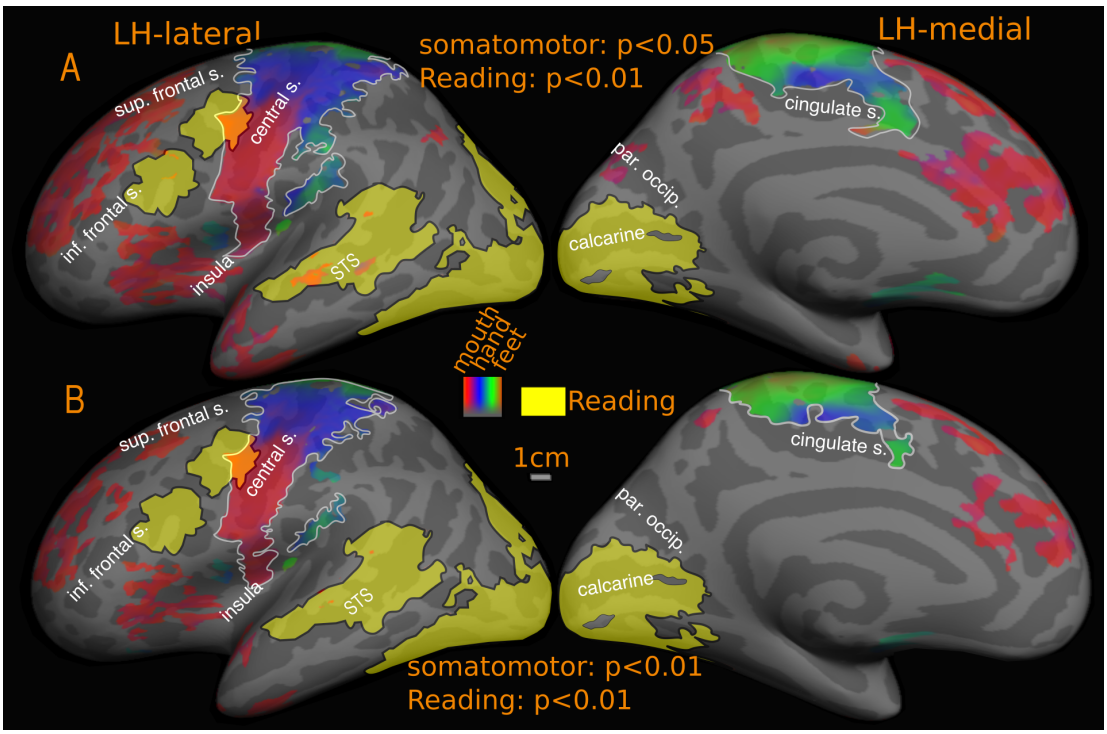

Figure 3.10: Overlap of READING (English vs. Hindi) with SOMATOMOTOR maps- GROUP

Reported p values are vertex thresholds used before cluster thresholding. All activations are cluster thresholded to p<0.05. Reading activation is illustrated at p<0.01 (vertex threshold) in A and B.

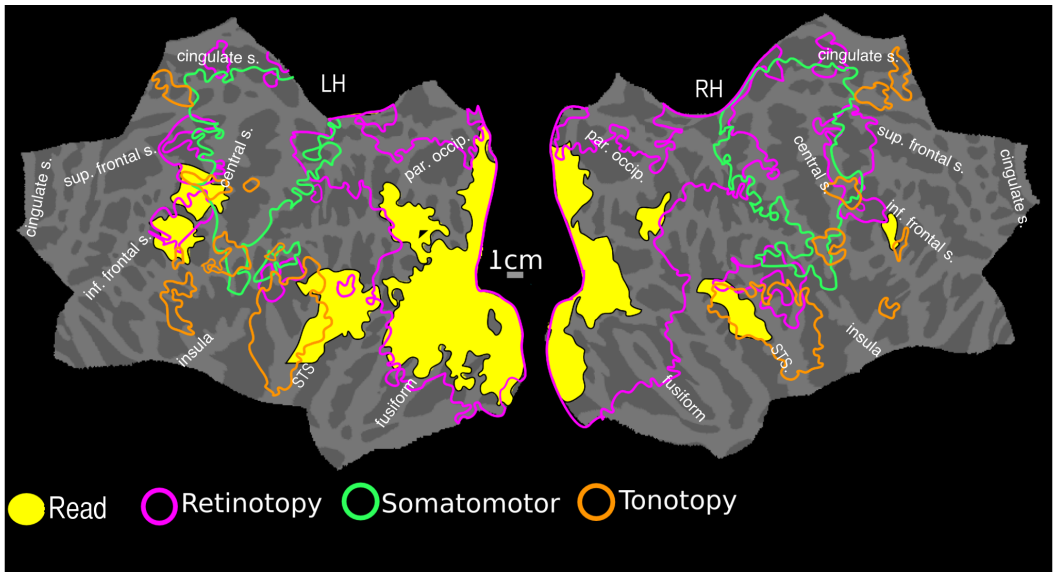

Figure 3.11: Overlap of READING (English vs. Hindi) with ALL MAPS- GROUP

Reading activation and maps are illustrated at vertex threshold p<0.01, cluster corrected to p<0.05

Reading overlap with somatomotor maps: In the cross-subject average, there is only one overlap zone, near the face/hand boundary bordering the central sulcus in M-I (Fig. 3.10). The overlapping region corresponds to 1.6% of total reading activation at higher threshold, increasing slightly to 2% at lower threshold. This constitutes 12% (high threshold) of the left

frontal reading activation, rising to 14% at low threshold. There was no overlap in right hemisphere or SMA.

Retinotopic maps (as a percentage of reading activation)			**Group**		**Subj-1**	**Subj-2**	**Subj-3**
			Higher threshold	Lower threshold			
	Left hemisphere	Overall	75	81	58	48	28
		Frontal	55	70	34	40	11
		Temporal	7	26	17	5	13
		Occipital	100	100	100	100	100
	Right hemisphere	Overall	73	81	83	81	Nil
		Frontal	Nil	62	69	38	Nil
		Temporal	8	15	18	Nil	Nil
		Occipital	100	100	100	100	Nil
Tonotopic maps (as a percentage of reading activation)	Left hemisphere	Overall	6	10	6	14	32
		Frontal	10	22	8	51	44
		Temporal	20	26	17	23	39
		Occipital	Nil	Nil	Nil	Nil	Nil
	Right hemisphere	Overall	13	20	10	7	54
		Frontal	6	84	8	33	Nil
		Temporal	74	85	71	29	61
		Occipital	Nil	Nil	Nil	Nil	Nil

Table 3.1: Quantitative estimates of overlap of Reading with Retinotopy and Tonotopy

3.5 Discussion

The results presented here provide a comprehensive qualitative and quantitative assessment of where, and by how much, processes relevant to naturalistic reading overlap with topological (neighbor-preserving) visual, auditory, and somatomotor maps using high-resolution surface-based fMRI across the entire cortex. Nearly 80 fMRI sessions were analyzed with a start-to-finish cortical-surface-based processing pipeline. This study combines recent advances in lower-level sensory-motor mapping with a higher-level

cognitive task (naturalistic reading with matched eye movements across conditions). There were two related objectives.

The first was to accurately localize regions of interest in naturalistic reading comprehension by determining their exact relation to low and high-level topological visual, auditory, somatosensory and motor maps. Topological mapping is a time-tested method for accurately defining the boundaries of cortical areas. The figures presented here are the first illustrations of the relative location of naturalistic reading comprehension activation and topological visual, auditory and somatomotor maps across the entire cortex in the same group of subjects. In the process, several previously unreported tonotopic maps in frontal cortex that partially overlapped frontal retinotopic maps were discovered. In anterior cingulate cortex, two additional new maps were found -- a visual map and a tonotopic map, both near the SMA but not overlapping each other, or the SMA. A strong reading (English vs. Hindi) activation overlapped the left anterior cingulate tonotopic map. The data sets presented here benefitted from the latest multi-band pulse sequences, allowing me to map the whole brain without losing temporal SNR, as well as from optimized sensory mapping stimuli, which together may account for why it was able to visualize those new maps.

Second objective was to provide a quantitative estimate for the level of overlap between activations observed during naturalistic reading comprehension and topological sensory-motor maps, which are driven by relatively low-level, sensory-motor stimuli. At least 80% of reading activations (English vs. Hindi) in the left hemisphere and 86% in the right hemisphere fall within regions containing topological visual, auditory, somatosensory, or motor maps in the group average. At least 65% of the reading activation in frontal cortex, 26% in temporal cortex, and 100% in parietal and occipital cortex falls within visual, auditory or somatomotor maps. The overlap figures rise to nearly 90% in frontal cortex and 50% in temporal cortex if the threshold for detecting topological mapping is lowered to $p<0.05$ (corrected). Given that smaller, higher-level maps are more difficult to visualize than large, metabolically active, early visual areas, these figures serve as a conservative rather than an overly optimistic estimate (see Gonzales-Castillo et al., 2012). It should be noted that the 'overlap' defined here could only be measured at the resolution of our fMRI voxels. An overlap voxel might be identified if the two kinds of signals were within the same neuron, within distinct but adjacent neurons, within different 50 micron wide minicolumns, or within

different ~1mm wide columns (see e.g., Lund et al., 1993), all of which could be within the same voxel.

While occipital cortex and immediately surrounding regions have long been considered to be quintessentially visual, language research has often regarded activation elsewhere as falling outside the bounds of vision. For example, the classical language areas in superior temporal cortex and frontal cortex are often considered to be non-visual. However, in the last decade or so, several additional retinotopic maps were discovered in frontal cortex (Hagler and Sereno, 2006; Hagler et al., 2007; Kastner et al., 2007), parietal cortex (Sereno et al., 2001, 2003; Huk et al., 2002; Schluppeck et al., 2005; Silver et al., 2005; Sereno and Huang, 2006; Swisher et al., 2007; Silver and Kastner, 2009) and temporal cortex (Sereno et al., 2003; Huang and Sereno, 2013). The higher-level retinotopic maps in frontal cortex were originally discovered using working memory and spatial attention paradigms (Hagler and Sereno, 2006; Kastner et al., 2007). Those studies suggested that topological maps may serve as a convenient method of allocating working memory, or maintaining pointers to specific content, even (or more so!) for tasks that don't explicitly require attention to spatial location, but that require attention to content. The present study shows that reading activation in frontal cortex falls largely within these retinotopic maps.

In addition to confirming previous reports of retinotopic maps in frontal cortex, new evidence was found for consistent tonotopy both in dorsolateral prefrontal cortex and ventral prefrontal cortex. While tonotopy in superior temporal cortex has been the subject of several studies (Talavage et al., 2000, 2004; Formisano et al., 2003; Humphries et al., 2010; Da Costa et al., 2011; Dick et al., 2012; Langers and Van Dijk, 2012) there is virtually no literature on tonotopy in human frontal cortex. There is, by contrast, a wealth of neuroimaging studies providing evidence that the human frontal lobe is active during general auditory tasks (Platel et al., 1997; Alain et al., 2001; Kiehl et al., 2001; Muller et al., 2001; Gaab et al., 2003; Arnott et al., 2004; Rämä et al., 2004; Koelsch et al., 2009). Neurophysiological and neuroanatomical findings in non-human primates show that both dorsolateral and ventral prefrontal cortex is reciprocally interconnected with auditory regions in the temporal cortex (Hackett et al., 1999; Romanski et al., 1999; Plakke and Romanski, 2014). The frontal reading activation overlaps the tonotopic maps in the region, perhaps for a

similar reason as for the retinotopic map overlap (e.g., memory allocation using topological maps as pointer buffers).

Any activation of higher-level visual and auditory areas during reading comprehension has often been dismissed with the claim that readable, understandable text (here English) attracts more attention than unreadable, incomprehensible text (here Hindi characters of the same word length, fixated with the same controlled pattern of saccades). An assumption prevalent in the literature is that comprehension and reading processes are dissociable from sustained attention, and that they can be dissociated by using a control task matched in attentional complexity. Recent research however suggests that attention is a cortex-wide dynamic process whereby resources are flexibly allocated to the attended function as opposed to a simple mechanism that merely modulates baseline response level (Çukur et al., 2013, Peelen & Kastner, 2014). But this also implies that subtractive analyses attempting to control for attention factors assuming a static modular nature of attention may be overly conservative. In the present study, any task-related attention and working memory processes are considered relevant and necessary for naturalistic reading comprehension and have not been subtracted out. Low level visual processing including saccade preparation and execution (eye movements), and task-irrelevant attention are controlled by subtracting out activation due to the combination of 'Hindi' font, directed naturalistic saccades, and the target detection task. In addition to facilitating a naturalistic reading experience, the presentation of text by highlighting the next word drives the exogenous attentional network (Posner, 1980) and triggers a saccade towards the highlighted spatial location. While spatial attention can be modulated without saccades, saccades rarely occur without being directed by attention. Substantial evidence exists suggesting that an eventual saccade target peripheral to fixation attracts attention during saccadic planning (Melcher & Colby, 2008; Zhao et al., 2012), and that attention then quickly returns to the centre of gaze after the saccade to the target has been made. Finally, the random colour change detection task performed by the subjects during the experiment across all conditions served as a control for endogenous attention. In all three conditions- English, Hindi and Dot, significant activation was observed bilaterally near intra parietal/postcentral sulcus, FEF, and dorsomedial frontal 'eye' fields, regions known to be activated by visuo-spatial attention and eye saccades (Pierrot-Deseilligny et al., 2004; McDowell et al., 2008; Müri, and Nyffeler, 2008; Jamadar et al., 2013; O'Reilly et al., 2013).

The activations in dorsomedial frontal ‘eye’ fields and parts of parietal cortex are fully attenuated in English vs. Hindi contrast (as well as in Hindi vs. Dot contrast, in fact Hindi and Dot has slightly better activations in these areas). In FEF, while the activation disappears in Hindi vs. Dot contrast, a good part of it is still highly significant in English vs. Hindi contrast, suggesting that the FEF may have a larger role in comprehension, an observation supported by other studies (Hasson et al., 2008; Choi et al., 2014).

However, not all frontal regions were activated for all three conditions. The more anterior activation near left inferior frontal sulcus/gyrus (a classical language region) overlapping with the DLPFC visual maps and tonotopic maps were unique to reading and comprehending English passages. Similarly the activation observed in left cingulate dorsomedial frontal 'ear' fields region is unique to the English condition. All the above activations fall largely within visual and tonotopic maps in those regions.

As mentioned above, part of the activation observed could be due to sustained attention and working memory processes engaged in reading meaningful passages; but the functional dissociation of reading processes was very specifically not the goal of the current study. Reading in real situations is a computationally intense, attention- and working memory-demanding contextual process that involves tying together information gleaned from linear symbol streams across seconds and minutes. The idea that these processes are recruited in language processing is not a new one (see Duncan et al., 2000). What is not clear though from the present literature is where the boundaries of these putative multi-functional regions or classical frontal language regions lie. Although we cannot distinguish between domain general processes and purely linguistic processing from the contrast used here, the present study does define precisely where reading activation zones are relative to topological cortical maps in the frontal cortex. Dissociating linguistic and non-linguistic elements in the frontal activation observed in the English vs. Hindi contrast is an important question and I believe similar contrasts using non-linguistic stimuli will help delineate functional specifications in this region, without downplaying comprehension specific processing taking place in these regions, one of the objectives of experiment described in chapter 4.

Despite being a silent reading task, there is also significant overlap with low-level tonotopic maps in the superior temporal gyrus. It has been reported previously that tonotopic maps in auditory cortex overlap with temporal voice areas (Belin, 2000) in STG (Moerel et

al., 2012). Additionally, silent active reading has been shown to activate temporal voice areas (Perrone-Bertolloti et al., 2012). The present results are consistent with these findings. These results also confirm a previous finding that the tonotopic maps overlapping reading activation in the STG have a bias towards the lower frequencies (Moerel et al., 2012), a range occupied by human voices.

There are regions of reading activation, notably in superior temporal cortex, that do not overlap with topological maps; and there are similar, though smaller, non-overlapping regions in frontal cortex near the pars opercularis region. Whether or not these regions are specialized for purely linguistic processing is an important question for future research. Some recent evidence suggests that these regions may have specific functions beyond language processing (see e.g., Dick et al., 2011). It is important to keep an open mind about 'levels': an apparently lower-level area may be performing language-specific functions while an apparently higher-level area may be performing other functions besides language.

Increased activation specific to reading meaningful paragraphs was also found in occipital cortex and adjacent regions in inferior/middle temporal lobes and in the fusiform gyrus. Although these regions are not often considered as significant for high level language processing, empirical evidence from lesion studies (Rubens and Kertesz, 1983) and invasive electrophysiology (Burnstine et al., 1990; Luders et al., 1991; Krauss et al., 1996; Mani et al., 2008) suggests that the 'basal temporal language area' in the inferior temporal lobe and fusiform gyrus is as strongly linked with language functions as classical language areas. Electrical stimulation of these regions not only interferes with reading and language understanding but also often leads to speech arrest. Judging from published reports, this area may overlap some of our inferotemporal retinotopy. The transcortical sensory aphasia, where the patient exhibits poor 'Wernicke'-like comprehension, is associated with brain lesions most often in inferior temporal cortex, sometimes including the basal temporal language area, but commonly also involving visual areas in the lateral aspect of the adjoining occipital lobe (Kertesz et al., 1982; Sharp et al., 2004). It is interesting in this context that picture 'lexical items' inserted into text sentences can be effortlessly integrated into ongoing linguistic discourse comprehension, even at faster-than-normal reading speeds (e.g., Potter et al., 1986). These results show that the regions activated during text comprehension in occipital cortex encompass a number of distinct visual areas, both low level (such as V1 and V2) as

well as higher level (such as ventral V3, MT, V8, posterior inferotemporal cortex, and LIP+). Taken together, this psychological, brain lesion, and neuroimaging data suggests that some aspects of linguistic meaning assembly may be taking place within intermediate level visual areas. It should be noted that not all activation observed in the occipital cortex for English vs. Fixation was significant for English vs. Hindi contrast. It was instructive to find out where these activations (for English vs. Hindi) lie relative to well-defined distinct retiniotopic maps in posterior occipital cortex.

In contrast to the substantial overlap with visual and auditory maps, somewhat surprisingly, rather less overlap of reading activations was found with somatomotor maps. The present study used simple informative passages dealing with natural phenomena, science, information about famous people and paintings, and so on, and did not attempt to select semantic content specific for any specific sensory modality; this may have resulted in less somatosensory content than visual and auditory content. A future direction would be to see if modality specific content modulated the amount of measured overlap with particular modality-specific topological maps. For somatomotor maps, the primary overlap zone was a frontal multimodal overlap zone adjoining primary motor cortex (see next).

There were multisensory maps in several locations including lateral prefrontal and in the extreme superior and posterior part of the lateral sulcus near the supramarginal gyrus. The frontal multisensory overlap zone also overlapped reading activation, but the posterior lateral sulcus zone did not. Note that 'multisensory' is defined in the restricted sense of voxels that contain topological maps in more than one modality (not voxels that merely respond to more than one modality).

The pattern of activations for the reading experiment across the whole cortex is similar to what was found in a recent natural reading experiment reported by Choi et al. (2014). Compared to Choi et al., this study utilized controlled/matched saccades as opposed to free eye movements, and a higher resolution, fully surface-based analysis stream as opposed to a volume-based cross-subject analysis only mapped to an average surface at the end. As with this study, the activation patterns in Choi et al. exhibited eye movement related activation patterns in IPS, the FEF, and the dorsomedial frontal eye fields, as well as unique activation for text in more anterior IFG. As observed here, Choi et al. also report no activations during

natural reading in somatosensory/motor cortex. Visual activation -- likely within retinotopic areas judging from our data -- was observed even when comparing text with pseudo-words -- a closer comparison than ones used here.

There is often an implicit assumption that whatever is going on in higher level visual areas can only count as being involved in language comprehension if it were equally activated by an auditory language understanding task -- that is, by this definition, there can be no modality-specific involvement in language comprehension. Given how poorly understood the cortical neural activity patterns underlying language comprehension currently are, it is important to keep an open mind about modality specificity or functional duplication. It seems quite possible that, for example, anaphor processing may employ modality-specific representations; the cortical computations and cortical areas involved in dereferencing an auditory "that" could well be different than for resolving a printed "that" that appeared in a particular location on the page. It is difficult to directly experimentally address the question of modality-specific language activations. For example, simultaneous, retinotopically overlapping visual tasks, widespread functional disruption of higher visual areas (e.g., by transcranial magnetic stimulation), or widespread lesions to higher visual areas would disrupt naturalistic reading comprehension itself -- the object of study.

Overall, the results presented here show that topological sensory-motor maps, which play crucial functional roles in primary sensory and motor areas, are also found in some of the brain regions involved in a higher-level cognitive function such as reading comprehension. This study provides the first comprehensive overview on the interface between a high-level complex cognitive process reading comprehension, and topologically organised visual, auditory, and somatomotor representations. Determining the specific roles played by the regions identified here remains an important question for future research in the field of topological sensory-motor maps as well as language.

~~~
~~~

Chapter 4

Cortical regions involved in narrative scene comprehension overlap both topological visual, auditory and somatomotor maps, as well as regions involved in reading comprehension

*This chapter is derived from: “Cortical regions involved in narrative scene comprehension overlap both topological visual, auditory and somatomotor maps, as well as regions involved in reading comprehension”. Sood, MR and Sereno MI (in prep).

Precis

This chapter builds on the results from the previous two chapters, and the data comes from a subset of subjects who participated in the reading comprehension and mapping experiments. The experiment consisted of a narrative scene comprehension task. The main objectives were to assess (1) how brain regions processing narrative comprehension using pictures are structured relative to topological sensory-motor maps and (2) to compare and contrast the nonlinguistic scene comprehension data with the linguistic reading comprehension data discussed in the previous chapter. The cumulative dataset from these five studies brings much improved accuracy and clarity to several important debates in the field including the degree to which sensory-motor regions are involved in comprehension, the significance of maps in higher-level cortical areas, the significance of comprehension-specific activity in lower-level visual areas, and the degree to which serial assembly processes in linguistic and non-linguistic comprehension utilising the same modality overlap. The results suggest that the reading and scene activations are remarkably aligned, and share common regions in the occipito-parietal, temporal and frontal cortex. The shared activations between reading and scene comprehension also largely overlap with topological cortical maps. Finally, there are regions that are specific to either reading or scene processing; in most cases, these overlap with topological maps in occipito-parietal, temporal and frontal cortex.

4.1 Introduction

Humans are exposed to rich visual environments from the time of their birth. The first words uttered by a child are often words which name objects in his visual world. For millennia, humans have told stories using sequential images, whether on cave walls or paintings, or in contemporary society, in picture-books or films (Cohn et al., 2014). What is the neural basis of pure picture based comprehension? A majority of the relevant research in scene comprehension is focussed on isolated scenes and objects. So far several scene selective regions have been identified in the posterior occipital cortex. Among them, the two best known regions are the parahippocampal place area (PPA), a region of the collateral sulcus near the parahippocampal-lingual boundary (Epstein & Kanwisher, 1998) and the

retrosplenial complex (RSC) (Bar & Aminoff, 2003). A third region, the occipital place area (OPA) (Dilks et al., 2013) has been found around the transverse occipital sulcus. All three of these regions respond preferentially to pictures depicting scenes, spaces and landmarks compared to pictures of faces or single movable objects (for a review, see Epstein & MacEvoy, 2011). Similarly the fusiform face area, a region in mid fusiform gyrus (Sergent et al., 1992; Kanwisher et al., 1997) and the occipital face area, a region in lateral occipital cortex in the vicinity of inferior occipital gyrus (Puce et al, 1996; Yovel and Kanwisher, 2005) show preferential selectivity to faces while a region in lateral occipital cortex inferior to V3A has been shown to prefer objects over scrambled objects.

Comparatively, only a few studies have looked across the whole brain when participants watched more naturalistic stimuli such as movies (Bartels and Zeki, 2004; Hasson et al., 2004, 2008; Haxby et al., 2011; Nishimoto et al., 2011, Huth et al., 2013). These studies have shown that the BOLD activity evoked by natural movies extend well beyond occipital cortex and is spread across temporal, parietal and frontal cortex. While considerable effort has gone into analysing the retinotopic map architecture underlying scene selective regions in the occipital cortex , no studies so far has looked at scene selective regions relative to topological sensory-motor maps in higher level cortices.

In the study presented here, the same subjects who took part in the reading comprehension and sensory-motor mapping experiments (described in previous chapters) participated in a 'picture based narrative comprehension' fMRI task. The subjects viewed a series of pictures adapted from wordless picture story books. Participant's saccades across each single- or multi-frame picture page were controlled by 'saccading' a transparent gaussian 'bubble'-style mask (at 1 Hz) to relevant points in the images chosen by offline comprehension testing. This experiment was designed in the same spirit as the reading comprehension, so that participants comprehended a narrative story assembled across 30-50 saccades, and so that the eye movements were exactly matched and controlled across conditions. The idea was to go beyond simple isolated scene comprehension and engage the brain in deriving meaning implied by a meaningful series of pictures. The data from this study was combined with four sets of cortical mapping and reading comprehension data that I had already collected, providing a unique data set that combined reading and picture comprehension with visual, auditory and somatomotor mapping in the same set of subjects.

There were two primary objectives behind this study. Firstly, to site narrative scene comprehension regions relative to topological retinotopic, tonotopic and somatomotor maps across the whole cortex. While initially it was thought that the scene/object selective regions in occipital cortex fell beyond the bounds of retinotopy, subsequent discoveries in retinotopic maps have shown that most of the scene/object selective regions in the posterior occipital cortex fall within or adjacent to retinotopic maps. There has not been a systematic effort to localise the higher level (beyond occipital cortex) scene processing regions relative to topological sensory-motor maps discovered in frontal, parietal and temporal lobe. This study will shed light on the underlying neural organisation of these regions and allows us to accurately site these regions with respect to known topological map locations.

Secondly, by combining this data with the reading comprehension data described in chapter 3, we can draw stronger inferences regarding the degree to which the serial assembly processes in linguistic and non-linguistic comprehension using the same modality intersect and diverge. Despite the obvious differences, comprehending a story from a series of pictures is in many ways akin to deriving meaning from reading a passage consisting of a series of words. Scene comprehension, like language is fundamentally serial in nature. The integration of successive glances in the comprehension of a visual scene (and even more in a series of pictures) requires a kind of serial assembly operation similar to the serial integration of word meaning in language comprehension. Isolated 250 msec glances taken out of context are as ambiguous as a single word taken out of discourse context (Sereno, 2014). Although a linguistic task such as reading and narrative visual comprehension involve cognitive processes unique to each (orthographic, phonological, lexical-syntactic for reading; object processing, relation to background processing, gist processing in scene comprehension), there are also several processes which could very well be shared between the two, such as semantic access, event segmentation, discourse structure building and so on. I hypothesised that the brain regions previously identified in reading comprehension (chapter 3) might at least be partially shared with the activation observed during this task, in both pre central and post central cortex.

Finally, as in the previous studies in this thesis, the data was analysed using a fully surface based group analysis pipeline which provides more precise cross-subject averaging. And by

suppressing individual differences through the re-use of the same subjects, we were able to draw stronger comparative conclusions.

4.2 Materials and Methods

4.2.1 Subjects

The data presented in this chapter come from nine (5 males) of our original 20 participants. The experimental protocols were approved by local ethics committees and participants gave their informed written consent prior to the scanning session.

4.2.2 Experimental Stimuli and Design

Narrative scene comprehension Experiment: The picture based comprehension experiment consisted of comprehending a coherent story from a series of pictures (no text captions of any kind). The stories presented in the experiment came from 12 wordless picture story books. Any text in the pictures was edited out in Photoshop. Each page of the book was not presented in its entirety. Instead, a transparent gaussian 'bubble'-style mask (fwhm: 512 pixels) was moved in a saccadic fashion over relevant parts of the page (at 1 Hz) and the subjects were instructed to move their eyes along with the mask to follow the story in the page. The mask locations were carefully chosen by offline comprehension testing. Each book's presentation time was thus determined by the total number of mask/saccade locations across all pages. The book presentation time varied between 30-50 seconds. Each book was presented in a separate run (12 runs in total). In each run, 3 conditions and a fixation screen were presented (Figure 4.1). In the main experimental condition (story), the pictures were presented in the same order as they appeared in the books. In the second condition (jigsaw), jigsawed version (each page fragmented into 40x40 pixel rectangular blocks and the blocks shuffled) of the book pages were presented. Although the page order remained same, the jigsaw made the book pages incomprehensible. The same Gaussian ‘bubble’ mask locations as those used for the 'story' condition were used. In the third condition (shuffle), the presentation order of the scenes in the book was shuffled. In the shuffle condition, the subjects eventually saw all the scenes that were seen in the 'story' condition, but the temporally coherent story structure was disrupted by shuffling. Since the jigsaw screen has a

rectangular grid pattern (which results in high spatial frequencies), a 40x40 pixel grid pattern was superimposed on the Story/Shuffle pages as well. The length of each of the three conditions were the same and equal to the number of mask locations used for the respective book. Before the start of each condition, a start screen was presented for 2 seconds. The book and the shuffle conditions were always separated by a jigsaw condition. In roughly half the runs (selected randomly) Story condition came before Jigsaw while in the rest, Shuffle condition came before jigsaw. The fixation screen (15 seconds in duration) was presented at random anywhere within the run. For all three experimental conditions, participants were instructed to saccade along with the mask location. The stimulus presentation mode used here, where different parts of the picture page was made visible briefly, served several purposes. In the spirit of the classic attention study by Posner (1980), the subject's exogenous attention is automatically drawn towards highlighted higher contrast regions in the peripheral visual field thus ensuring exogenous attentional control across all experimental conditions. This presentation mode also ensured that participants made controlled eye saccades (and extremely similar eye movements across conditions) as opposed to uncontrolled eye movements if the picture pages were presented unmasked for free viewing. Additionally, this presentation mode ensured all subjects had much more similar viewing experience when comprehending the picture stories.

In order to further ensure that participants stayed attentive and made similar eye-movements for all conditions, they were asked to press a button when a red dot was presented (at random) at the centre of the gaussian mask. When the task occurred in the fixation screen, the fixation dot turned red for a duration of 1 second. The level of comprehension achieved for the stories were measured with a questionnaire afterwards. Participants were informed of this quality control process before the scan.

The stimulus presentation framework was programmed in C/OpenGL/X11. The stories were adapted from the following 12 wordless picture books: *Flotsam* by David Wiesner , *Journey* by Aaron Becker, *Freefall* by David Wiesner, *Tuesday* by David Wiesner, *Goodnight Gorilla* by Peggy Rathmann, *The grey lady and the strawberry snatcher* by Molly Bang, *Window* by Jeannie Baker, *Oops* by Arthur Geisert, *Belonging* by Jeannie Baker, *Changes Changes* by Pat Hutchins, *Deep in the forest* by Brinton Turkle and *Pancakes for breakfast* by Tomie dePaola.

Although this task involved a lot more than isolated scene comprehension, for simplicity of description, I will use ‘scene comprehension’ to describe the task in the rest of this chapter.

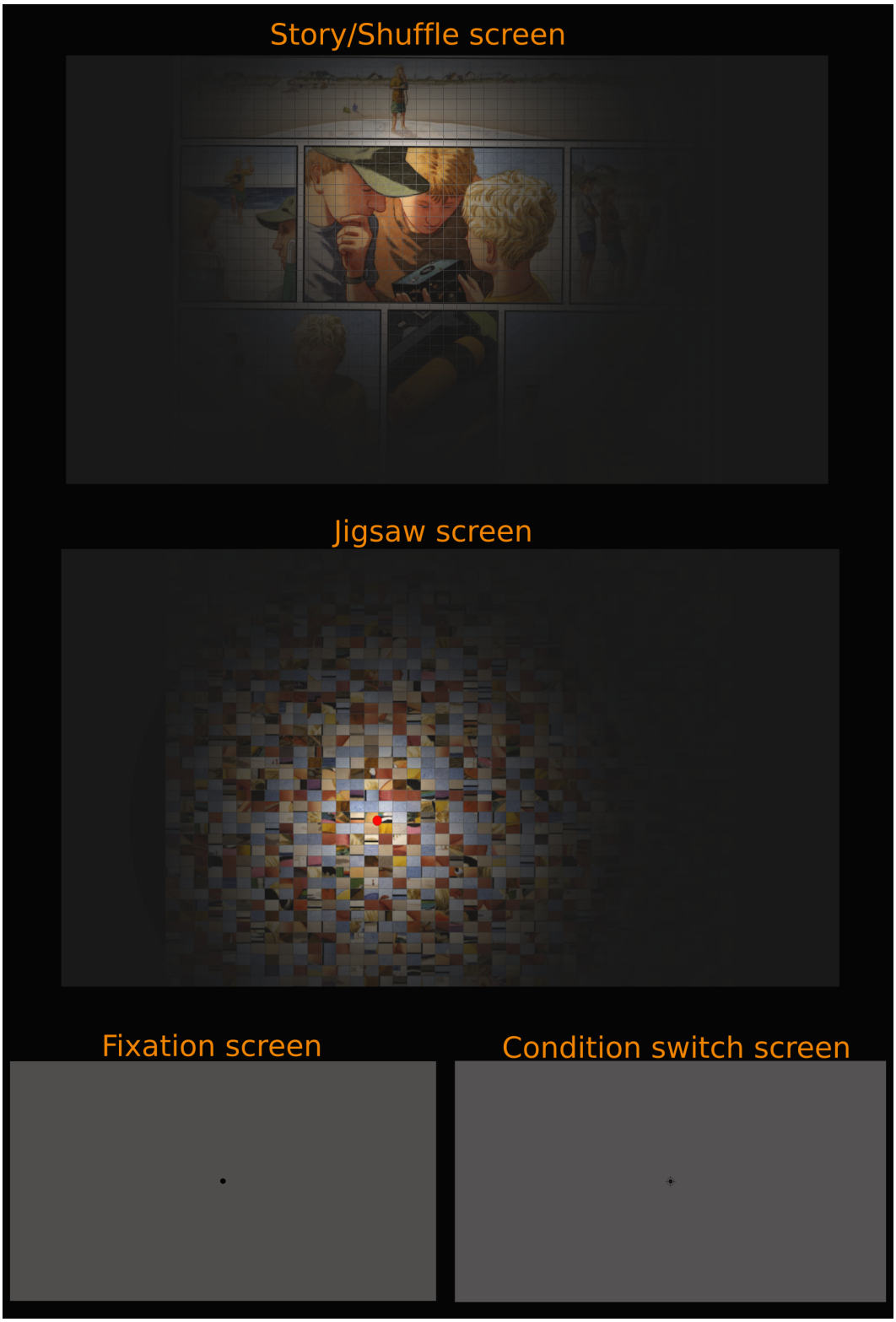

Figure 4.1: Stimuli screens

4.2.3 Experimental Set-Up

The stimuli were back projected at HDMI (1920 x 1080 pixels) resolution onto a screen inside the bore of the magnet almost flush with the back of the head coil that was visible to the subjects via a mirror; viewing distance was 30 cm. Memory foam cushions (NoMoCo Inc.) were packed around the head to provide additional passive scanner acoustical noise attenuation and to stabilize head position. Responses were made via an optical-to-USB response box (LUMItouch, Photon Control, Burnaby, Canada) situated under their right hand. I used a 30 channel head coil, with the eye coils removed (as opposed to the standard 32 channel head coil) for these scans. The lack of eye coils greatly improved the viewing experience (preventing disruptive saccade-direction-dependent blocking of the view of one or the other eye) without affecting the signal-to-noise in any part of the brain except for a slight reduction at the extreme tip (< 5mm) of the orbitofrontal pole.

4.2.4 Imaging Parameters

Functional images were acquired on a 1.5 T whole-body TIM Avanto System (Siemens Healthcare), at the Birkbeck /University College London Centre for NeuroImaging (BUCNI), with RF body transmit and a 30-channel receive head coil. For all subjects, images were acquired using multiband EPI (40 slices, 3.2x3.2x3.2mm, flip=75°, TE=54.8ms, TR=1sec, accel=4) (Moeller et al., 2011). To allow longitudinal relaxation to reach equilibrium, 8 initial volumes were discarded from each run for multiband EPI. For each imaging session, a short (3 min) T1-weighted 3D MPRAGE (88 partitions, voxel resolution 1x1x2mm, flip angle=7°, TE=4ms, TI=1000ms, TR=1370ms, mSENSE acceleration=2x, slab-selective excitation) was acquired with the same orientation and slice block centre as the functional data (‘alignment scan’), for initial alignment with the high-resolution scans (acquired as part of the previous experiments) used to reconstruct the subject’s cortical surface.

4.3 Data Analysis

The analysis of picture-story comprehension data utilised the FSL-Freesurfer cortical surface based pipieline used also for the analysis of reading experiment data (chapter 3). The cortical surface reconstructions (discussed in chapters 2 & 3) were utilized for data analysis

of picture-story data as well. The overlap analysis with topological visual, auditory and somatomotor maps followed the same methods described in chapter 3.

Analysis of picture-story data: The data analysis utilised the FSL-Freesurfer cortical surface based analysis pipeline followed in the reading experiment (Chapter 3). The single subject fMRI data was motion corrected and skull stripped using FSL tools (MCFLIRT and BET). First level fMRI analysis was carried out by applying the General Linear Model (GLM) within FEAT using FILM prewhitening (FSL, version 5) with motion outliers (detected by fsl_motion_outliers) being added as confound regressors if there was more than 1mm motion (as identified by MCFLIRT). All subjects had minimal motion (maximum displacement well under 1 mm). The high-pass filter cut-off was estimated using the FSL Feat tool based on the power spectra of the design matrices. Three main explanatory variables were modelled and controlled: story, jigsawed story and shuffled story. Button press responses to target 'red dot' were modelled as the fourth regressor. In order to capture slight deviations from the model, temporal derivatives of all explanatory variables convolved with FEAT's double gamma hemodynamic response function (HRF) were included. The registration from functional to anatomical (6 DOF) and standard space (12 DOF) was first done using FSL's FLIRT and further optimized using boundary based registration (bbregister; FreeSurfer) similar to the procedure for the reading experiment. A fixed effects analysis was performed across 12 runs from an individual subject to get group FEAT (GFEAT) results of first-level contrast of parameter estimates (COPEs) and their variance estimates (VARCOPEs) in the standard space. Across-subject group analysis was then carried out on the cortical surface using FreeSurfer tools. The GFEAT results of each subject were first sampled to individual cortical surfaces and then resampled to the spherical common average reconstructed surface (fsaverage). Surface based spatial smoothing of 3mm FWHM was applied on the icosahedral sphere. A mixed effects GLM group analysis was performed on the average surface using the mri_glmfit program from FreeSurfer. Significance maps were thresholded at $p<0.01$ and were then corrected for multiple comparisons with cluster-based correction using in-house program surfclust (analysis program provided by Martin Sereno), with clusters greater than 40 mm^2 (on a smoothwm surface) excluded yielding a corrected significance of $p<0.05$. Finally corrected significance values ($p<0.05$) of scene comprehension activation were displayed on the fsaverage surface.

The single subject raw data was not spatially smoothed in 3D, although a 10 step (~3mm FWHM) surface level smoothing is applied for final illustration of the results. Hence the 3D, Gaussian random field based cluster correction provided by FSL is not appropriate for multiple comparison correction of the language data. I have instead used the surface based cluster correction using surfclust. The GFEAT results were sampled to their respective anatomical surface, thresholded at $p<0.001$ ($Z=3.09$) and corrected for multiple comparisons with cortex surface clusters smaller than 30 mm^2 excluded, achieving a corrected p-value of 0.01.

The target (detecting the occasional 'red dot') presentation timings and the button press events were logged during the experiment and analysed to assess the performance of the task. For each participant, the number of targets detected and the mean response time in each condition were calculated. The cross-subject mean response time and target detection rates were assessed for significant differences across conditions.

4.4 Results

As in the previous chapter, I begin by first illustrating the *amplitude* of the vertex-wise response for all relevant scene contrasts. The next set of results present the overlap of scene activation with retinotopic, tonotopic and somatomotor maps. The last set of results illustrate the overlap between scene, reading and maps.

The main scene contrast utilised for overlap analysis with sensory-motor maps is story vs. jigsaw contrast. The scene activation is illustrated as transparent overlays over single modality phase hue maps, finally leading up to a summary outline figure containing all four kinds of data. For clarity, in later overlap figures, only positive activation (for story vs. jigsaw) after thresholding and cluster correction is shown. The overlap results for different modalities are illustrated for three individual subjects and then for the group as a whole. For the cross-subject average, the sensory-motor maps are illustrated for two separate vertex thresholds; $p<0.05$ (lower threshold) and $p<0.01$ (higher threshold), corrected for multiple comparisons using cluster thresholding at $p<0.05$. As in the Reading data (chapter 3), the scene data illustrated here uses a vertex threshold of $p<0.01$ in all cross-average images. For

the individual subjects, results are illustrated at a vertex threshold of $p<0.001$, corrected to $p<0.01$ for both scene and mapping data.

For overlap with reading activation, the cross-subject scene contrast (story-jigsaw) is illustrated as a transparent overlay over the reading (English-Hindi) activation. The scene and reading group average data are depicted for two vertex thresholds $p<0.01$ and $p<0.05$, cluster corrected to $p<0.05$. An extra omnibus figure shows the sensory-motor map locations added as outlines over the scene-language overlap illustration.

All 9 subjects who participated in the scene experiment gave satisfactory performance in the target detection task, and comprehension assessment, as well as having motion well under our threshold of 1 mm. The activation for the target detection regressor (button press regressor) was used as an extra quality check to decide whether the subject performed the task as per the instructions during each run. All our subjects had comparable performance across conditions in the target detection task and motor activation for the target regressor. The mapping results illustrated here are same as those illustrated in chapter 2 and 3.

4.4.1 Target detection response

The target detection response time was calculated as the time it took for participants to respond to the target after the target presentation start time, target was presented for a second after the start time. On average, participants took 1.08 seconds ± 0.01 (SEM) to respond to the target when it occurred in story, 1.13 seconds ± 0.09 (SEM) in Jigsaw, 1.08 seconds ± 0.05 (SEM) in shuffle and 1.38 ± 0.06 (SEM) in fixation. A Wilcoxon matched-pairs signed-ranks test indicated no significant differences between ‘story’ (median= 1.06 seconds) and ‘jigsaw’ (median=1.08 seconds) ($Z=-0.06$, $p=0.95$) or between ‘story’ and ‘shuffle’ (median = 1.31 seconds; $Z=-0.42$, $p=0.68$). The differences between ‘story’ and ‘fixation’ (median = 1.31 seconds) was found to be significant ($Z=-2.67$, $p=0.008$).

On average, participants managed to detect 73% ± 0.06 (SEM) targets in the ‘Story’ condition, 80.9% ± 0.03 (SEM) in ‘Jigsaw’ condition, 79.6% ± 0.07 (SEM) in ‘Shuffle’ condition and 93.6% ± 0.03 (SEM) in ‘fixation’. A Wilcoxon matched-pairs signed-ranks test was carried out to assess statistical significance of the average success rate. The median success rate for targets in story, jigsaw, shuffle and fixation were 71.4%, 85.7%, 83.3% and 100% respectively. There were no significant differences between ‘story’ and ‘jigsaw’ or

'story' and 'shuffle' (story-jigsaw: Z=-1.41, p=0.16; story-shuffle: Z=-0.771, p=0.44). The performance in fixation condition was significantly better (Z=-2.2, p=0.03), not surprisingly as the target was easier to discern in the fixation condition.

4.4.2 Scene Activation:

Figures 4.2, 4.3 and 4.4 illustrate the average cross-subject activation for a stairstep of t-values (all above a minimum threshold of $p<0.05$, uncorrected) for each condition (story, jigsaw and shuffle) relative to fixation (Fig. 4.2), and those for two main contrasts, story vs. jigsaw and story vs. shuffle (Fig. 4.3 and Fig. 4.4).

In the cross-subject activation for Story vs. Jigsaw (Fig. 4.3(top) and 4.4A), the most extensive activation is observed in the posterior occipital cortex. The left hemisphere activation covers the entire lateral occipital cortex. There are several branches which extend beyond lateral occipital, one branch extends into the temporal lobe, stretching across MT and posterior STS reaching up to STG. Another offshoot reaches up to intraparietal sulcus (IPS) covering regions in superior parietal lobules. The next offshoot stretched nearly half the length of the inferior temporal gyrus and extended ventrally onto the fusiform gyrus joining the medial activation covering most of collateral sulcus and part of parahippocampal cortex, stretching across lingual gyrus, calcarine sulcus and reaching beyond parieto-occipital sulcus. There is also strong activation in precuneus. The occipital cortex has been known to have several scene selective regions (parahippocampal place area, retrosplenial complex, occipital place area) and object selective regions (lateral occipital cortex) and face selective regions (fusiform face area, occipital face area). The activation observed for Story vs. Jigsaw is consistent with the above findings (PPA and RSC locations annotated in figures are based on the functional localizations identified by Nasr et al. (2011) on fsaverage surface). Regions in occipital cortex which did not show a significant difference in activation between Story and Jigsaw included early visual areas such as V1, V2 (especially the foveal regions) and the adjoining cuneus cortex.

In the left frontal cortex, there are two distinct activation zones — one on the precentral sulcus near FEF (visible at a lower threshold of $p<0.05$) and another near the inferior frontal sulcus (IFS) in the pars opercularis region. In the left temporal cortex, apart from the

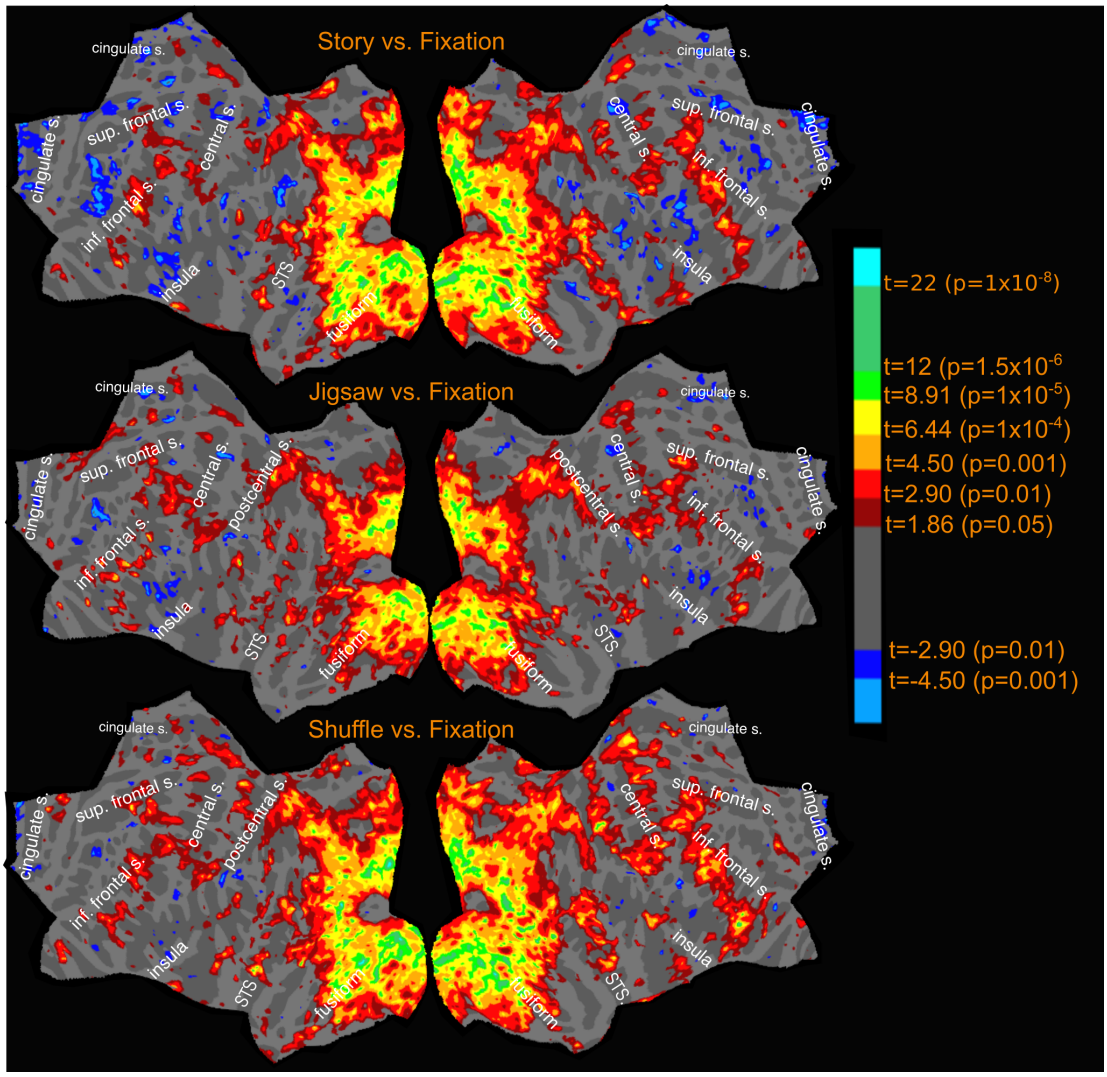

Figure 4.2: Narrative scene comprehension- Activation amplitude profile (uncorrected) for relevant contrasts

occipital branch extending into the temporal cortex across MT, there is a well separated inferior, anterior activation zone in the superior temporal sulcus.

The activation pattern in the right hemisphere, though similar has some notable differences. The posterior occipital cortex activation is similar to their left hemisphere counterparts, but more spread out covering a larger total extent of cortical area. In the right temporal cortex, there is significant activation along the entire superior temporal sulcus. The right frontal cortex also exhibit more extensive activation with activation spread along precentral sulcus.

The single subject activation for Story vs. Jigsaw was strikingly similar to the cross-subject profile, with activated regions corresponding to the regions described above.

In the shuffle condition, subjects saw exactly the same scenes as in the story condition, but in a different temporal order. The activation pattern for Shuffle vs. Fixation is very similar to Story vs. Fixation as expected. Although not obvious in Figure 4.2, there is significant

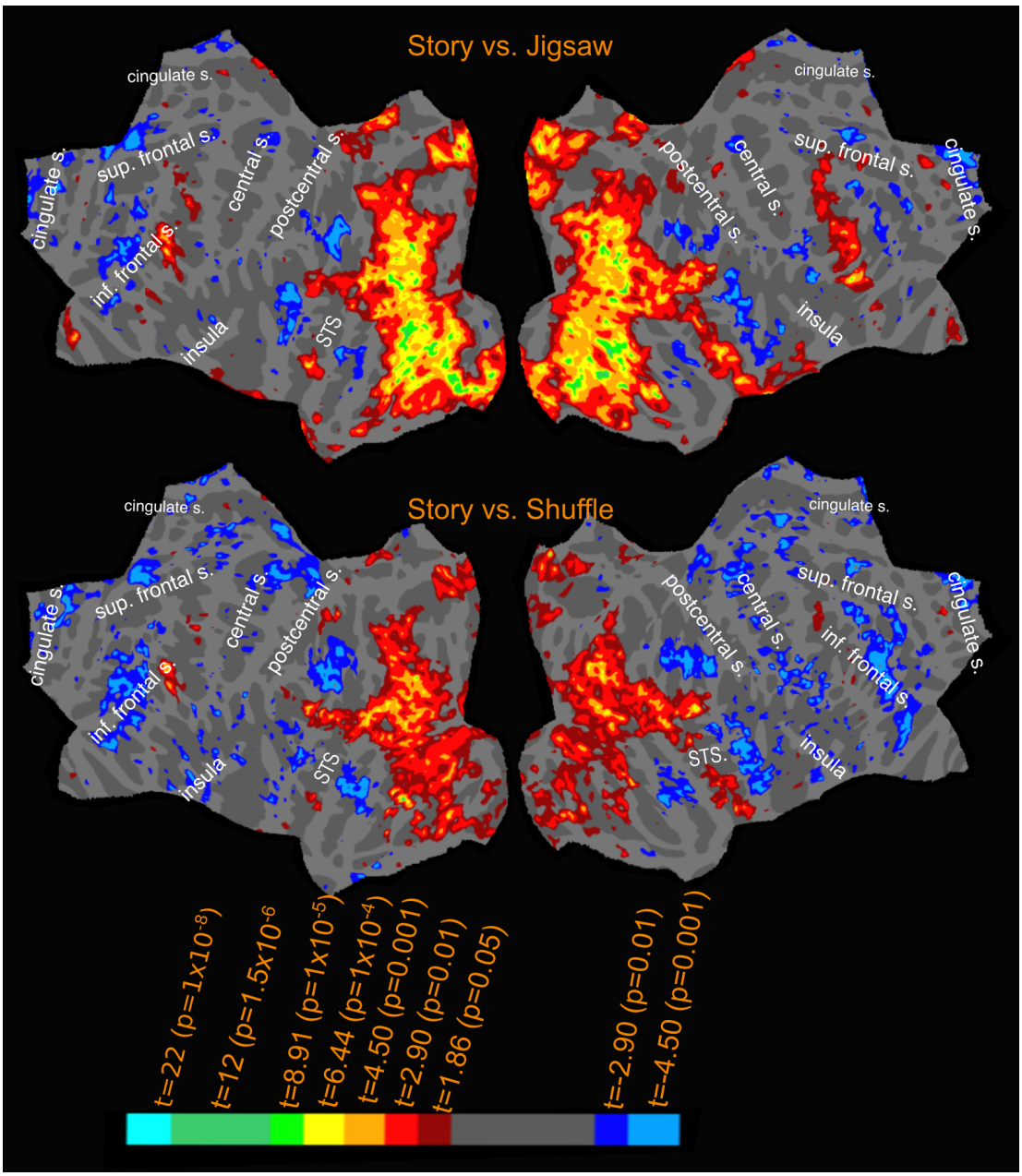

Figure 4.3: Narrative scene comprehension- Activation amplitude profile (uncorrected) for relevant contrasts (continued)

differences between Story and Shuffle conditions and the activation pattern for Story vs. Shuffle show remarkable alignment to the regions activated in Story vs. Jigsaw condition, albeit with a much lower significance value. In the left hemisphere, significant activation (Figure 4.3, 4.4B) was observed in the lateral occipital cortex, in the branch leading up to STG, as well as in the anterior STS and in the inferior frontal cortex. The activations observed in inferior frontal cortex, anterior STS and part of lateral occipital cortex were exclusive to Story and Shuffle conditions and was absent in the Jigsaw condition. All these regions were still significantly more active in the Story condition as compared to the Shuffle

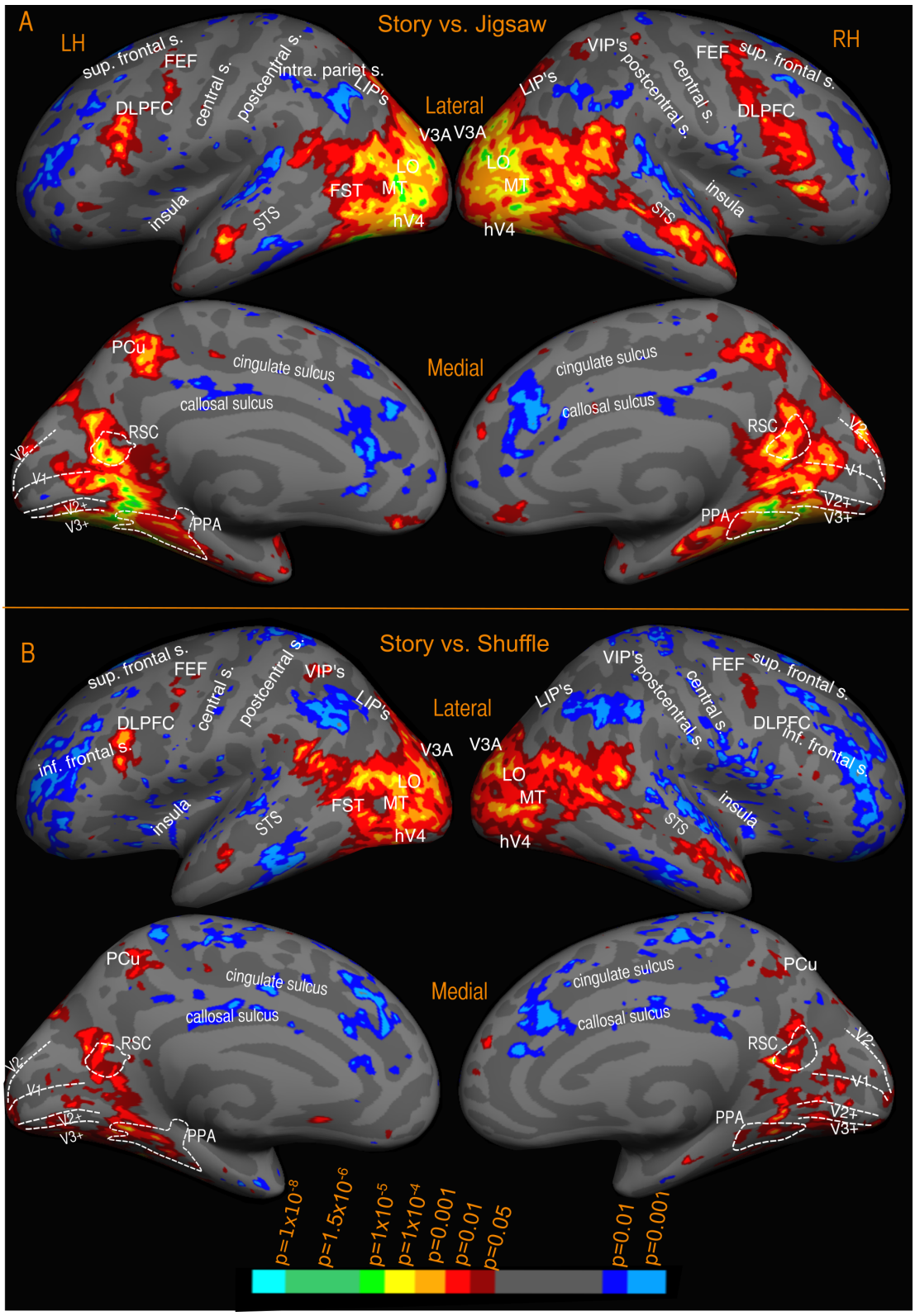

Figure 4.4: Narrative scene comprehension- Activation amplitude profile (uncorrected) for relevant contrasts (annotated lateral and medial views)

condition. On the medial wall, the activation profiles of Story and Shuffle (vs. Fixation) look very similar, while Jigsaw had no activation notably in precuneus and reduced activation in parieto-occipital sulcus and in the region of left PPA. Unlike the lateral occipital cortex, the

medial activation for Story-Shuffle condition was more attenuated. There was however less extensive but significant activation in precuneus, and along the parieto-occipital sulcus extending across RSC and the peripheral regions of early visual areas joining up with activation in the vicinity of PPA .

The activation pattern for Story vs. Shuffle in right hemisphere was similar, with most of lateral occipital and right STS activation still significantly higher for Story than in Shuffle. Much of the activation observed in right frontal cortex for Story vs. Jigsaw was not observed in Story vs. Shuffle condition and the medial activation was largely reduced showing the same pattern as in left hemisphere.

4.4.3 Overlap of scene (Story vs. Jigsaw) activation with visual, auditory, and somatomotor maps

The main contrast used in the overlap figures to assess scene comprehension was story vs. Jigsaw. In the figures depicting overlap with sensory-motor maps, transparent bright yellow regions outlined in black depict the regions that showed significantly higher activation when viewing story compared to jigsaw.

For the cross-subject activations, the visual, auditory, and somatomotor activations were assessed for two different hard vertex wise thresholds before cluster exclusion correction: $p<0.01$ (higher threshold) and $p<0.05$ (lower threshold). Scene activation used a single higher hard vertex threshold of $p<0.01$. For single subject activations, scene, retinotopic, and tonontopic maps were hard thresholded at $p<0.001$, corrected to $p<0.01$. Among the single subjects included below, subject-3 represents the same subject-3 who participated in Reading experiment. Subjects 1 and 2 are different from the single subjects illustrated in Reading experiment. The overlap estimates below, are expressed as the percentage of scene activation intersecting with sensory-motor maps. The results include an overall estimate, where the percentage of total scene activation overlapping with retinotopic, tonotopic and somatomotor maps is reported for each hemisphere. Additionally, each region (frontal, temporal and occipito-parietal) for scene activation is considered separately, and corresponding overlap is expressed as a percentage of the regional scene activation. Overlap estimates are summarised in Table 4.1

Scene overlap with retinotopic maps: The retinotopy/scene overlap for the cross-subject surface average is shown in Figures 4.5 and 4.6. Most of the scene activation in occipito-parietal cortex, falls within retinotopic regions in both hemispheres. Part of the activation in parahippocampal cortex, parieto-occipital sulcus and precuneus on the medial side falls outside the bounds of retinotopy. While the posterior superior temporal activation largely falls within retinotopy, the activation along STS does not overlap with retinotopic maps. There is also significant overlap in the frontal cortex, and the activation near inferior frontal sulcus partially overlaps with retinotopic maps.

Overall, at higher threshold (Figure 4.5) more than 65% of the cross-subject scene activation in both hemispheres falls within retinotopic areas (LH: 80%, RH: 67%) rising up to more than 70% at lower threshold (LH: 85%, RH: 74%) (Figure 4.6). In occipito-parietal cortex, the estimates are 84% in LH and 77% in RH at higher threshold, rising to 89% and 83% respectively when the threshold is lowered. In the temporal cortex, there is only a modest overlap with retinotopy with 3% of LH and 12% of RH activation overlapping with retinotopy at higher threshold rising to 17% and 23% respectively at lower threshold. There is also substantial overlap in the frontal cortex with around 54% of LH and 15% of RH activation falling within retinotopic regions at higher threshold rising to 75% and 47% respectively at lower threshold.

For the individual subjects (Figures 4.7, 4.8), the overall left hemisphere retinotopy/scene overlap in LH was 66% for subject-1, 55% for subject-2 and 75% for subject-3 , while the right hemisphere overlap was 60% for subject-1, 72% for subject-2 and 56% for subject-3.

Zooming in on individual regions, as with the cross-subject average, there is more than 60% overlap between scene and retinotopy in occipito-parietal cortex in both hemispheres (subject-1: 73%, subject-2: 60%, subject-3: 77% in LH and subject-1: 70%, subject-2: 78%, subject-3: 64% in RH). In the left hemisphere frontal and temporal scene activation, overlap with retinotopy is 33% and 13% in subject-1 and 39% and 29% in subject-2 and 18% and 51% for subject-3. The corresponding overlaps for the right hemisphere of these subjects are 27% (frontal) and 33% (temporal) for subject-1, 53% (frontal) and 47% (temporal) for subject-2 and 16% (frontal) and 17% (temporal) for subject-3.

In the retinotopic map underlays illustrated in Figures 4.5-4.8, the green colour indicates lower contralateral visual field, blue indicates horizontal meridian and red indicates upper

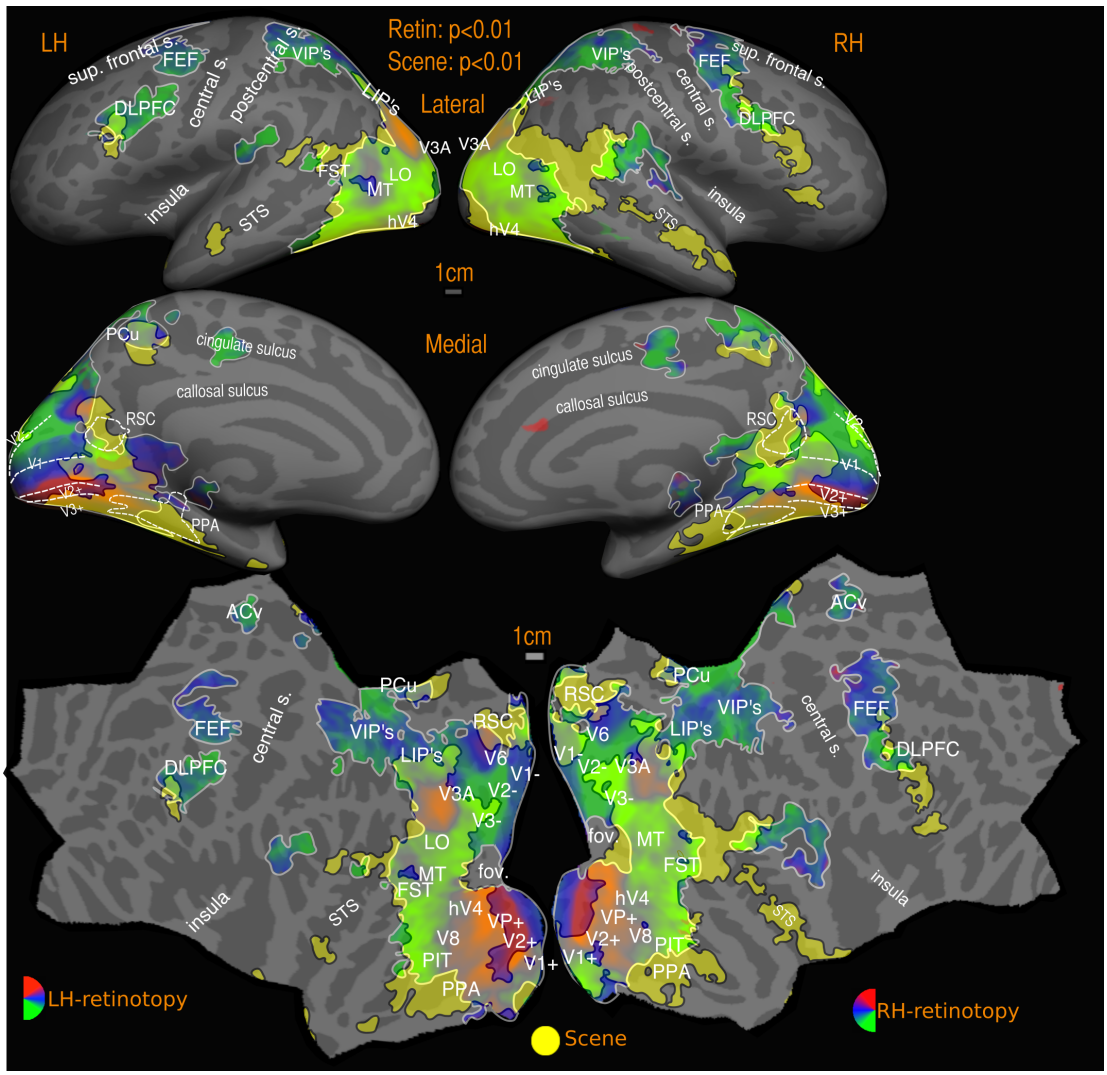

Figure 4.5: Overlap of SCENE (Story vs. Jigsaw) with RETINOTOPIC maps- GROUP (higher threshold)

Reported p values are vertex thresholds used before cluster thresholding. All activations are cluster thresholded to p<0.05.

visual field. In the group results, in both hemispheres the occipital scene activation on the lateral side overlaps roughly equally with lower, middle, and upper visual fields. In higher-level retinotopic areas, there was a slight predominance of horizontal meridian and lower visual fields (at an individual level some subjects did not show this bias, as observed in subject 1 selected for scene overlap analysis). There are two reasons for this. First, because retinotopic maps in higher-level visual areas are smaller, slight inter-subject displacements in the location of these maps has a tendency to reduce the range of polar angles in the average map. This 'regression toward the horizontal meridian' results in an overrepresentation of the horizontal meridian in the average. Another possible source of a horizontal meridian and particularly lower field emphasis is that subjects in our direct-view experiments had to lower their gaze somewhat to fixate the centre of the close-up screen. Given that there is evidence

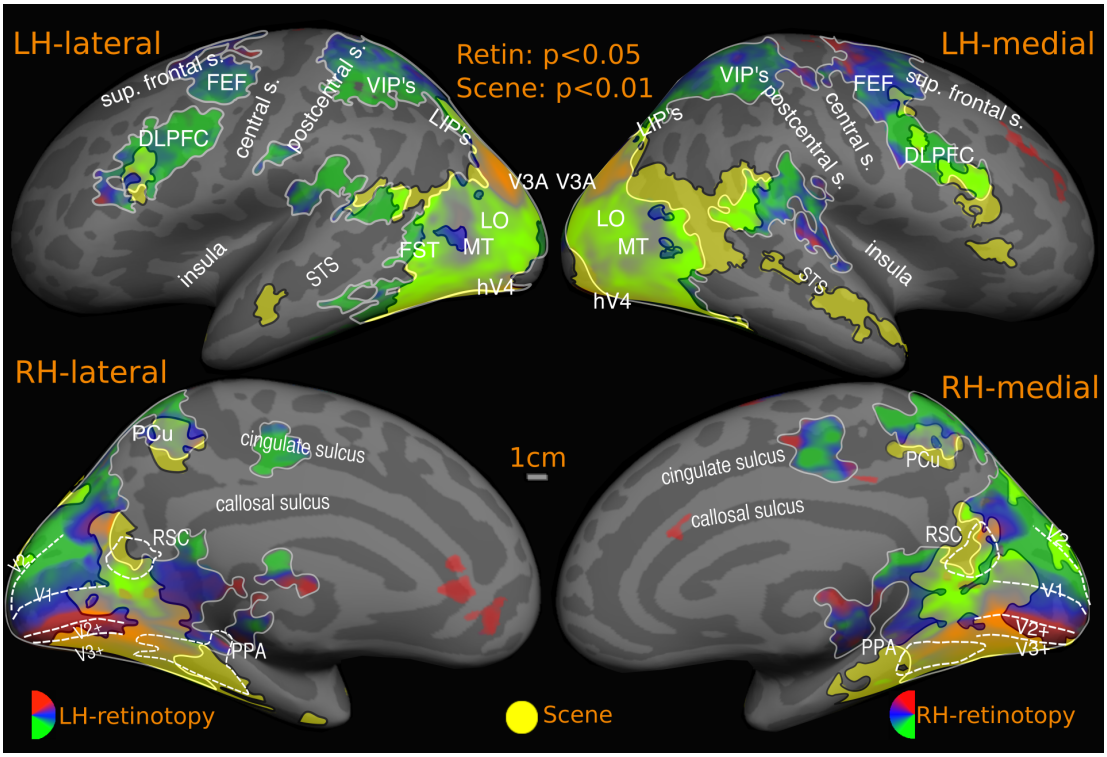

Figure 4.6: Overlap of SCENE (Story vs. Jigsaw) with RETINOTOPIC maps- GROUP (lower threshold)

Reported p values are vertex thresholds used before cluster thresholding. All activations are cluster thresholded to p<0.05.

for head-centered remapping of receptive fields in some higher visual areas (e.g., see Sereno and Huang, 2006), the lowered gaze may have remapped the entire visual field toward the lower field, resulting in an overemphasis of the lower field in both individual subjects as well as the average.

Scene overlap with tonotopic maps: In the left temporal cortex, the tonotopic maps overlap partially the activation in posterior STG, but the significant activation in the anterior STS is outside the bounds of tonotopic maps. The frontal lobe scene activation also substantially overlaps with frontal tonotopic maps. These are also potential sites of multi-sensory integration since these regions contain both retinotopic and tonotopic maps. These findings are consistent in the cross-subject average as well as in individuals.

The overall tonotopy/scene overlap (Fig. 4.9) estimates for cross-subject average are 0.19% (LH) and 1.4% (RH) for the higher threshold, and 1% (LH) and 6% (RH) for the lower threshold in the cross-subject average. In left temporal cortex, the level of overlap is 3% at the higher threshold and 6% at the lower threshold. In the right hemisphere, temporal scene activation is more extensive compared to left hemisphere, and the tonotopy overlap estimates

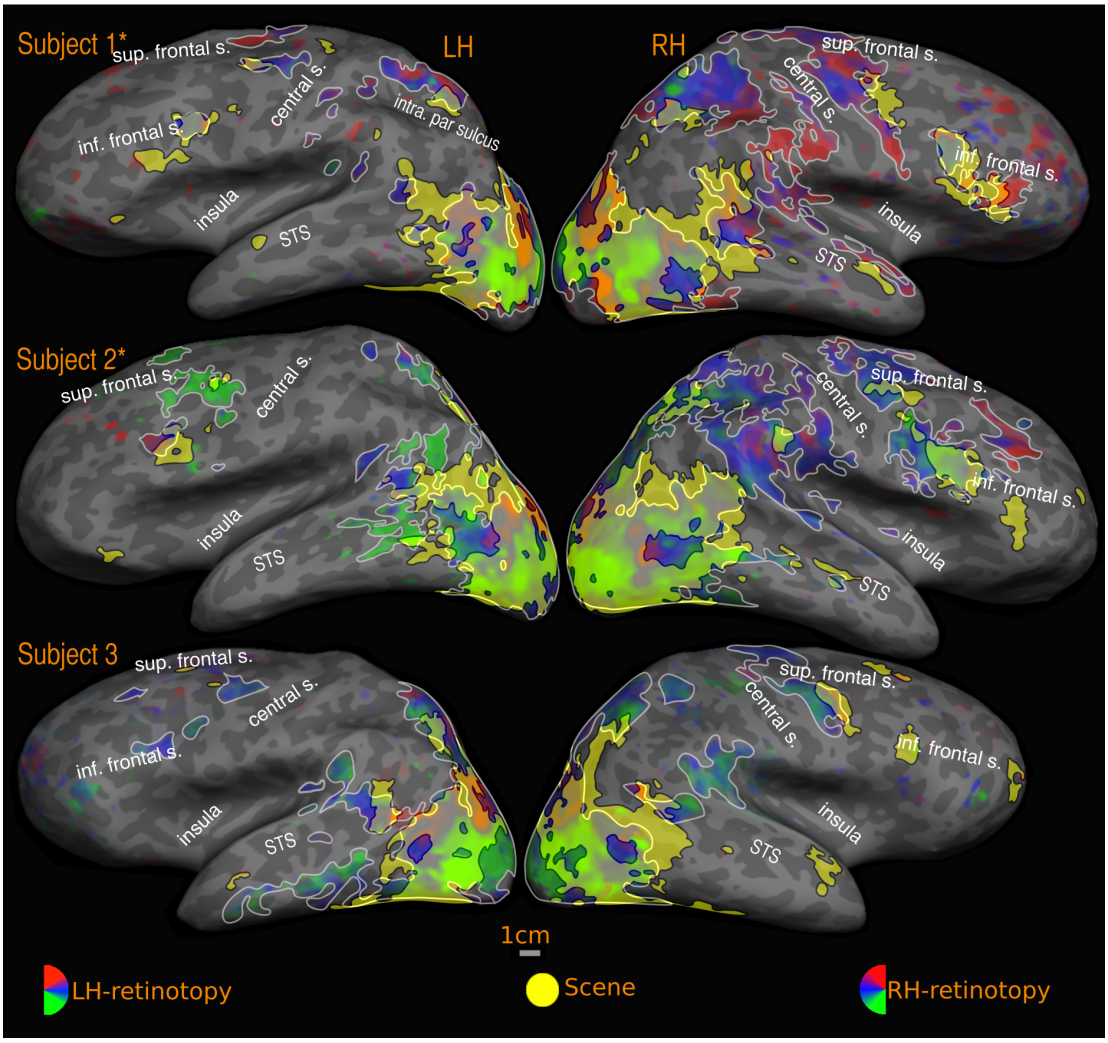

Figure 4.7: Overlap of SCENE (Story vs. Jigsaw) with RETINOTOPIC maps- individual SUBJECTS (Lateral view).

Activations are illustrated at p<0.001, corrected to p<0.01. Subject-3 is same as corresponding subject in Reading experiment. Subjects 1 and 2 are different.

are 11% at higher threshold rising to 34% at lower threshold. The tonotopic maps also overlap with frontal scene activation in both hemispheres: 3% (higher threshold) and 42% (lower threshold) in left hemisphere and 6% (higher threshold) and 60% (lower threshold) in the right hemisphere.

Among the individual subjects, subject-1 and subject-2 exhibit a similar profile to the higher threshold group profile (note that the single subject activations are thresholded at p<0.001), while subject-3 has a much more extensive overlap with tonotopic maps. Overall, around 0.2% in subject-1, 0.5% in subject-2 and 3% in subject-3 overlapped with tonotopy in the left hemisphere. Around 4%, 3% and 9% overlap was observed in the right hemisphere for subject-1, subject-2 and subject-3 respectively. Looking at the regional activations, in subject-1, 2% of left frontal activation and 21% of right frontal activation overlaps with

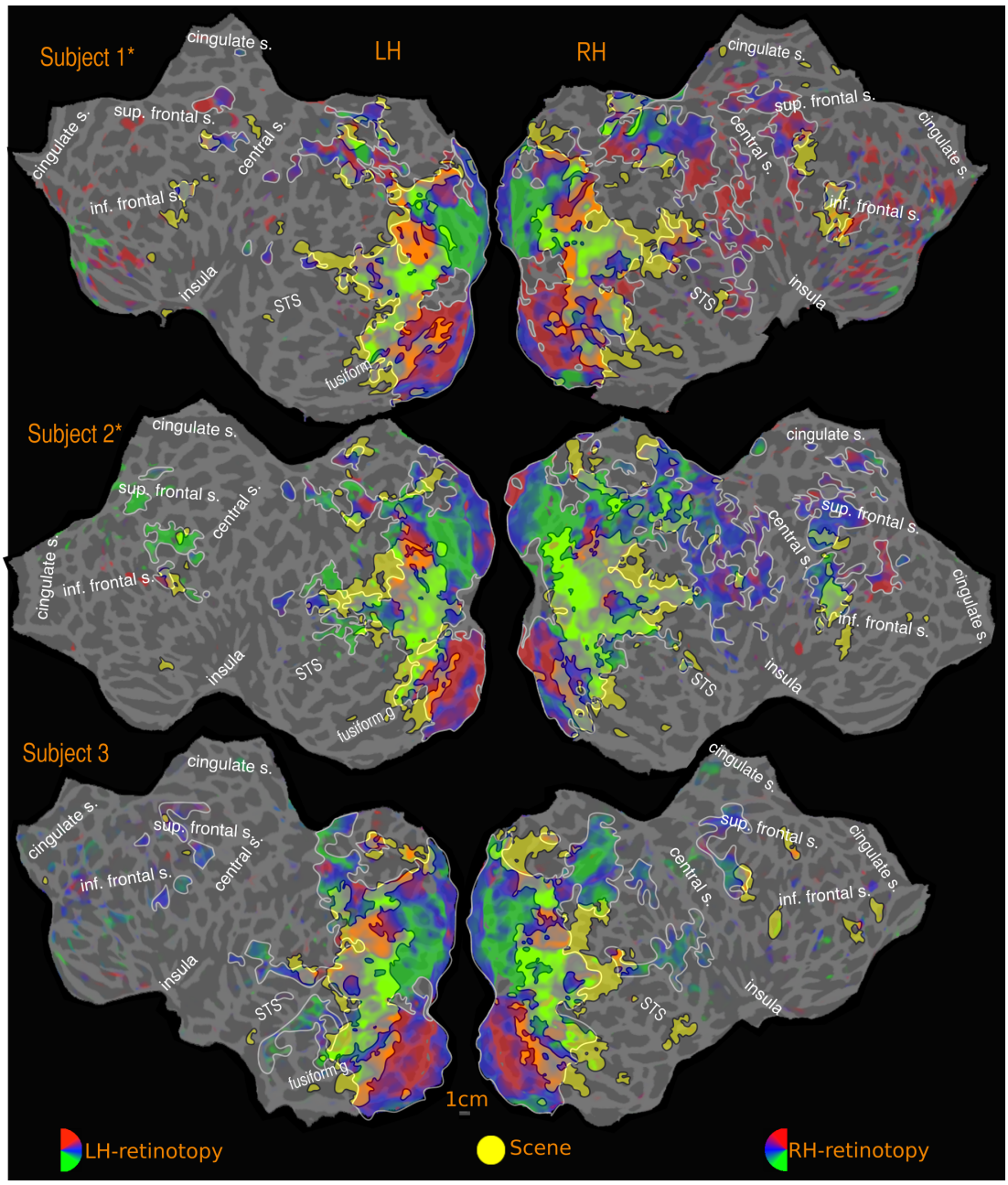

Figure 4.8: Overlap of SCENE (Story vs. Jigsaw) with RETINOTOPIC maps- individual SUBJECTS (Flat view).

Activations are illustrated at p<0.001, corrected to p<0.01.

tonotopy. No overlap is observed in left temporal cortex and 18% overlap was observed in right temporal cortex. For subject-2, there is no overlap in the left frontal cortex and a 1% overlap in right frontal cortex, with the corresponding figures in temporal cortex being 5% in left hemisphere and 32% in the right hemisphere. In subject-3, none of the frontal scene activation in left hemisphere overlaps with tonotopy, while in the right hemisphere around 40% of frontal activation is within tonotopic maps. The corresponding figures for temporal cortex are 53% in left hemisphere and 56% in the right hemisphere.

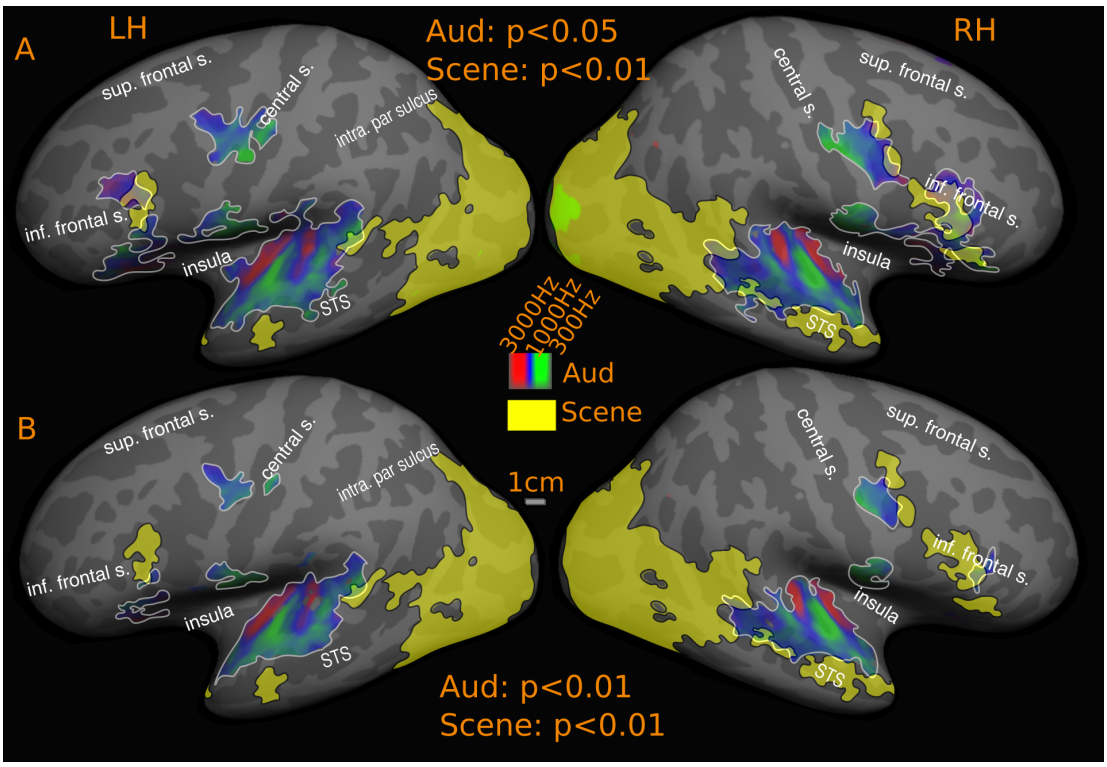

Figure 4.9: Overlap of SCENE (Story vs. Jigsaw) with TONOTOPIC maps- GROUP
Reported p values are vertex thresholds used before cluster thresholding. All activations are cluster thresholded to p<0.05. Scene activation is illustrated at p<0.01 (vertex threshold) in A and B. Tonotopic activation is illustrated at two different vertex thresholds- p<0.05 (A) and p<0.01 (B).

In the group results, the overlap between scene and tonotopy in the temporal lobe in both hemispheres falls within the low to middle frequency range, narrowly avoiding the adjacent high frequency region in STG and well away from the high frequency regions in the lateral sulcus. The situation in frontal cortex is more mixed. In the left frontal cortex, the overlapping region near the inferior frontal sulcus in the pars opercularis region is dominated by mid-low frequencies on the inferior end and by high-mid range frequencies on the superior end. In the right frontal cortex, the scene activation along the precentral sulcus overlaps mainly with high-mid range frequencies. In the inferior frontal sulcus (IFS), the overlapping regions fall predominantly in mid frequency range, with a lower and equal share of high and low frequencies. The overlapping region ventral to IFS in the right hemisphere is dominated by low-mid frequencies at the inferior end

Scene overlap with somatomotor maps: In the cross-subject maps, there is no overlap between scene and somatomotor activation in the left hemisphere. The precentral scene activation (at p<0.05, Figures 4.3 and 4.4A) lies just outside the mouth encoded portion of the somatomotor maps. In the right hemisphere, the precentral region overlaps the outer edge

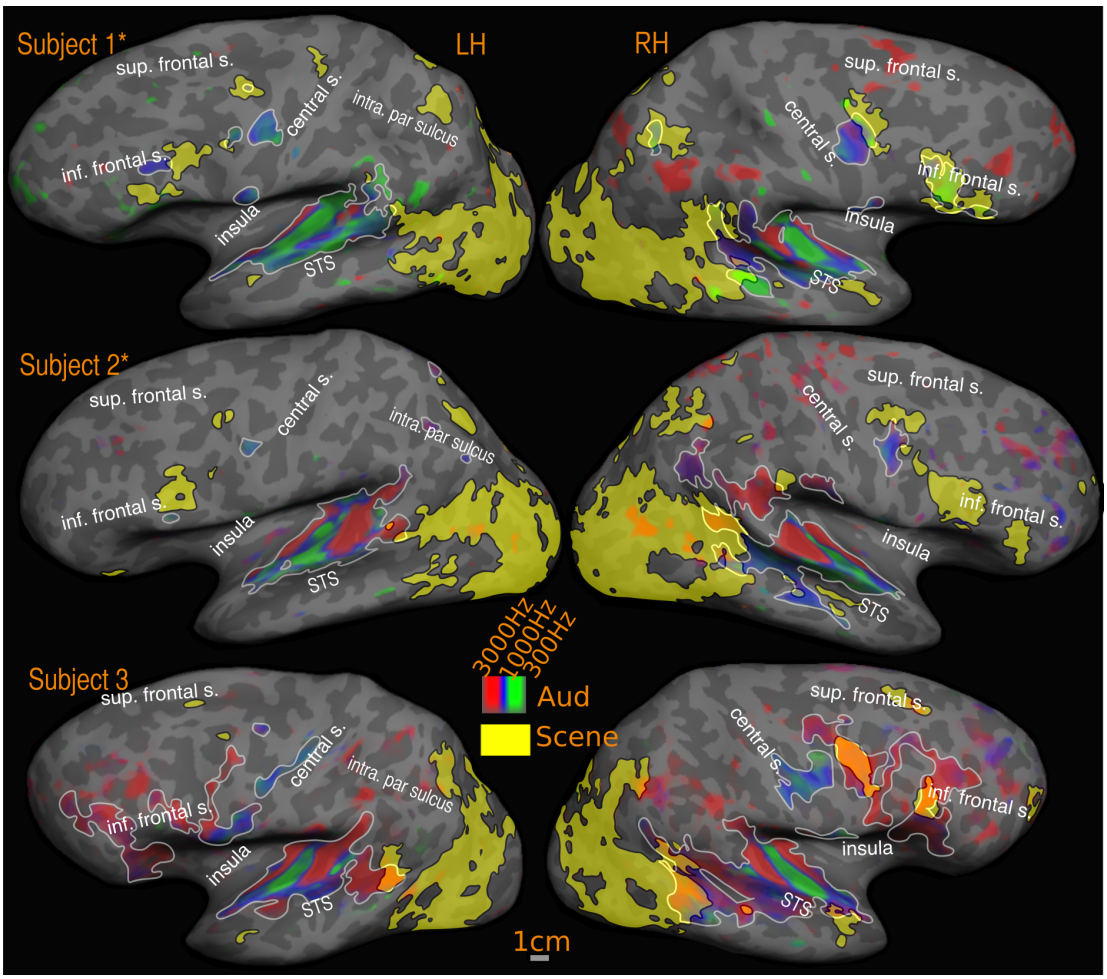

Figure 4.10: Overlap of SCENE (Story vs. Jigsaw) with TONOTOPIC maps- SUBJECTS

All activations are illustrated at vertex threshold p<0.001, cluster thresholded to p<0.01.

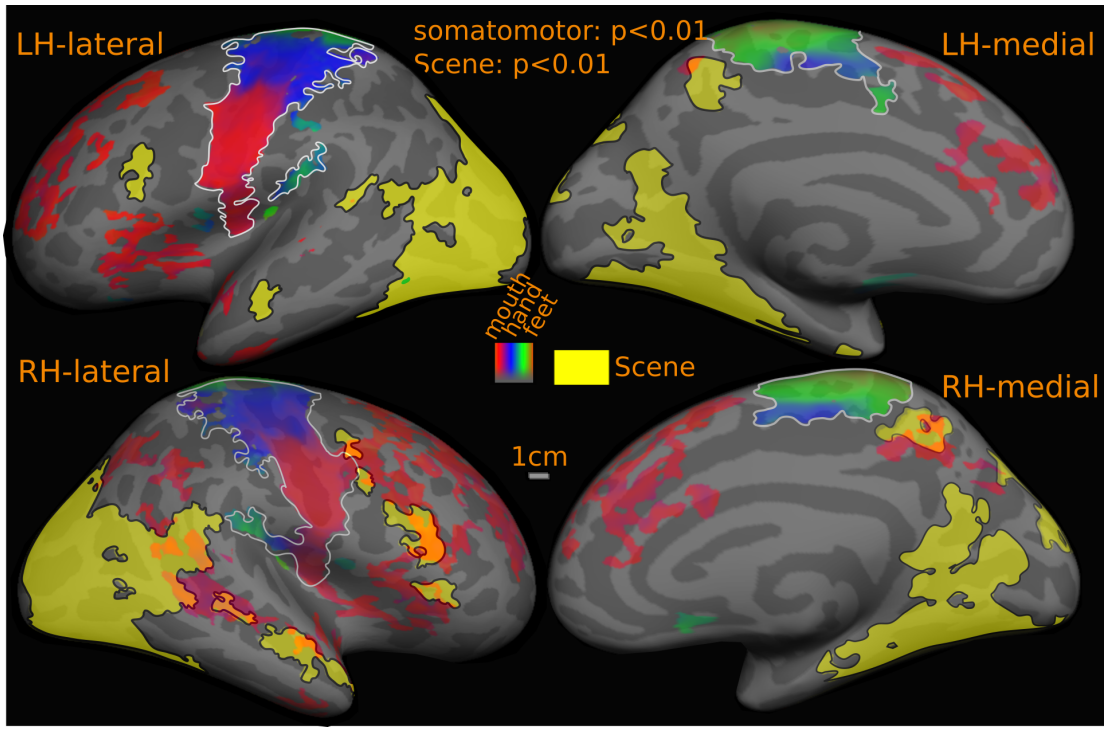

Figure 4.11: Overlap of SCENE (Story vs. Jigsaw) with SOMATOMOTOR maps- GROUP

All activations are illustrated at vertex threshold p<0.01, cluster thresholded to p<0.05.

of mouth encoded portion of the body map.

Retinotopic maps (as a percentage of scene activation)			**Group**		**Subj-1**	**Subj-2**	**Subj-3**
			Higher threshold	Lower threshold			
	Left hemisphere	Overall	80	85	66	55	75
		Frontal	54	75	33	39	18
		Temporal	3	17	13	29	51
		Occipital	84	89	73	60	77
	Right hemisphere	Overall	67	74	60	72	56
		Frontal	15	47	27	53	16
		Temporal	12	23	33	47	17
		Occipital	77	83	70	78	64
Tonotopic maps (as a percentage of scene activation)	Left hemisphere	Overall	0.2	1	0.2	0.5	3
		Frontal	3	42	2	Nil	Nil
		Temporal	3	6	Nil	5	53
		Occipital	Nil	Nil	Nil	Nil	Nil
	Right hemisphere	Overall	1	6	4	3	9
		Frontal	6	60	21	1	40
		Temporal	11	34	18	32	56
		Occipital	Nil	Nil	Nil	Nil	2

Table 4.1: Quantitative estimates of overlap of Scene with Retinotopy and Tonotopy

4.4.4 Comparison between Scene (Story-Jigsaw) and Reading (English-Hindi) comprehension activation

The results support the classical observation that reading is more left lateralised while picture-based comprehension activates right hemisphere regions more extensively. While the extent and spread differs, the activated regions are remarkably aligned in both reading and scene comprehension, with main activity observed in occipital, temporal and frontal cortex.

In the occipital cortex, on the lateral side, reading activation is more constrained with very little activity in the lateral occipital region adjoining V3A as compared to scene. On the medial wall, there is significant foveal activation along the primary visual areas V1 and V2

for reading, while scene activation in these regions is more peripheral. The medial scene activation largely avoids V1,V2, the remainder of the cuneus and lingual cortex, and covers more scene specific regions such as parahippocampal cortex, RSC, parieto-occipital cortex

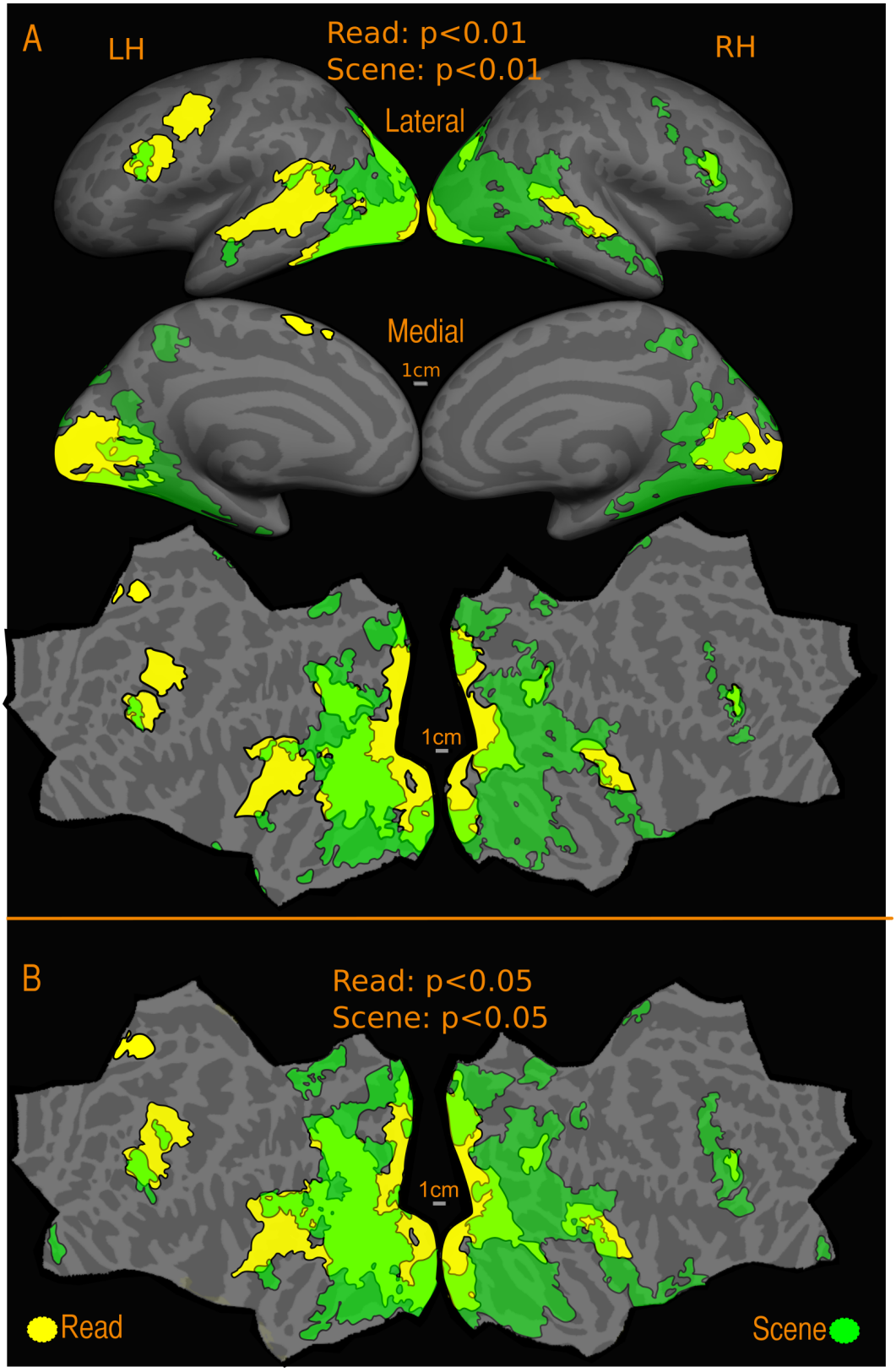

Figure 4.12: Overlap of SCENE (Story vs. Jigsaw) with READING (English vs. Hindi)-GROUP . Reported p values are vertex thresholds used before cluster thresholding. All activations are cluster thresholded to p<0.05.

and precuneus, none of which are active for reading. There is little or no activation for reading in the above mentioned regions activated during picture-based comprehension.

In the temporal cortex, reading has prominent activation in the left hemisphere, with extensive activation along superior temporal gyrus/sulcus and middle temporal gyrus. The

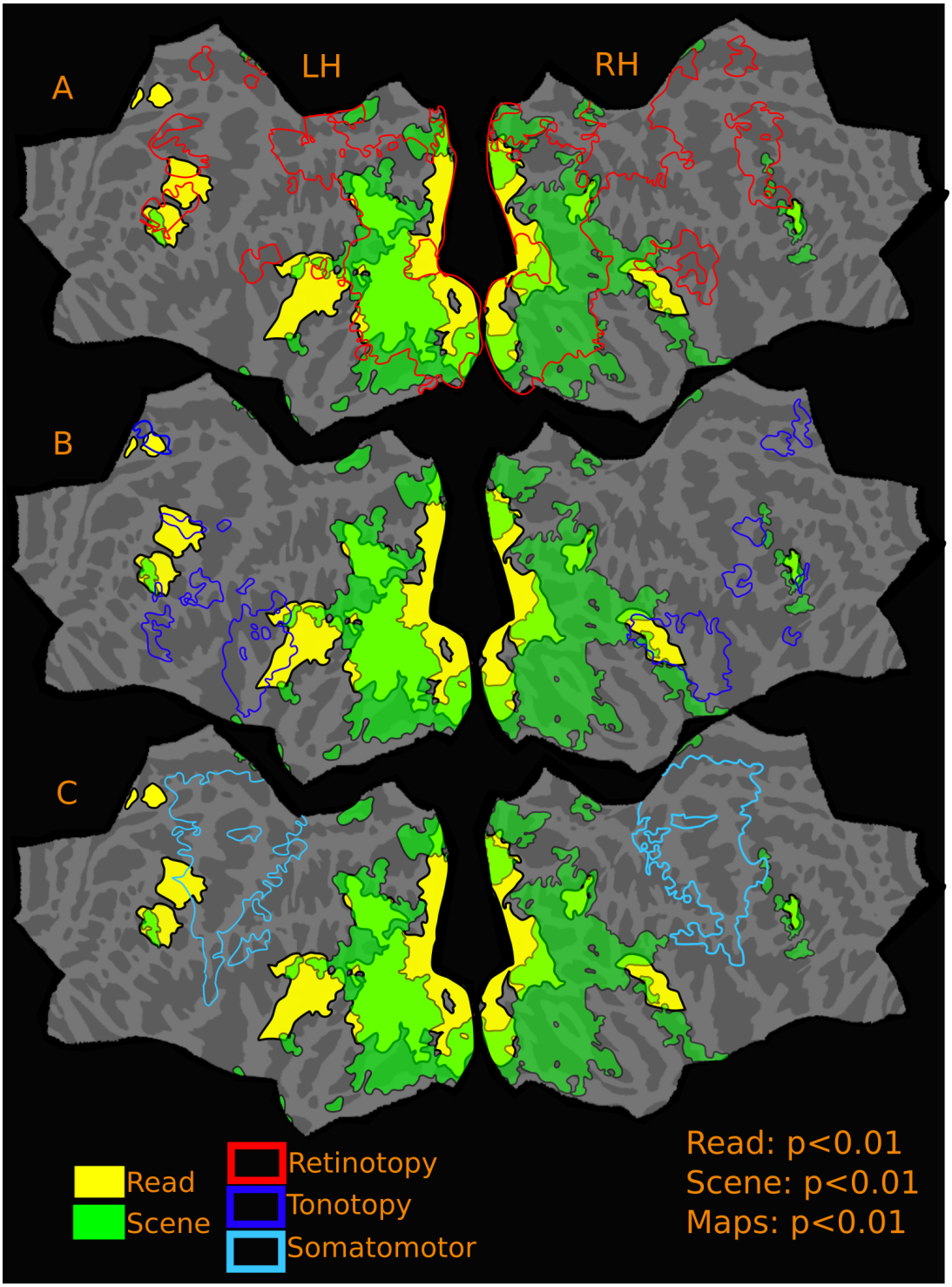

Figure 4.13: Overlap of SCENE, READING with ALL MAPS (at higher threshold) - GROUP
Reported p values are vertex thresholds used before cluster thresholding. All activations are cluster thresholded to p<0.05.

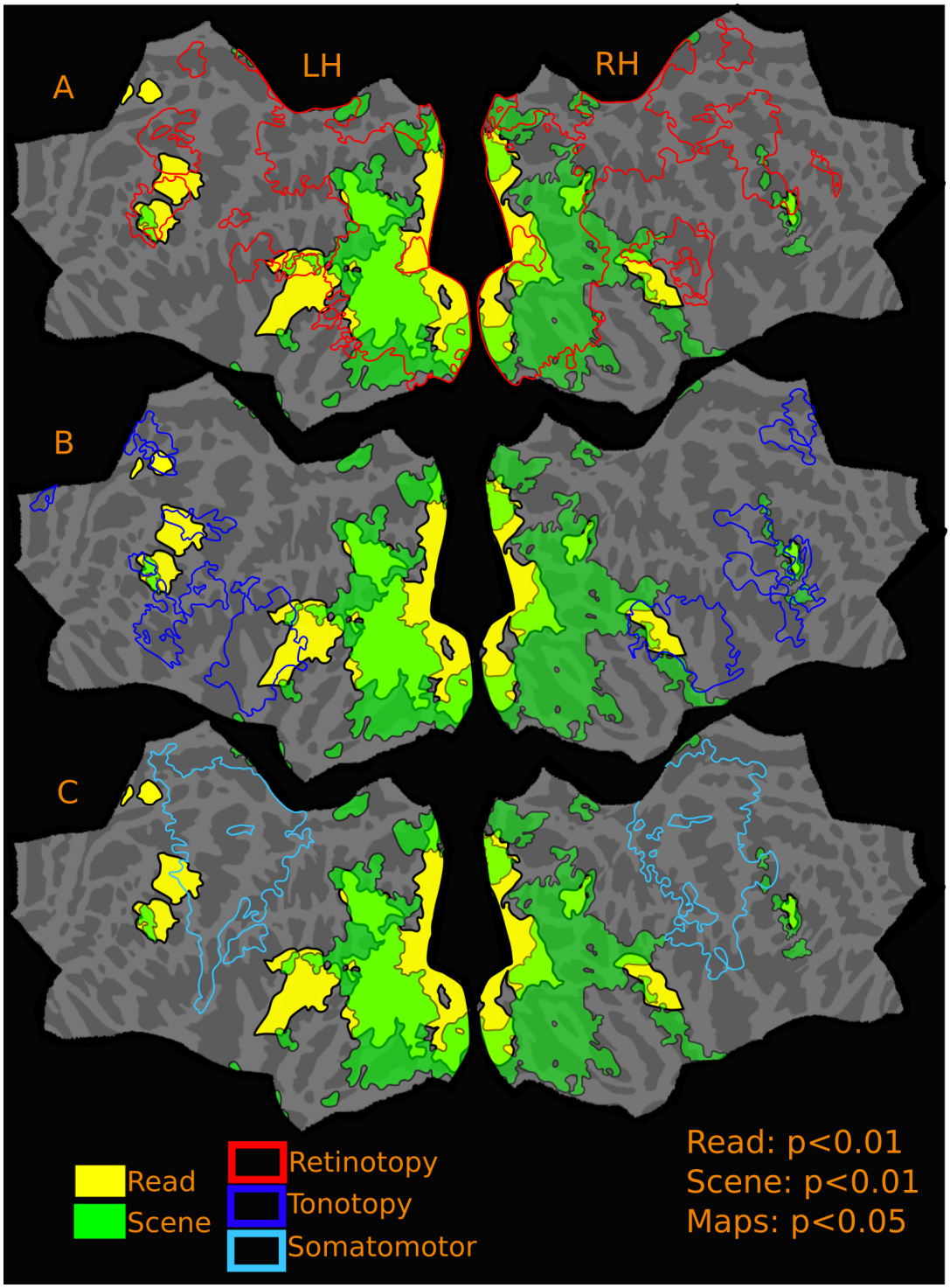

Figure 4.14: Overlap of SCENE, READING with ALL MAPS (at lower threshold) - GROUP
Reported p values are vertex thresholds used before cluster thresholding. All activations are cluster thresholded to p<0.05.

main overlapping region for reading and scene is in the posterior superior STS/STG. The more anterior/inferior activation zone in left STS for scene is largely non-overlapping with reading activation. In the right hemisphere, temporal activation is more extensive for scene and although there is a good degree of overlap with reading activation in STS, there is considerable anterior activation in STS outside the bounds of reading activation. Although

reading activation did not have activation in anterior temporal lobes, the standard EPI pulse sequence used for 3 subjects (of the 17 included subjects) didn't include this region within its scanning block, which might have contributed to lack of significant reading activation in anterior temporal cortex in the cross-subject average. (as explained in chapter 3). Hence, it is possible that the anterior scene activation could have a larger overlap with reading than what is depicted here.

The frontal activation zones for both reading and scene are well aligned. The frontal activation in left hemisphere is much more extensive for reading than for scene. There is a prominent overlapping scene activation near inferior frontal sulcus in the pars opercularis region, as well as a less significant ($p<0.05$) activation zone in the precentral sulcus near the FEF region, also overlapping with reading activation. On the right hemisphere, scene activation is more extensive and is spread along the precentral sulcus all the way up to pars triangularis region.

The medial cingulate region activated for reading (only present when reading English) and overlapping with the tonotopic map in the region (figures 4.13, 4.14), is not activated for any conditions in the scene experiment. This could be a bonafide language-specific region.

4.5 Discussion

The study presented in this chapter provides a comprehensive qualitative and quantitative assessment of where and by how much processes relevant to narrative scene comprehension overlap with topological sensory-motor maps as well as activation observed during naturalistic reading comprehension using high-resolution surface-based fMRI across entire cortex. This study builds up on the results presented in the previous chapters (chapters 2 and 3) and was conducted on a subset of the subjects who participated in the previous studies. There were two main objectives.

The first was to accurately localise regions of interest in narrative scene comprehension by determining their exact relation to low and high-level topological visual, auditory, somatosensory and motor maps. Topological mapping is a time-tested method for accurately defining the boundaries of cortical areas. The figures presented here are the first illustrations of the relative location of ‘narrative scene comprehension’ activation and topological visual, auditory and somatomotor maps across the entire cortex in the same group of subjects.

Additionally, the results provide a quantitative estimate for the level of overlap between activations observed during narrative scene comprehension and topological sensory-motor maps, which are driven by relatively low-level sensory-motor stimuli. At a higher threshold of $p<0.01$, nearly 80% of cross-subject scene activations in left hemisphere and 67% in right hemisphere fall within regions containing topological sensory-motor maps. When the threshold for sensory-motor maps is lowered ($p<0.05$), these figures rise to 85% and 74% in left and right hemispheres respectively.

The second main objective was to compare and contrast the activation during narrative scene comprehension with that observed during narrative reading comprehension, and assess them relative to topological sensory-motor maps. The reading and scene stimuli both used controlled eye saccades and naturalistic serial comprehension of stories, making the comparative analysis combined with the cortical maps, the first such available complete data set.

The main features of this study that differentiate it from other scene comprehension studies or natural movie studies were the following. 1. The study's main focus was comprehension of 12 different narrative picture stories evolving over 30 to 50 seconds and subjects were tested for their comprehension afterwards. 2. In contrast to majority of neuroimaging studies that use rapid serial visual presentation, the presentation mode used here allowed naturalistic eye movements which were carefully controlled during viewing of the images. 3. The analysis method, as highlighted in previous studies in this thesis utilised a cortical surface based group averaging as opposed to volume based group analysis commonly employed in majority of scene comprehension studies.

It was anticipated that the activation includes scene selective regions identified previously by other studies. The scene activation observed in occipital cortex is consistent with previous findings and includes brain regions associated with PPA (Epstein and Kanwisher, 1998; Nasr et al., 2011), RSC (Bar & Aminoff, 2003; Nasr et al., 2011), FFA (Kanwisher et al., 1997), LO (Hasson et al., 2008; Huth et al., 2012; Dilks et al., 2013) and precuneus (Lacoboni et al., 2004; Huth et al., 2012). The retinotopic maps in occipital cortex and the localisation of above mentioned regions relative to retinptopic maps are well explored. Consistent with previous findings (Arcaro et al., 2009; Huang and Sereno, 2013) the activation in parahippocampal cortex and RSC partially overlaps with retinotopic maps. There is extensive

activation not just restricted to previously known scene regions in occipital cortex. The activation along fusiform gyrus where FFA is localised, the LO region anterior to V3A, where the lateral occipital place area resides, and the lateral inferior occipital gyrus, a region where occipital face area is often localised, are all within regions activated in narrative scene comprehension. These regions are all known to have retinotopic maps (Wandell et al., 2007; Huang and Sereno, 2013), and these results confirm this.

While there has been considerable focus on exploring the underlying map structure and localising scene selective regions in posterior occipital cortex with respect to retinotopic maps in the region, there has been very little effort so far in exploring the relation of higher-level (beyond occipital cortex) regions activated in naturalistic scene comprehension with respect to topological visual, auditory and somatomotor maps also found in higher level cortices. In temporal cortex, bilateral activation in posterior superior temporal sulcus extending on to STG was found. The posterior STS (pSTS) has been linked to processing of faces (Haxby et al., 2000; Hoffman and Haxby, 2000), on biological motion (Grossman et al, 2005) and in social perception (Lahnakoski et al., 2012). Posterior STS has also been positively activated as a higher level region relevant for temporally coherent comprehension in Lerner et al (2011). The results presented here show that the posterior STS activation during narrative scene comprehension is fully contained within the extensive reading activation found in the superior temporal cortex and majority of the superior temporal scene activation overlaps with retinotopy towards the posterior end, and the rest of the anterior activation in STG overlaps with tonotopic maps. The anterior-inferior STS activation, which is present even in Story-Shuffle contrast is largely non-overlapping with topological maps. The activation along the STS in the right hemisphere overlaps partially with tonotopic maps on the posterior superior end.

In frontal cortex, there is considerable activation for each condition- Story, Jigsaw and Shuffle relative to Fixation. The Story and Shuffle condition activates precisely the same regions in the frontal lobe, where as the main shared activation zone with Jigsaw is the activation spread across superior frontal sulcus and the activation in the post central sulcus region. Only the activation present in inferior frontal sulcus and a small region near lateral FEF are significantly more active than Jigsaw in both Story and Shuffle conditions. Of this, only the inferior frontal sulcus activation is still significantly active in Story-Shuffle

condition. This region of activation is also overlapping with both retinotopic and tonotopic maps within the region, and is mostly contained within the English-Hindi reading activation.

The eye movement control network consisting of IPS/postcentral sulcus, dorsomedial eye fields and lateral FEF regions (and also observed for all three conditions in the reading experiment) are significantly activated for all three scene conditions. The activation in IPS/ postcentral and dorsomedial frontal eye fields disappears in Story vs. Jigsaw contrast and Story vs. Shuffle contrast. The lateral FEF activation is much reduced in Story vs. Jigsaw and even more attenuated in Story vs. Shuffle.

The zone near inferior frontal sulcus however was only activated for Story and Shuffle conditions, and there was significant activation (slightly attenuated in total area) even in Story vs. Shuffle condition. In the reading experiment, the activation around this region was also present only while reading English, and not present in Hindi or Dot. This region could be a bonafide candidate for serial narrative comprehension relevant processing, as it was only activated while semantically rich content was presented (via text or scene), and the activation was significantly better when the temporal coherence of the narrative improved (as in the Story case as opposed to Shuffle). This activation is nearly completely covered by retinotopic and tonotopic maps.

All left frontal scene activation is fully contained within the reading activation, with reading activation more extensive than the scene activation. The activation around lateral FEF region in left hemisphere showed considerable differences in reading and scene, with lateral FEF far more extensively activated in reading than in scene. In the right frontal cortex, the reading activation is a subset of the scene activation, with scene activation completely overlapping and extending beyond the reading activation. The right frontal scene activation is largely contained within maps and has partial overlap individually with all three maps. The right hemisphere scene activation is almost fully attenuated in Story vs. Shuffle condition, suggesting these regions are relevant for isolated scene processing as well.

The functional role of frontal cortex, and how this can be differentiated is an intensely debated research question. Any activation of higher-level visual and auditory areas in this region during comprehension tasks has often been dismissed as attention related. Recent research however suggests that attention is a cortex-wide dynamic process whereby resources are flexibly allocated to the attended function as opposed to a simple mechanism that merely

modulates baseline response level (Çukur et al., 2013, Peelen & Kastner, 2014). But this also implies that subtractive analyses attempting to control for attention factors assuming a static modular nature of attention may be overly conservative. Instead, I suggest that the functional differentiation of this region is best done the way illustrated here. The reading contrast (English vs. Hindi) and the scene contrast (Story vs. Jigsaw) are relatively matched in the attentional demands, without downplaying comprehension specific activations. The differential pattern of activity observed in frontal cortex for these two contrasts, suggest that not all activation there can be put down to purely multi-domain processes.

An interesting and rather unexpected finding from this study is that more or less same network of regions are activated for Story vs. Shuffle contrast. These two conditions were identical except for the temporal coherence of the evolving story aspect. The previous study by Hasson et al. (2008) utilising silent movies, where temporally coherent stimuli was compared with temporally scrambled version, did not find any significant response amplitude differences in higher level cortical regions such as temporal, frontal and parietal cortex although there was significant differences in response reliability (a correlation based measure). The results presented here show that nearly all higher level regions (except the right frontal regions) activated in Story vs. Jigsaw contrast also had significant activation for Story vs. Shuffle (considerably lower significance values, but still $p<0.05$), a result inconsistent with the previous report. This could be because of the differences in the stimulus or/and due to the more sensitive surface based averaging utilised in this study.

It is also noteworthy that most of the lateral occipital regions showed highly significant activation in Story vs. Shuffle contrast. The basic pattern of activation is very similar to Story vs. Jigsaw, although the Shuffle condition was semantically far richer and closer to Story condition than Jigsaw. This result suggest that occipital regions may play a more significant role than is usually appreciated in high level semantics processed over a long temporal scale. In contrast to lateral occipital cortex, the activation in medial occipital cortex was attenuated in Story vs. Shuffle contrast. This was not surprising as scene selective regions here are known to be heavily involved in processing isolated scenes. However, while the activation is not as extensive as in Story vs. Jigsaw contrast, there is still significant activation in these regions in Story vs. Shuffle condition.

Similar to reading data, very little overlap was found with somatomotor maps. These results are however consistent with previous studies using silent movies (Hasson et al., 2008), which also did not find any scene specific activation in the somatomotor regions.

~~~
~~~

Chapter 5

General Discussion

The aim of this thesis was to provide improved data upon which to evaluate several important debates in the field including the significance of maps in higher-level cortical areas, the degree to which sensory-motor regions are involved in comprehension, the significance of comprehension-specific activity in lower-level visual areas, and the degree to which serial assembly processes in linguistic and non-linguistic comprehension utilise the same set of modality specific maps. In the experiments described in this thesis, I systematically explored the three-way interplay between cortical sensory-motor maps and brain regions processing narrative reading and scene comprehension. These fields are often explored separately, and these different kinds of experiments are usually conducted on different groups of individuals. Same set of subjects participated in the five different fMRI experiments described in this thesis, and the data comes from ~90 individual fMRI sessions. Two different analysis methods were utilised for data analysis — Fourier based phase-encoded analysis for mapping experiments and the GLM based mass univariate analysis for narrative reading and scene comprehension — though both are fundamentally linear analysis methods, and are, in fact, quite closely related (Rio et al., 2013). All experiments utilised a more accurate cortical surface based group averaging pipeline as opposed to the volume based averaging much more commonly used in high level cognitive experiments.

The contrasts I have used in these studies also require further mention. A typical method utilized in high-level cognitive experiments is to use close control conditions to deduce the functional significance of brain activations. They are surely informative, but they are also based on the assumption that cognitive processes realised in the brain are modular in nature. The emerging evidence (for eg: Huth et al., 2012; Çukur et al., 2013, Peelen and Kastner, 2014) from a variety of sources does not support this conclusion. Secondly, if a certain brain region is critical for two different tasks (performed separately in an fMRI session), a subtractive analysis of brain activations during these two tasks will negate the significance of this critical brain region. This risk is much higher when the control conditions are extremely close to that of the experimental condition. Hence, I argue that using very close contrasts runs the risk of being overly conservative and may impede a deeper understanding of the full evolving picture of brain activity. In this thesis, the contrast used to assess reading activation was reading English vs. unfamiliar Hindi. This contrast highlighted activations supporting processes traditionally referred to as linguistic (orthographic, syntactic, word level

processing), but it also included activations due to more domain general processes such as semantic access, working memory, attention, serial assembly of the evolving concepts over a long time scale. To further distinguish the functional significance of the activated regions during reading experiment, I utilized a non-linguistic but comprehension-intensive narrative scene task, presented in a naturalistic but controlled manner similar to the reading stimuli. As hypothesised, there were visual as well as higher level regions common to both reading (English vs. Hindi) and scene (Story vs. Jigsaw). In the following sections I discuss the overall findings in this thesis. In the text below, 'reading' refers to English vs. Hindi contrast and 'scene' refers to Story vs. Jigsaw contrast, unless otherwise stated.

New retinotopic and tonotopic maps associated with cognitive functions

In addition to confirming previous findings of retinotopic maps in posterior occipital, frontal, parietal and temporal cortex, the tonotopic maps in lateral sulcus/superior temporal cortex and the somatomotor maps in the somatomotor cortex, the mapping experiments uncovered several sensory maps previously unreported in the literature. One of the key new maps reported here is a visual map adjacent to SMA in the anterior cingulate cortex. In non-human primates, it has long been known that the anterior cingulate supplementary motor areas are directly adjoined by the dorsomedial frontal eye fields (Schiller and Chou, 1998; Purcell et al., 2012). So far, there have not been any reports on topological maps in a similar region in humans. The data presented here may provide the first observation of the topological organization of the human equivalent of the dorsomedial frontal eye fields, which possess a retinotopic map of the contralateral visual field. While retinotopy in this region is reported here for the first time, there have been a number of reports of activation in this region associated with visuo-spatial attention and eye movements (Mesulam et al., 2001; Pierrot-Deseilligny et al., 2004; McDowell et al., 2008; Jamadar et al., 2013; O'Reilly et al., 2013). In the narrative reading and scene comprehension experiments, all relevant conditions (English, Hindi, Dot in Reading experiment and Story, Jigsaw, Shuffle in Scene experiment) had significant activation in this region, confirming the previous reported findings.

A new tonotopic map (the dorsomedial frontal 'ear' fields), adjacent to the dorsomedial retinotopic map and separated by SMA was also found. There is a strong reading activation aligned with the tonotopic map in the left hemisphere. As this activation is absent in the

scene experiment as well as for all conditions except English in the reading experiment, this could be a bonafide language-specific site.

In addition to cingulate maps, previously unreported tonotopic maps were found in the frontal cortex. All frontal tonotopic maps partially overlap with retinotopic maps in the region as well. In the polysensory zone (see chapter 2 results), it was found that there is an overlapping tonotopic map in addition to previously reported visual and motor maps.

Moreover, the mapping experiments revealed the distribution of topological sensory-motor maps across whole cortex allowing a unique insight into where these maps overlap. Several new overlapping regions are identified including the frontal cortex and lateral sulcus region in addition to confirming previously found multisensory map regions (Graziano and Cooke, 2006; Huang et al., 2012) in VIP, and the polysensory zone on the anterior bank of central sulcus (Huang and Sereno, 2013).

Common areas for reading and scene activations and their relation to maps

Reading and scene contrasts activate mainly similar cortical regions- in occipito-parietal, frontal and temporal cortex. In the occipito-parietal cortex, the common regions activated include V8, hV4, MT, posterior IT, fusiform gyrus, peripheral V1 and V2 and LIP (lateral intraparietal) region. All the activated regions in occipito-parietal cortex common to reading and scene contrasts fall within retinotopic maps. In the left temporal cortex, both reading and scene activation extend across MT into posterior superior STS/STG cortex. The scene activation in this region is fully contained within more extensive reading activation found in the superior temporal cortex. Except for a small region in STS, most of this shared activation in both hemispheres fall within retinotopic and tonotopic maps in the region. In the left frontal cortex, on the lateral side, the scene activation is a subset of the reading activation, and the shared activation near the inferior frontal sulcus near the vicinity of Broca's area (Broca, 1861) is mostly contained within the retinotopic and tonotopic maps. This common activation zone was also significantly active in Story vs. Shuffle condition. Considering that this region was active for reading, scene and in story-shuffle contrasts, this could be a candidate region relevant for narrative comprehension common for all of the above three contrasts. In the right frontal cortex, reading activation is a subset of scene activation; and again the shared activation is contained mainly within tonotopic maps. In the lateral FEF

region in left hemisphere, both reading and scene activation (at $p<0.05$) is present along with the presence of all three maps. This is the only region where all three modality maps overlap, although there are several other regions where maps from two modalities overlap. The dorsomedial frontal eye fields is another region activated uniformly for all conditions in both experiments (reading and scene), and as already discussed this region overlaps with retinotopy. In summary, there are shared activations across entire cortex and most of these shared activations are overlapping with topological sensory-motor maps.

Distinct areas for reading and scene activations and their relation to maps

There are some distinct differences between reading and scene activation. Reading is heavily left lateralised. Scene activations, though more balanced than reading activation, are still more extensive in the right hemisphere. In the left temporal lobe, activation is extensive for reading and most of it is not shared with scene. This distinct continuous activation zone (for reading) covers most of STG and STS. Tonotopy overlaps this region partially, but a significant portion (50-75%) of this activation does not overlap with any maps. In the right hemisphere however, the distinct reading activation observed in STS is completely overlapping with tonotopic maps. The data suggests that left temporal lobe (also well known as the region where classical Wernicke's area is situated) is more specialised for reading, considering the total lack of scene activation in most of the reading activated regions in the left superior temporal cortex. In the left frontal cortex the reading activation is more extensive than scene activation, and most of the distinct reading activation in this region falls within mapped areas. Distinct reading activation in the occipital cortex is mainly in the foveal regions in the primary visual areas, scene activation here is more peripheral. All distinct reading activation in the occipital cortex falls within retinotopy. There is also a distinct reading activation in the left anterior cingulate cortex, which overlaps with newly found tonotopic map.

For the main scene contrast, in left hemisphere most of the temporal and frontal activation is a subset of the reading activation as described in the previous section. The scene activation in the left anterior inferior STS extending into MTG, does not have any overlapping maps either. In the right temporal cortex, there is activation along the STS, and the anterior STS activation is non-overlapping with either reading or tonotopic maps in the region. However it

is possible that reading-specific activation extends to this region, but was not detected as a result of the EPI pulse sequence used for 3 subjects, where the scanning block didn't include the anterior most regions of temporal lobe (as explained in chapter 3, 4). In right frontal cortex, the scene activation is more extensive and the reading is a subset of scene activation. Most of right frontal scene activation falls within topologically mapped regions. There are distinct scene activations also in occipital cortex which are not shared with reading. In the left hemisphere, where reading activation is more extensive, the regions distinct for scene include activations in parahippocampal cortex (PPA region), RSC, precuneus and in LO. Among these PPA, RSC and the precuneus activations are partially covered by retinotopy. The distinct LO region and the surrounding lateral regions shared with reading is also active in Story vs. Shuffle contrast. Although occipital regions are not often associated with high level cognition, the fact that significant activation is observed in most of the activated lateral occipital regions for a much closer contrast suggest that these regions may play a significant role in narrative comprehension. In the right hemisphere, there is very little lateral occipital activation for reading, while scene activation is more spread out than its left hemisphere counterparts. Apart from the regions mentioned in left hemisphere, the scene regions non-overlapping with retinotopy includes regions beyond MT in superior posterior MTG area.

In summary there are distinct regions unique to both reading and scene comprehension. For reading these are primarily in left hemisphere, mainly including activations in superior temporal cortex, frontal cortex and anterior cingulate cortex. Among these, the frontal and anterior cingulate activations largely overlap with maps while a good proportion of left temporal activation is not covered by any maps. For scene comprehension, the main distinct regions are in posterior occipital cortex, as well as in right temporal and frontal cortex. There are distinct regions in posterior occipital cortex that are not fully covered by retinotopy, as well as the right anterior temporal activation which falls beyond tonotopic maps in the region. A significant portion of occipital activation and right frontal activation distinct to scene are overlapping with maps.

Differential activations for reading and scene in frontal cortex

Although there are reading and scene specific activation in frontal cortex, these activations also have distinct coverage. The fronto-parietal regions are often considered multi-domain

sites associated with cognitive processes which are shared across domains (e.g. attention, see Duncan et al., 2000). There is considerable evidence in the literature for frontal activation during all sorts of language tasks. Comparatively, less work has been done to identify the relevance of these regions for picture based comprehension. But studies using natural movies and even silent movies have reported activation in frontal cortex, although where they fall relative to language activations or the attentional network was not previously very well defined. The results presented in chapters 3 and 4 show that not all activation during reading is shared with scene activation and vice versa. As discussed in the previous section, there are activation sites distinct for reading and scene comprehension in frontal cortex. The reading (English vs. Hindi) and scene (Story vs. Jigsaw) contrasts used in this thesis were controlled for eye movements and were similar in their attentional demands. Hence the distinct reading/ scene regions identified here are candidate regions for specialised linguistic processing or scene processing. Siting these regions relative to topological maps in the area, provides a much more precise anatomical localization than those that are available in the literature. Not all activation found in the frontal cortex was distinct, and there was common frontal activation zones in all relevant conditions in the reading experiment as well as in scene, some of which could be attributed to the eye control network discussed below.

Activation patterns in eye control network

In all reading conditions (English, Hindi, Dot) as well as in all scene conditions (Story, Jigsaw, Shuffle), significant activation was observed bilaterally near intraparietal/postcentral sulcus, FEF, and dorsomedial frontal 'eye' fields, regions known to be activated by visuo-spatial attention and eye saccades (Pierrot-Deseilligny et al., 2004; McDowell et al., 2008; Müri, and Nyffeler, 2008; Jamadar et al., 2013; O'Reilly et al., 2013). The activations in dorsomedial frontal 'eye' fields and parts of parietal cortex are fully attenuated in English vs. Hindi and Story vs. Jigsaw contrasts. In lateral FEF, while the activation disappears in Hindi vs. Dot contrast, a good part of it is still highly significant in English vs. Hindi contrast. While there is lateral FEF activation for Story vs. Jigsaw condition, this is much less significant and far less extensive than the activation observed in English vs. Hindi. More work needs to be done to assess what exactly contributes to this differential activation patterns in lateral FEF.

Chapter 6

Magnetic Resonance Imaging (MRI) and Functional MRI: A conceptual overview

6.1 Magnetic resonance imaging (MRI): Basic concepts

fMRI is a non invasive technique which allows us to indirectly measure neural activity while subjects perform cognitive tasks in an MRI scanner. Since fMRI does not involve any ionizing radiation and has excellent spatial resolution and adequate temporal resolution, it has become hugely popular with research involving human subjects. During fMRI scanning, the neural activity is inferred from changes in the measured T_2* signal as a result of changes in intracerebral blood oxygenation, a mechanism termed as the blood oxygen level dependent effect (BOLD). In this section, I will provide a conceptual overview of magnetic resonance imaging (MRI) on which fMRI relies on. The following sections deal with the principles behind BOLD signal and the specific pulse sequences used for scanning.

Magnetic fields

MRI is based on the principles of Nuclear magnetic resonance (NMR) discovered in 1940's by Block and Purcell (Bloch et al., 1946; Purcel et al., 1946). fMRI is a special form of MRI which can measure neural activity in real time and uses the same basic principles as MRI. All atomic particles such as protons and neutrons possess an intrinsic quantum property called spin. MRI techniques measure the effects of changing the spin precession direction and targets nuclei with an odd number of nucleons (protons and neutrons) such as ^{1}H and ^{13}C.

Because of their abundance in human tissue in the form of water, the hydrogen atom is the most commonly imaged atomic nucleus. The hydrogen nucleus consists of a single positively charged proton. The spinning positive charge of the proton can be thought of as inducing a local magnetic field, the spin magnetic moment. In the absence of an external field, the hydrogen nuclei magnetic moments are randomly oriented and the bulk material has no net magnetisation. However, when a strong external magnetic field, B0 is applied, the individual spins align or anti-align with the magnetic field at the 'quantum mechanical angle' with respect to the B0 field. Spins rapidly precess around the B0 axis at a precession frequency known as resonance frequency or Larmor frequency, which is directly proportional to the B0 field strength.

There are two possible states for precessing protons, one parallel to the external field and the other anti-parallel. Protons precessing parallel to an external field are in a lower energy

state than those which are anti-parallel. There are always more protons in the lower energy state than those in the higher, with the exact proportions dependent on the temperature and the field strength. This difference in proportions result in a weak net equilibrium magnetisation, M0 aligned with the field. By convention, the direction along the external magnetic field, B0 is assigned the Z direction in a cartesian co-ordinate system. At the level of an individual nucleus, the precessing proton has a magnetic component projecting into the XY-plane. However averaging across all nuclei, this 'transverse magnetisation' in the XY-plane cancels out to zero. Hence in the presence of an external magnetic field, the bulk material only possess the 'longitudinal magnetisation', M0, aligned with the external field B0.

Generating an MR signal

The equilibrium magnetism M0 is not directly observable as it is many orders of magnitude weaker than the external field, B0. In order to generate a measurable MR signal, the magnetic properties of atomic nuclei are perturbed and the energy returned during their recovery to the equilibrium state is measured. If energy is supplied externally, spins can be excited from the low to the high energy state and the spin precision directions can be effectively aligned. This energy transfer occurs by way of an oscillating radio frequency (RF) electro magnetic field (B1) applied perpendicular to the main magnetic field B0. When the oscillation frequency of the B1 field matches the resonance/Larmor frequency of the proton (64MHz for a proton in a 1.5 Tesla field), energy transfer is most efficient. The application of RF pulse at the Larmor frequency causes some protons to absorb energy and transition into the high energy state. This tips the net magnetisation vector (M) towards the transverse plane. The longer the RF pulse is on or the stronger the strength of B1 field, the larger this tipping angle would be. A common tipping angle employed in MRI is a 90^{o} tip, which tips the net magnetisation fully into the transverse plane. The final tip angle achieved is said to be the 'flip angle' of the RF pulse. When the required flip angle is achieved, the oscillating RF transmitter pulse is turned off. The resulting magnetic field in the transverse plane oscillating at the Larmor frequency generates an oscillating electric current in a receiver coil by way of electromagnetic induction. Theoretically, transmitter and receiver coils can be one and the same, but in

practice they are usually separate coils, both tuned to transmit/receive at the resonance frequency.

The MR signal detected through receiver coils does not remain stable forever. After spin excitation, the net magnetisation is tipped from the longitudinal axis into the transverse plane. Because the net magnetisation reflects the vector sum of many individual spins, its amplitude depends on the coherence between those spins, being greatest when they all precess at the same phase and with the same frequency. But over time, the spins lose coherence. Spatially proximate spins may interact, causing some spins to precess at higher frequencies and some lower. The differences in precession frequencies cause spins to get out of phase with each other, which lead to an exponential decay in the MR signal that is described by a time constant called T_2. Furthermore, any spatial inhomogeneities in the magnetic field will cause different spins to experience different magnetic fields over time, again causing some to precess more rapidly than others. This effect is additive to that of T_2 decay, and the combined effects of spin-spin interactions and magnetic field inhomogeneities is described by the time constant T_2*. As a result of T_2* decay, spins lose coherence relatively quickly (typically within a few tens of milliseconds) resulting in a diminishing net magnetisation in the transverse plane. As the spin system loses energy, it recovers back to the same state it was in before the excitation- with the net magnetisation aligned along the longitudinal axis. The longitudinal component of the recovery is slow, typically on the order of a few hundreds of milliseconds and is described by the time constant T_1 recovery. Together, these changes in the MR signal are called relaxation. The change in transverse magnetisation is termed transverse relaxation while the changes in longitudinal magnetisation is known as longitudinal relaxation. The regrowth of longitudinal magnetisation is too slow to generate electromagnetic waves, and so the RF coil only detects the transverse magnetization. The parameters governing these two types of relaxation differ across tissues, and this allows a single MRI scanner to collect many types of images.

Image formation

The MR signal generated as a result of the application of B0 and B1 fields (described above) alone are insufficient to produce tomographic MR images, since all hydrogen nuclei will experience roughly the same magnetic field and will resonate in a similar manner

irrespective of where in space they are located. In order to spatially distinguish them, additional manipulations are required. The critical innovation that made MR imaging viable was the introduction of superimposed gradient (spatially varying) magnetic fields. Because the precession frequency is proportional to the strength of the magnetic field, gradient magnetic fields cause atomic nuclei in different spatial locations to precess at different rates. By dividing the MR signal into components with different precession frequencies, we can generate maps (or images) that provide information about the characteristics of those atomic nuclei.

A common step in producing an MR image involves restricting the MR signal to one two-dimensional slice at a time, termed as slice selection. This is achieved by applying a gradient magnetic field along the z direction, which varies the magnetic field experienced by nuclei at different z positions. Hence the precession frequency of the brain tissue varies along the Z direction. The RF pulse oscillation frequency is varied to match the precession frequency of the required slice. This step selects (causes coherent precision in) nuclei in a particular slice (typically 1-10mm thick) along the Z axis.

However, the net signal still reflects the sum of all the signals generated across the slice, and the remaining localization in the XY plane is done with the application of two more gradients- a phase-encoded (PE) gradient along the Y axis and a frequency-encoded (FE) gradient along the X axis. During the interval between the RF transmitter pulse and data acquisition, the phase-encoded gradient typically is switched on and off, which will cause the transverse magnetisation at different Y positions to precess at different rates, such that the phase differences between the signals at two positions along the Y axis increases linearly with time. After the gradient is turned off, all spins will return to Larmor frequency, but the phase will be position dependent along the PE axis. This is one phase encoding step. In each phase-encoding step, the phase differences induced will correspond to the contribution from a particular spatial frequency in the Y axis within the tissue being imaged. The frequency encoding process then produces further phase evolution of the signal from a voxel with the rate of change of the phase (i.e. frequency) proportional to the X-position, encoding a particular spatial frequency in the X axis. The signal is being read out when the frequency encoding gradient is on so that multiple spatial frequencies are successively measured. The above steps allow us is to interrogate all possible spatial frequencies (within limits) within

the image. Once all of these signals are collected the application of discrete Fourier transform converts the 2D spatial frequency distribution into a 2D spatial distribution of the density of the excited nuclei.

6.2 BOLD Signal

The BOLD effect relies upon differences in magnetisation between oxygenated (oxyHb) and deoxygenated haemoglobin (deoxyHb). Because of the presence of unbound iron containing haem groups, deoxyHb is paramagnetic in nature (Pauling & Coryell, 1936) and it alters the magnetic field into which it is introduced. When the surrounding magnetic field is altered, the precessing protons nearby will experience different field strengths. This causes them to precess at different frequencies, resulting in a more rapid decay of transverse magnetisation (i.e. a shorter T2*). Thus MR measurements sensitive to T2* will show higher MR signal where blood is oxygenated and lower MR signal where blood is deoxygenated. The magnitude of the BOLD effect increases with the square of the strength of the static magnetic field. This effect was first illustrated by Ogawa and colleagues in 1990 (Ogawa & Lee 1990; Ogawa et al. 1990a; Ogawa et al. 1990b).

Although the relationship between neural activity in a given region and changes in blood oxygenation is still not fully understood, there is empirical evidence that BOLD signal changes indeed reliably reflect neural activity changes (Logothetis et al. 2001; Logothetis 2003). The BOLD signal however correlates better with local field potentials (LFPs) rather than neuronal spiking activity, thereby reflecting the incoming inputs into an area as well as the processing of this input information by local brain circuitry. This makes sense since neurons devote much more energy to controlling ionic currents through the dense banks of ion channels on their dendrites than they allocate for controlling the much more sparsely spaced voltage-gated channels on their myelinated axons. The temporal resolution of BOLD signal is lower than other techniques such as EEG. The dynamics of the neurovascular response implies the BOLD signal takes a number of seconds to evolve, peaking at around 6-10 seconds (Logothetis 2003). However, fMRI has much better spatial resolution compared to EEG and does not suffer from the inverse problem for signal localization. The functional images in this thesis were acquired at 3.2x3.2x3.2 (multiband sequence) and at 3.2x3.2x3.8

(standard EPI sequence). The spatial resolution at which images are acquired is not always the eventual spatial resolution as any spatial smoothing applied to the images at the preprocessing stage of data analysis can reduce spatial specificity, as does variations in individual anatomy when a group analysis is performed. For the experiments described in this thesis, no smoothing was applied at the individual subject analysis stage, and a minimal 3 mm (FWHM) smoothing was applied at the group level (explained in respective chapters).

6.3 Pulse Sequences used in this thesis

There were two types of images acquired for analysis in the experiments described in this thesis: Anatomical structural images for cortical surface reconstruction and functional images for experimental tasks. Below, I provide a brief overview of the different pulse sequences (programmed set of changing magnetic gradients, defined by a set of parameters) utilized in this thesis.

The structural imaging used a T_1-weighted 3D MPRAGE pulse sequence (Mugler III and Brookeman,1990). Images are called T_1-weighted if the relative signal intensity of voxels within the image depends on the T_1 value (time it takes for tissue to regain longitudinal magnetisation after the application of RF pulse) of the tissue. At very short TR's (time between two consecutive RF pulses), there is no time for longitudinal magnetisation to recover and thus no MR signal for either tissue. Conversely for long TR, all longitudinal magnetisation recovers for both tissues. At intermediate TR's there are clear differences between two tissues which has two different T_1 values, with tissue with a shorter T_1 recovering more rapidly and generating a greater MR signal (which is dependent on M0). The magnetisation-prepared rapid acquisition gradient echo (MP RAGE) is the most widely used T_1-weighted 3D gradient echo sequence that incorporates an MP inversion pulse to increase T_1 weighting. These sequences can give excellent contrast, such as between gray matter (GM) and white matter (WM) because the centre of k-space (which most strongly affects contrast) can be acquired at a time when the longitudinal magnetization of gray matter passes through zero, yielding almost no signal in comparison to the more rapidly recovering white matter. In order to obtain a T_1 weighted image, the unrecordable longitudinal magnetization is first quicky converted to recordable transverse magnetization.

For functional imaging, two T_2* weighted pulse sequences were utilized: EPI and multi band. 3 subjects's mapping and reading data were acquired using EPI, a more traditional protocol, while all other data acquisition utilized the more recently introduced multi band pulse sequence. As discussed previously, T_2* weighted images are sensitive to the amount of deoxygenated haemoglobin present, and is the contrast basis for fMRI. The EPI sequence was first introduced by Mansfield in 1977 (Mansfield, 1977). Compared to the techniques that preceded it, EPI allowed the fast acquisition of MR images by facilitating an entire slice to be acquired in one pulse repetition time (TR).

The multi band sequence utilized for most of the functional data collection in this thesis is a relatively recent technique, where multiple slices are excited and acquired simultaneously. Each RF coil channel then receives a linear combination of the signals from each of the slices, weighted by the coil sensitivity profiles, which can be used to reconstruct the signal for individual slices (Moeller et al., 2011). This allowed much faster data acquisition than possible with EPI, and facilitated whole brain coverage without loosing temporal SNR.

~~~
~~~

References

Adrian ED (1940): Double representation of the feet in the sensory cortex of the cat. J Physiol 98:16–18.

Alain C, Arnott SR, Hevenor S, Graham S, Grady CL (2001): “What” and “where” in the human auditory system. Proc Natl Acad Sci. U.S.A. 98:12301–12306.

Alexander MP, Naeser MA, Palumbo C (1990): Broca’s area aphasias: Aphasia after lesions including the frontal operculum. Neurology 40:353-362.

Arcaro MJ, McMains SA, Singer BD, Kastner S (2009): Retinotopic organization of human ventral visual cortex. J Neurosci 29(34):10638-52.

Arnott SR, Binns MA, Grady CL, Alain C (2004): Assessing the auditory dual-pathway model in humans. Neuroimage 22:401–408.

Bandettini PA, Jesmanowicz A, Wong EC, Hyde JS (1992): Processing strategies for time course data sets in functional MRI of the human brain. Magn Reson Med 30:161- 173.

Bar M, Aminoff E (2003): Cortical analysis of visual context. Neuron 38:347–358.

Bartels A, Zeki S (2004): Functional brain mapping during free viewing of natural scenes. Hum. Brain Mapp. 21:75–85.

Barton B, Venezia JH, Saberi K, Hickok G, Brewer AA (2012): Orthogonal acoustic dimensions define auditory field maps in human cortex. Proc Natl Acad Sci 109:20738-20743.

Basso A, Lecours AR, Moraschini S, Vanier M (1985): Anatomoclinical Correlations of the Aphasias as Defined through Computerized Tomography : Exceptions. Brain Lang 26:201–229.

Belin P, Fillion-Bilodeau S, Gosselin F (2008): The Montreal Affective Voices: a validated set of nonverbal affect bursts for research on auditory affective processing. Behavior research methods 40:531–539.

Belin P, Zatorre RJ, Lafaille P, Ahad P, Pike B (2000): Voice-selective areas in human auditory cortex. Nature 403:309 –312.

Berker EA, Berker AH, Smith A (1986): Translation of Broca’s 1865 report. Localization of speech in the third left frontal convolution. Arch Neurol. 43(10): 1065-72.

Bilecen D, Seifritz E, Scheffler K, Henning J, Schulte A-C (2002): Amplitopicity of the human auditory cortex: an fMRI study. Neuroimage 17:710-718.

Binder JR, Desai RH (2011): The neurobiology of semantic memory. Trends Cogn Sci 15:527–536.

Bloch F, Hansen WW, Packard M (1946): Nuclear Induction. Physical Review 70: 460

Bremmer F, Schlack A, Shah NJ, Zafiri O, Kubischik M, Hoffman K-P, et al. (2001): Polymodal motion processing in posterior parietal and premotor cortex: A human fMRI study strongly implies equivalencies between humans and monkeys. Neuron 29(1): 287–296.

Brodmann K (1909): "Vergleichende Lokalisationslehre der Grosshirnrinde" (in German). Leipzig: Johann Ambrosius Barth.

Broca P (1861): Nouvelle observation d'aphe´mie produite par une le´sion de la troisie`me circonvolution frontale. Bulletins de la Socie´te´ d'anatomie (Paris), 2e serie 6: 398–407.

Broca P (1865): Sur le siege de la faculte du langage articule. Bulletin de la Societe d'anthropologie 6: 337–93.

Burnstine TH, Lesser RP, Hart J, Uematsu S, Zinreich SJ, Krauss GL, Fisher RS, Vining EPG, Gordon B (1990): Characterization of the basal temporal language area in patients with left temporal lobe epilepsy. Neurology 40:966-970.

Burton H, Videen TO, Raichle ME (1993): Tactile-vibration-activated foci in insular and parietal-opercular cortex studied with positron emission tomography: mapping the second somatosensory area in humans. Somatosens Motor Res 10:297–308.

Chainay H, Krainik A, Tanguy M, Gerardin E, Bihan DLe (2004): Foot , face and hand representation in the human supplementary motor area. Neuroreport 15(5):1–5.

Choi W, Desai RH, Henderson JM (2014): The neural substrates of natural reading: a comparison of normal and nonword text using eyetracking and fMRI. Front Hum Neurosci, 8:1-11. Article 1024.

Clare MH, Bishop GH (1954): Responses from an association area secondarily activated from optic cortex. J Neurophysiol 17:271-277.

Cohn N, Jackendoff R, Holcomb PJ, Kuperberg GR (2014): The grammar of visual narrative: Neural evidence for constituent structure in sequential image comprehension. Neuropsychologia 64C:63–70.

Colby CL, Duhamel JR, Goldberg ME (1993): Ventral intraparietal area of the macaque: anatomic location and visual response properties. J Neurophysiol 69:902–914.

Cowey A (1964): Projection of the Retina on to Striate and Prestriate Cortex in the Squirrel Monkey, Saimiri Sciureus. J Neurophysiol 27:366-393.

Cox RW (2012): AFNI: what a long strange trip it's been. NeuroImage 62:743–747.

Çukur T, Nishimoto S, Huth AG, Gallant JL (2013): Attention during natural vision warps semantic representation across the human brain. Nature Neurosci 16:763–770.

Da Costa S, Van der Zwaag W, Miller LM, Clarke S, Saenz M (2013): Tuning in to sound: frequency-selective attentional filter in human primary auditory cortex. J Neurosci 33:1858-1863.

Da Costa S, Van der Zwaag W, Marques JP, Frackowiak RSJ, Clarke S, Saenz M (2011): Human primary auditory cortex follows the shape of Heschl's gyrus. J Neurosci 31:14067-14075.

Dick F, Lee HL, Nusbaum H, Price CJ (2011): Auditory-motor expertise alters "speech selectivity" in professional musicians and actors. Cereb Cortex 21:938-948.

Dick F, Tierney AT, Lutti A, Josephs O, Sereno MI, Weiskopf N (2012): In vivo functional and myeloarchitectonic mapping of human primary auditory areas. J Neurosci 32:16095–16105.

Dilks D, Julian J, Paunov A, Kanwisher N (2013): The occipital place area is causally and selectively involved in scene perception. J Neurosci 33(4): 1331-1336

Disbrow E, Roberts T, Krubitzer L (2000): Somatotopic organization of cortical fields in the lateral sulcus of Homo sapiens: evidence for SII and PV. J Comp Neurol 418:1–21.

Duncan J, Seitz RJ, Kolodny J, Bor D, Herzog DH, Ahmed A, Newell FN, Emslie H (2000): A Neural Basis for General Intelligence. Science 289:457–460.

Engel SA (2012): The development and use of phase-encoded functional MRI designs. NeuroImage 62(2): 1195–200.

Engel SA, Glover GH, Wandell BA (1997): Retinotopic organization in human visual cortex and the spatial precision of functional MRI. Cereb Cortex 7:181–192

Engel SA, Rumelhart DE, Wandell BA, Lee AT, Glover GH, Chichilnisky EJ, Shadlen MN (1994): fMRI of human visual cortex. Nature 369:525-525.

Epstein R, Kanwisher N (1998): A cortical representation of the local visual environment, Nature 392:6–9.

Epstein RA, MacEvoy SP (2011). Making a scene in the brain. In L. Harris & M. Jenkin (Eds.). Vision in 3d Environments. Cambridge: Cambridge University Press. p 255-279.

Ercsey-Ravasz M, Markov NT, Lamy C, Van Essen DC, Knoblauch K, Toroczkai Z, Kennedy H (2013): A predictive network model of cerebral cortical connectivity based on a distance rule. Neuron 80:184-197.

Felleman DJ, Van Essen DC (1991): Distributed hierarchical processing in the primate cerebral cortex. Cereb Cortex 1:1–47.

Ferrier D (1874): The localisation of function in the brain. Proc R Society of London 22: 229-232

Fischl B, Sereno MI, Dale AM (1999a): Cortical Surface-Based Analysis. II. Inflation, flattening, and a surface-based coordinate system. Neuroimage 9:195-207.

Fischl B, Sereno MI, Tootell RB, Dale AM (1999b): High-resolution intersubject averaging and a coordinate system for the cortical surface. Hum Brain Mapp. 8:272–284.

Formisano E, Kim DS, Di Salle F, Van de Moortele PF, Ugurbil K, Goebel R (2003): Mirror-symmetric tonotopic maps in human primary auditory cortex. Neuron 40:859-869.

Franceschini S, Gori S, Ruffino M, Pedrolli K, Facoetti A (2012): A causal link between visual spatial attention and reading acquisition. Curr Biol 22(9):814–819.

Gaab N, Gaser C, Zaehle T, Jancke L, Schlaug G (2003): Functional anatomy of pitch memory—an fMRI study with sparse temporal sampling. Neuroimage 19:1417–1426.

Gabrieli JDE, Norton ES (2012): Reading abilities: importance of visual-spatial attention. Curr Biol 22(9):298–299.

Gallese V, Lakoff G (2005): The Brain's concepts: the role of the Sensory-motor system in conceptual knowledge. Cogn Neuropsychol 22: 455–79.

Geschwind N (1970). The organization of language and the brain. Science 170: 940- 4.

Grossman ED, Donnelly M, Price R, Pickens D, Morgan V, Neighbor G (2000) Brain areas involved in perception of biological motion. J Cogn Neurosci 12(5):711–720.

Gonzalez-Castillo J, Saad ZS, Handwerker DA, Inati SJ, Brenowitz N, Bandettini PA (2012): Whole-brain, time-locked activation with simple tasks revealed using massive averaging and model-free analysis. Proc. Natl. Acad. Sci 109:5487–5492.

Grafton ST, Woods RP, Mazziotta JC, Phelps E (1991): Somatotopic Mapping of the Primary Motor Cortex in Humans: Activation Studies With Cerebral Blood Flow and Positron Emission Tomography. J Neurophysiol 66(3):735-743.

Graziano, M (2006): The organization of behavioral repertoire in motor cortex. Annu Rev Neurosci 29:105–34.

Graziano MSA, Cooke DF (2006): Parieto-frontal interactions, personal space, and defensive behavior. Neuropsychologia 44(6): 845–59.

Greve DN, Fischl B (2010): Accurate and robust brain image alignment using boundary based Registration. Neuroimage 48:63–72.

Hackett TA, Preuss TR, Kass JH (2001): Architectonic identification of the core region in auditory cortex of macaques, chimpanzees, and humans. J. Comp. Neurol. 441:197-222.

Hackett TA, Stepniewska I, Kaas JH (1999): Prefrontal connections of the parabelt auditory cortex in macaque monkeys. Brain Research 817:45–58.

Hagler DJ, Riecke L, Sereno MI (2007): Parietal and superior frontal visuospatial maps activated by pointing and saccades. NeuroImage 35:1562–77.

Hagler DJ Jr, Sereno MI (2006): Spatial maps in frontal and prefrontal cortex. Neuroimage 29:567-577.

Hari R, Reinikainen K, Kaukoranta E, Hamalainen M, Ilmoniemi R, Penttinen A, Salminen J, Teszner D (1984): Somatosensory evoked cerebral magnetic fields from SI and SII in man. Electroencephalogr Clin Neurophysiol 57:254–263.

Hasson U, Nir Y, Levy I, Fuhrmann G, Malach R (2004): Intersubject synchronization of cortical activity during natural vision. Science 303: 1634-1640.

Hasson U, Yang E, Vallines I, Heeger DJ, Rubin N (2008): A hierarchy of temporal receptive windows in human cortex. J Neurosci 28(10):2539–50.

Haxby JV, Hoffman EA, Gobbini MI (2000): The distributed human neural system for face perception. Trends Cogn Sci 4:223–233.

Hebb D (1949): The Organization of Behavior: A Neuropsychological Theory. New York (NY). John Wiley.

Herdener M, Esposito F, Scheffler K, Schneider P, Logothetis NK, Uludag K, Kayser C (2013): Spatial representations of temporal and spectral sound cues in human auditory cortex. Cortex 49(10): 2822-33.

Hodge CJJ, Huckins SC, Szeverenyi NM, Fonte MM, Dubroff JG, Davuluri K (1998): Patterns of lateral sensory cortical activation determined using functional magnetic resonance imaging. J Neurosurg 89:769–779.

Hoffman EA, Haxby JV (2000): Distinct representations of eye gaze and identity in the distributed human neural system for face perception. Nature Neurosci 3:80–84.

Holmes G (1918): Distrubances of vision by cerebral lesions. Bre. J. Opthal 2:353–384.

Holmes G, Lister WT (1916): Disturbances of vision from cerebral lesions, with special reference to the cortical representation of the macula. Brain. 39:34–73.

Huang R-S, Chen C, Tran AT, Holstein KL, Sereno MI (2012): Mapping multisensory parietal face and body areas in humans. Proc. Natl. Acad. Sci. U.S.A. 109:18114–198119.

Huang R-S, Sereno MI (2013): Bottom-up Retinotopic Organization Supports Top-down Mental Imagery. Open Neuroimag J 7:58–67.

Huk AC, Dougherty RF, Heeger DJ (2002): Retinotopy and functional subdivision of human areas MT and MST. J Neurosci 22:7195-7205.

Humphries C, Liebenthal E, Binder JR (2010): Tonotopic organization of human auditory cortex. Neuroimage 50:1202-1211.

Huth AG, Nishimoto S, Vu AT, Gallant JL (2012): A continuous semantic space describes the representation of thousands of object and action categories across the human brain. Neuron 76(6):1210–24.

Head H (1915): Hughlings Jackson on Aphasia and Kindred Affections of Speech. Brain 38: 1-190.

Hubel DH, Wiesel TN (1965): Receptive Fields and Functional Architecture in Two Nonstriate Visual Areas (18 and 19) of the Cat. J Neurophysiol 28:229-289.

Inouye T (1909): Die Sehstroungen bei Schussverietzungen der kortikalen Sehsphare. Leipzig, Germany: W. Engelmann

Jamadar SD, Fielding J, Egan GF (2013): Quantitative meta-analysis of fMRI and PET studies reveals consistent activation in fronto-striatal-parietal regions and cerebellum during antisaccades and prosaccades. Front. Psychol 4:749.

Jenkinson M, Bannister PR, Brady JM, Smith SM (2002): Improved optimisation for the robust and accurate linear registration and motion correction of brain images. NeuroImage 17:825-841.

Jenkinson M, Smith SM (2001): A global optimisation method for robust affine registration of brain images. Med Image Anal 5:143-156.

Kaas JH (1983): What , if Anything , is SI? Organization of First Somatosensory Area of Cortex. Physiol Rev 63(1):206-31

Kaas JH (1997): Topographic maps are fundamental to sensory processing. Brain Res. Bull 44:107–112.

Kaas JH, Hackett TA (2000): Subdivisions of auditory cortex and processing streams in primates. Proc Natl Acad Sci 97:11793-11799.

Kanwisher N, McDermott J, Chun MM (1997): The fusiform face area: a module in human extra striate cortex specialised for face perception. J Neurosci. 17:4302-4311.

Kastner S, DeSimone K, Konen CS, Szczepanski SM, Weiner KS, Schneider KA (2007): Topographic maps in human frontal cortex revealed in memory-guided saccade and spatial working-memory tasks. J Neurophysiol 97:3494-3507.

Kertesz A, Sheppard A, MacKenzie R (1982): Localization in transcortical sensory aphasia. Arch Neurol 39:475-478.

Kevan A, Pammer K (2008): Making the link between dorsal stream sensitivity and reading 19(4):67–70.

Kiehl KA, Laurens KR, Duty TL, Forster BB, Liddle PF (2001): Neural sources involved in auditory target detection and novelty processing: an event-related fMRI study. Psychophysiology 38:133–142.

Koelsch S, Schulze K, Sammler D, Fritz T, Muller K, Gruber O (2009): Functional architecture of verbal and tonal working memory: an FMRI study. Hum Brain Mapp 30:859–873.

Krauss GL, Fisher R, Plate C, Hart J, Uematsu S, Gordon B, Lesser RP (1996): Cognitive effects of resecting basal temporal language areas. Epilepsia 37:476–483.

Lacoboni M, Lieberman MD, Knowlton BJ, Molnar-Szakacs I, Moritz M, Throop CJ, Fiske AP (2004): Watching social interactions produces dorsomedial prefrontal and medial parietal BOLD fMRI signal increases compared to a resting baseline. NeuroImage 21(3): 1167–73.

Lahnakoski JM, Glerean E, Salmi J, Jääskeläinen IP, Sams M, Hari R, Nummenmaa L (2012): Naturalistic fMRI Mapping Reveals Superior Temporal Sulcus as the Hub for the Distributed Brain Network for Social Perception. Front Hum Neurosci 6: 233-245.

Langers DRM, van Dijk P (2012): Mapping the tonotopic organization in human auditory cortex with minimally salient acoustic stimulation. Cereb Cortex 22:2024-2038.

Langner G, Sams M, Heil P, Schulze H (1997): Frequency and periodicity are represented in orthogonal maps in the human auditory cortex: evidence from magnetoencephalography. J. Comp. Physiol. A 181:665-676.

Lerner Y, Honey CJ, Silbert LJ, Hasson U (2011): Topographic mapping of a hierarchy of temporal receptive windows using a narrated story. J Neurosci 31(8):2906–15.

Leyton SSF, Sherrington CS (1917): Observations on the excitable cortex of the chimpanzee, orangutan and gorilla. Q J Exp Physiol 11:135–222.

Lin W, Kuppusamy K, Haacke EM, Burton H (1996): Functional MRI in human somatosensory cortex activated by touching textured surfaces. J Magn Reson Imag 6:565–572.

Lichtheim L (1885): On aphasia. Brain, 7:433–485.

Logothetis NK, Pauls J, Augath M, Trinath T, Oeltermann A (2001): Neurophysiological investigation of the basis of the fMRI signal. Nature 412: 150- 7.

Logothetis NK (2003): The underpinnings of the BOLD functional magnetic resonance imaging signal. J Neurosci 23: 3963-71.

Luders H, Lesser RP, Hahn J, Dinner DS, Morris HH, Wyllie E, Godoy J (1991): Basal temporal language area. Brain 114:743–754.

Lund JS, Yoshioka T, Levitt JB (1993): Comparison of intrinsic connectivity in different areas of macaque monkey cerebral cortex. Cereb Cortex 3:148-162.

Mahon BZ, Caramazza A (2008): A critical look at the embodied cognition hypothesis and a new proposal for grounding conceptual content. Journal of physiology 102:59–70.

Maldjian JA, Gottschalk A, Patel RS, Pincus D, Detre JA, Alsop DC (1999): Mapping of secondary somatosensory cortex activation induced by vibrational : an fMRI study. Brain Res 824:291–295.

Mani J, Diehl B, Piao Z, Schuele SS, Lapresto E, Liu P, Nair DR, Dinner DS, Lüders HO (2008): Evidence for a basal temporal visual language center: cortical stimulation producing pure alexia. Neurology 71:1621–1627.

Mansfield P (1977): Multi-planar imaging using NMR spin echoes. Journal of Physics C 10(3): 55-58

Mugler III JP, Brookeman R (1990): Three-Dimensional Magnetization-Prepared Rapid Gradient-Echo Imaging (3D MP RAGE). Magn Reson Med 15: 152–157.

Marshall WH, Woolsey CN, BARD R (1937): Cortical representation of tactile sensibility as indicated by cortical potentials. Science 85: 333-390.

Mayeux R, Kandel ER (1991): Disorders of language: the aphasias. In: Principles of Neural Science (Kandel ER, Schwartz JH, Jessell TM, 3rd ed). pp839-851. London: Prentice Hall.

McDowell JE, Dyckman KA, Austin BP, Clementz BA (2008): Neurophysiology and neuroanatomy of reflexive and volitional saccades: evidence from studies of humans. Brain Cogn 68:255–270.

Meier JD, Aflalo TN, Kastner S, Graziano MSA (2008): Complex organization of human primary motor cortex: a high-resolution fMRI study. J Neurophysiol 100(4): 1800–12.

Melcher D, Colby CL. Trans-saccadic perception (2008): Trends Cogn Sci 12(12):466– 473.

Merzenich M, Kaas JH (1980): Principles of organization of sensory-perceptual systems in mammals. In: Progress in Psychobiology and Physiological Psychology, edited by J. M. Sprague and A. N. Epstein. New York: Academic. p. 1-41.

Mesulam, MM, Nobre AC, Kim YH, Parrish TB (2001): Heterogeneity of Cingulate Contributions to Spatial Attention. Neuroimage 13: 1065–1072.

Mohr JP (1976): Broca's area and Broca's aphasia. In H. Whitaker (Ed.), Studies in neurolinguisics (pp. 201–236). New York: Academic.

Mohr JP, Pessin MS, Finkelstein S, Funkenstein HH, Duncan GW, & Davis KR (1978): Broca aphasia: Pathologic and clinical. Neurology 28:311–324.

Moeller S, Yacoub E, Olman CA, Auerbach E, Strupp J, Harel N, Kâmil U (2011): Multiband Multislice GE-EPI at 7 Tesla, With 16-Fold Acceleration Using Partial Parallel Imaging With Application to High Spatial and Temporal Whole-Brain FMRI. Magn. Reson Med 5:1144–1153.

Moerel M, De Martino F, Formisano E (2012): Processing of natural sounds in human auditory cortex: tonotopy, spectral tuning, and relation to voice sensitivity. J Neurosci 32(41): 14205–16.

Monti MM (2011): Statistical Analysis of fMRI Time-Series: A Critical Review of the GLM Approach. Front Hum Neurosci 5: 28-55.

Muller RA, Kleinhans N, Courchesne E (2001): Broca's area and the discrimination of frequency transitions: a functional MRI study. Brain Lang 76:70–76

Müri RM, Nyffeler T (2008): Neurophysiology and neuroanatomy of reflexive and volitional saccades as revealed by lesion studies with neurological patients and transcranial magnetic stimulation (TMS). Brain Cogn 68:284–292.

Nadeau SE, Rothi LJG, Crosson BA (2000): Aphasia and Language: Theory to Practice. Guilford Press, New york, NY. 418 p.

Nasr S, Liu N, Devaney KJ, Yue X, Rajimehr R, Ungerleider LG, Tootell RBH (2011): Scene-selective cortical regions in human and nonhuman primates. J Neurosci 31(39): 13771–85.

Nishimoto S, Vu AT, Naselaris T, Benjamini Y, Yu B, Gallant JL (2011): Reconstructing visual experiences from brain activity evoked by natural movies. Curr. Biol. 21:1641-1646.

Ogawa S, Lee TM (1990): Magnetic resonance imaging of blood vessels at high fields: in vivo and in vitro measurements and image simulation. Magn Reson Med. 16(1):9–18.

Ogawa S, Lee TM, Nayak AS, Glynn P (1990a): Oxygenation-sensitive contrast in magnetic resonance image of rodent brain at high magnetic fields. Magn Reson Med. 14(1):68–78.

Ogawa S, Lee TM, Kay AR, Tank DW (1990b): Brain magnetic resonance imaging with contrast dependent on blood oxygenation. Proc Natl Acad Sci U S A 87: 9868-72.

O'Reilly JX, Schüffelgen U, Cuell SF, Behrens TEJ, Mars RB, Rushworth MFS (2013): Dissociable effects of surprise and model update in parietal and anterior cingulate cortex. Proc Natl Acad Sci 110(38): 3660–9.

Pantev C, Hoke M, Lehnertz K, Lütkenhöner B (1989): Neuromagnetic evidence of an amplitopic organization of the human auditory cortex. Electroencephalogr Clin. Neurophysiol. 72:225-231.

Pauling L, Coryell CD (1936): The Magnetic Properties and Structure of Hemoglobin, Oxyhemoglobin and Carbonmonoxyhemoglobin. Proc Natl Acad Sci U S A 22: 210-6.

Peelen MV, Kastner S (2014): Attention in the real world: toward understanding its neural basis. Trends Cogn Sci 18(5): 242–250.

Penfield W, Boldrey E (1937): Somatic motor and sensory representation in the cerebral cortex of man as studied by electrical stimulation. Brain 60: 389–443.

Penfield W, Jasper H. 1954. Epilepsy and the functional anatomy of the human brain. Boston, MA: Little, Brown & Co. 896p.

Penfield W, Rasmussen T. 1950. The Cerebral Cortex ofMan.Macmillan,NewYork. 248p.

Penfield W, Welch K (1951): The supplementary motor area of the cerebral cortex; a clinical and experimental study. AMA Arch Neurol Psychiatry 66(3): 289-317.

Perrone-Bertolotti M, Kujala J, Vidal JR, Hamame CM, Ossandon T, Bertrand O, … Lachaux J-P (2012): How silent is silent reading? Intracerebral evidence for top-down activation of temporal voice areas during reading. J Neurosci 32(49):17554–62.

Pierrot-Deseilligny C, Milea D, Müri RM (2004): Eye movement control by the cerebral cortex. Curr. Opin. Neurol. 17:17–25.

Plakke B, Romanski LM (2014): Auditory connections and functions of prefrontal cortex. Front Neurosci 8:1–13.

Platel H, Price C, Baron JC, Wise R, Lambert J, Frackowiak RS, Lechevalier B, Eustache F (1997): The structural components of music perception. A functional anatomical study. Brain 120:229–243.

Polonara G, FabriM, Manzoni T, Salvolini U (1999): Localization of the first and second somatosensory areas in the human cerebral cortex with functional MR imaging. Am J Neuroradiol 20:199–205.

Posner MI (1980): Orienting of attention. Q J Exp Psychol 32:3–25.

Potter MC, Kroll JF, Yachzel B, Carpenter E, Sherman J (1986): Pictures in sentences: understanding without words. J Exp Psychol: General 115:281-294.

Puce A, Allison T, Asgari M, Gore JC, McCarthy G (1996): DiVerential sensitivity of human visual cortex to faces, letter strings, and textures: a functional magnetic resonance imaging study. J Neurosci 16:5205–5215.

Pulvermüller F, Fadiga L (2010): Active perception: sensorimotor circuits as a cortical basis for language. Nat Rev Neurosci 11:351–360.

Purcell BA, Weigand PK, Schall JD (2012): Supplementary eye field during visual search: salience, cognitive control, and performance monitoring. J Neurosci 32(30):10273–85.

Purcell EM, Torrey HC, Pound RV (1946): Resonance Absorption by Nuclear Magnetic Moments in a Solid. Phys Rev 69:37.

Rämä P, Poremba A, Sala JB, Yee L, Malloy M, Mishkin M, Courtney SM (2004): Dissociable functional cortical topographies for working memory maintenance of voice identity and location. Cereb Cortex 14:768–780.

Rio DE, Rawlings RR, Woltz LA, Gilman J, Hommer DW (2013): Development of the Complex General Linear Model in the Fourier Domain: Application to fMRI Multiple Input-Output Evoked Responses for Single Subjects. Computational and Mathematical Methods in Medicine.

Rizzolatti G, Luppino G, Matelli M (1998): The organization of the cortical motor system: new concepts. Electroencephalogr Clin Neurophysiol. 106:283–296.

Romanski LM, Tian B, Fritz J, Mishkin M, Goldman-Rakic PS, Rauschecker JP (1999): Dual streams of auditory afferents target multiple domains in the primate prefrontal cortex. Nature Neurosci 2:1131–1136.

Rubens AB, Kertesz A (1983): The localization of lesions in transcortical aphasias. In: Kertesz A . Localization in Neuropsychology. 1st ed. Academic Press. p 245-268.

Saygin AP, Sereno MI (2008): Retinotopy and attention in human occipital, temporal, parietal, and frontal cortex. Cereb Cortex 18:2158–68.

Schiller PH, Chou IH (1998): The effects of frontal eye field and dorsomedial frontal cortex lesions on visually guided eye movements. Nature Neurosci 1:248–253.

Schira MM1, Tyler CW, Breakspear M, Spehar B (2009): The foveal confluence in human visual cortex. J Neurosci 29:9050-9058.

Schluppeck D, Glimcher P, Heeger DJ (2005): Topographic organization for delayed saccades in human posterior parietal cortex. J Neurophysiol 94:1372-1384.

Schmahmann J, Pandya D (2009): Fiber Pathways of the Brain. Oxford(UK): Oxford University Press.

Seifritz E, Di Salle F, Esposito F, Herdener M, Neuhoff JG, Scheffler K (2006): Enhancing BOLD response in the auditory system by neurophysiologically tuned fMRI sequence. Neuroimage 29:1013-1022.

Seitz RJ, Roland PE (1992): Vibratory stimulation increases and decreases the regional cerebral blood f lowand oxidative metabolism: a positron emission tomography (PET) study. Acta Neurol Scand 86:60–67.

Sereno MI (2014): Origin of symbol-using systems: speech, but not sign, without the semantic urge. Philosphical Transactions of the Royal Society Biological Sciences. 369:20130303.

Sereno MI, Allman JM (1991): Cortical visual areas in mammals. In Leventhal AG. 1st ed. The Neural Basis of Visual Function. London (UK). Macmillan. p 160-172.

Sereno MI, Dale AM, Reppas JB, Kwong KK, Belliveau JW, Brady TJ, Rosen BR, Tootell RB (1995): Borders of multiple visual areas in humans revealed by functional magnetic resonance imaging. Science 268:889–893.

Sereno MI, Huang R-S (2006): A human parietal face area contains aligned head-centered visual and tactile maps. Nature Neurosci 9(10): 1337–43.

Sereno MI, Huang R-S (2014): Multisensory maps in parietal cortex. Curr Opin Neurobiol 24(1): 39–46.

Sereno MI, Lutti A, Weiskopf N, Dick F (2013): Mapping the human cortical surface by combining quantitative T1 with retinotopy. Cereb Cortex 23:2261–2268.

Sereno MI, Pitzalis S, Martinez A (2001): Mapping of contralateral space in retinotopic coordinates by a parietal cortical area in humans. Science 294:1350-1354.

Sereno MI, Saygin AP, Hagler DJ Jr (2003): Retinotopy in parietal and temporal cortex. Neuroimage 19:S1523.

Sergent J, Ohta S, MacDonald B (1992): Functional neuroanatomy of face and object processing: a positron emission tomography study. Brain 115: 15-36.

Sharp DJ, Scott SK, Wise RJS (2004): Retrieving meaning after temporal lobe infarction: the role of the basal language area. Ann Neurol 56:836-846.

Silver MA, Kastner S (2009): Topographic maps in human frontal and parietal cortex. Trends Cogn Sci 13:488–495.

Silver MA, Ress D, Heeger DJ (2005): Topographic maps of visual spatial attention in human parietal cortex. J Neurophysiol 94:1358-1371.

Simmons W, Barsalou L (2003): The similarity-in-topography principle: reconciling theories of conceptual deficits. Cogn. Neuropsychol 20:451–486.

Smith SM, Jenkinson M, Woolrich MW, Beckmann CF, Behrens TEJ, Johansen-Berg H, Bannister PR, De Luca M, Drobnjak I, Flitney DE, R. Niazy, Saunders J, Vickers J, Zhang Y, De Stefano N, Brady JM, and Matthews PM (2004): Advances in functional and structural MR image analysis and implementation as FSL. NeuroImage 23(S1):208-19.

Sperry RW (1943): Effect of 180 degree rotation of the retinal field on visuomotor coordination. J Exp Zool 92:263-279.

Swisher JD, Halko MA, Merabet LB, McMains SA, Somers DC (2007): Visual topography of human intraparietal sulcus. J Neurosci 27:5326-5337.

Talavage TM, Ledden PJ, Benson RR, Rosen BR, Melcher JR (2000): Frequency- dependent responses exhibited by multiple regions in human auditory cortex. Hear Res 150: 225-244.

Talavage TM, Sereno MI, Melcher JR, Ledden PJ, Rosen BR, Dale AM (2004): Tonotopic organization in human auditory cortex revealed by progressions of frequency sensitivity. J Neurophysiol 91:1282-1296.

Thivierge J-P, Marcus GF (2007): The topographic brain: from neural connectivity to cognition. Trends Neurosci 30:251–259.

Thompson JM, Woolsey CN, Talbot SA (1950): Visual areas I and II of cerebral cortex of rabbit. J Neurophysiol 13:277-288.

Tusa RJ, Palmer LA, Rosenquist AC (1978): The retinotopic organization of area 17 (striate cortex) in the cat. J Comp Neurol 177:213-235.

Venkatesan L, Barlow SM, Popescu M, Popescu A (2014): Integrated approach for studying adaptation mechanisms in the human somatosensory cortical network. Exp Brain Res 232(11): 3545–54.

Wandell BA, Dumoulin SO, Brewer AA (2007): Visual field maps in human cortex. Neuron 56:366–383.

Wernicke C (1874): The symptom complex of aphasia. Reprinted in English in Proc. Boston Colloq. Philos. Sci. 4: 34-97.

Woolsey CN (1943): “Second” somatic receiving areas in the cerebral cortex of cat, dog and monkey. Fed Proc 2:55–56.

Woolsey CN (1944): Additional observations on a “second” somatic receiving area in the cerebral cortex of the monkey. Fed Proc 3:53.

Woolsey CN, Fairman D (1946): Contralateral, ipsilateral, and bilateral representation of cutaneous receptors in somatic areas I and II of the cerebral cortex of pig, sheep, and other mammals. Surgery 19: 684–702.

Woolsey CN (1964): Cortical localization as defined by evoked potential and electrical stimulation studies. In: Cerebral localization and organization (Schaltenbrand G, Woolsey CN, eds), Madison, WI: University of Wisconsin. pp 17–26.

Woolsey CN, Settlage PH, Meyer DR, Sencer W, Pinto Hamuy T , Travis, AM (1952): Patterns of localization in precentral and ‘supplemen- tary’ motor areas and their relation to the concept of a premotor area. Res. Publ. Assoc. Nerv. Ment. Dis. 30: 238–264.

Woolsey CN,Wang G (1945): Somatic sensory areas I and II of the cerebral cortex of the rabbit. Fed Proc 4:79.

Yovel G, Kanwisher N (2005): The neural basis of the behavioral face inversion effect. Curr Biol 15:2256–2262

Zhao M (2012): Eye movements and attention: The role of pre-saccadic shifts of attention in perception, memory and the control of saccades. Vision Res 74:40–60.

Zeharia N, Hertz U, Flash T, Amedi A (2012): Negative blood oxygenation level dependent homunculus and somatotopic information in primary motor cortex and supplementary motor area. Proc Natl Acad Sci 109:18565–18570.